

Thesis
C78

Thesis
C78

- Library
U. S. Naval Postgraduate School
Annapolis, Md.

AIR INLETS FOR TURBOJET ENGINES
THROUGH THE TRANSONIC SPEED RANGE

A thesis
Submitted to the Graduate Faculty
of the
University of Minnesota

by
James J.^{Coyle} Coyle

In Partial Fulfillment of the Requirements
For the Degree of
Master of Science

July 15, 1949

TABLE OF CONTENTS

Chapter	Page
I. Diffuser Analysis--Introduction	1
II. Performance of a Diffuser	5
1. Characteristics of Diffuser Flow.. . . .	5
2. Diffuser Efficiency	9
3. Diffuser Discharge Limitations	15
4. External Drag Considerations	18
III. Diffuser Losses	21
1. Shock Loss	22
2. Entrance Loss	28
3. Yawing Effect	32
4. Expansion Loss	33
A. Boundary Layer in a Diffuser	35
B. Point of Laminar Separation	38
C. Mixing Length	40
D. Point of Separation of the Turbulent Boundary Layer	40
E. Means of Delaying Separation	44
5. Friction Loss	47
6. Turning Loss	50
7. Obstructions in the Flow	53
8. Leakage Loss	56
9. Exit Loss	57
IV. Geometric Considerations	59
1. Inlet Duct Location	59
2. Area Ratios and Diffuser Length	63
3. Velocity Ratio	67
V. Typical Diffuser Problem	73
VI. Present Air Inlet Design Features	86
VII. Conclusions and Recommendations	97
Appendix I--Symbols	101
References	102

LIST OF FIGURES

1. Effect of Ram Recovery Ratio on the Maximum Available Net Thrust of a Turbo-jet Engine at Sea Level.
2. Effect of Ram Recovery Ratio on Specific Fuel Consumption at Maximum Available Net Thrust of a Typical Turbo-jet Engine at Sea Level.
3. Change in Net Thrust and Specific Fuel Consumption for an Increase of Ram Recovery Ratio from 0.70 to 0.90.
4. Comparison of Test Results with Theoretical Expectations for Diffusers with Internal Shock.
5. Ram Recovery Ratio Across a Normal Shock.
6. Theoretical Pressure Recovery Ratio after "n" Compression Shocks, n - 1 oblique Shocks Plus One Normal Shock.
7. Effect of Exit Cone Angle on the Performance of Two Supersonic Diffusers.
8. Velocity Decrement Obtainable before Laminar Separation Occurs.
9. Improvement of Diffuser Efficiency with Suction.
10. Effect of Radius Ratio and Deflection Angle on Turning Losses in Ducts.
11. Influence of Aspect Ratio on Turning Losses in Ducts.
12. Effect of Gap/Chord Ratio on Resistance Coefficient.
13. Losses in Expanding Entries.
14. Obstruction Loss Coefficient in a Duct.
15. Length of Constant Area Duct Following a Diffuser Necessary for Complete Pressure Recovery.
16. Variation of Area Ratio with Entrance Mach Number to Give an Exit Mach Number of 0.3.
17. Length of Conical Diffuser Required for Various Entrance Mach Numbers.

18. Diffuser Geometry for Illustrative Problem.
19. Shape of Diffuser Entrance and Static Pressure Distribution.
20. Internal Conditions in the Diffuser.
21. Friction Effects in the Diffuser.
22. Friction Losses in the Duct Connecting the Diffuser and the Compressor
23. Variation of Velocity Ratio with Flight Mach Number.
24. Variation of Flow Density with Flight Mach Number and Altitude.

CHAPTER I

DIFFUSER ANALYSIS--INTRODUCTION

On September 15, 1948, a North American F-86A set a new world air speed record of 670.981 mph at Muroc, California. The average mach number of this speed trial was 0.87. The F-86A is powered by a General Electric-Allison J-35 turbojet engine. This was the fourth time in twenty seven months that the world air speed record was broken by a turbo-jet powered aircraft. On December 22, 1947, an aviation magazine published a report that the Bell XS-1, a rocket powered aircraft, had exceeded a flight mach number of 1.0 at altitude. Meanwhile, other experimental aircraft such as the Douglas D-558-II, the Bell XS-2, the Douglas XS-3, and the Northrop XS-4 are being developed for investigating transonic flight.

On the basis of this information it is obvious that rapid strides are being made in the field of aviation. As flight speeds approach and pass the speed of sound new problems arise which influence the design of aircraft and aircraft engines. Foremost among these problems is the phenomenon that air at these flight mach numbers is compressible, and behaves in a quite different manner than it does at relatively low speeds.

The question also arises as to which type of propulsion system is best fitted for use at speeds near the speed of sound. The commonly recognized types of propulsion systems for airborne vehicles are the reciprocating engine driven propeller, the turbine driven propeller, the turbo-jet, the ram-jet, and the rocket. Only the last mentioned is independent of air supply for the generation of power.

At high speeds propeller efficiency declines rapidly so the use of a propeller driven aircraft near the speed of sound is not practical. This is further indicated by the present speed advantage of jet powered aircraft over propeller driven aircraft. The rocket, since it is independent of air supply, appears to have a big advantage, but it is so inefficient at low supersonic mach numbers that its fuel demands severely restrict the flight duration. Its use in present experimental type aircraft is based upon a desire to reach supersonic speeds, if only for a short duration, to obtain data to prove and develop aerodynamic designs for supersonic flight. It should be noted that auxiliary means are used to bring these aircraft up to high speed before the rocket power is utilized. The XS-1 is air launched from another aircraft, and the B-558-II has a turbo-jet engine for subsonic flight.

The ram-jet engine has a restricted use due to design limitations. It is efficient for only one flight

mach number, and cannot develop sufficient thrust to reach this design point unaided. Furthermore, at flight mach numbers below 1.5 the turbo-jet is theoretically more efficient.

After considering the principal disadvantages of the other types of propulsion systems, the suitability of the turbo-jet for transonic operation will be considered. Fig. 1, which was obtained from Ref. 1, shows the variation of thrust with flight velocity at various values of ram recovery ratio%. Ram recovery ratio is a measure of diffuser efficiency, and is defined thus:

$$\text{Ram recovery ratio} = \frac{P_2^0 - P_0}{P_0^0 - P_0}$$

As can be seen, thrust does vary with flight velocity, particularly with low values of ram recovery ratio. Thrust is even more sensitive to engine rpm. The turbo-jet's moving parts consist of a directly coupled turbine and compressor. The characteristics of these two units are such that peak efficiency occurs at a particular design engine speed, variations from this design point result in reduced engine performance. Fig. 1 reveals that the thrust decreases with flight velocity down to a minimum, and then increases with further speed increase if the ram recovery ratio is sufficiently high.

Fig. 2 shows the variation of specific fuel consumption with flight velocity with various ram recovery ratios. These curves are also a measure of the

efficiency of a turbo-jet unit. They show that for high ram recovery ratios, the specific fuel consumption increases with flight velocity but tends to level off after reaching some maximum value. From a study of Figs. 1 and 2 the conclusion can be drawn that the turbo-jet offers efficient operation from the static thrust condition to speeds near the speed of sound provided the diffuser ram recovery ratio is sufficiently high. These curves would show the same trends if they were extrapolated into the range of low supersonic mach numbers. The improvement in performance with increased ram recovery ratio is shown in Fig. 3. For example, it shows that for an airplane flying at 650 mph at sea level an increase in ram recovery ratio from 0.70 to 0.90 will result in an 15.2 per cent increase in net thrust and a 9.5 per cent decrease in specific fuel consumption. Such figures indicate the importance of high diffuser efficiency.

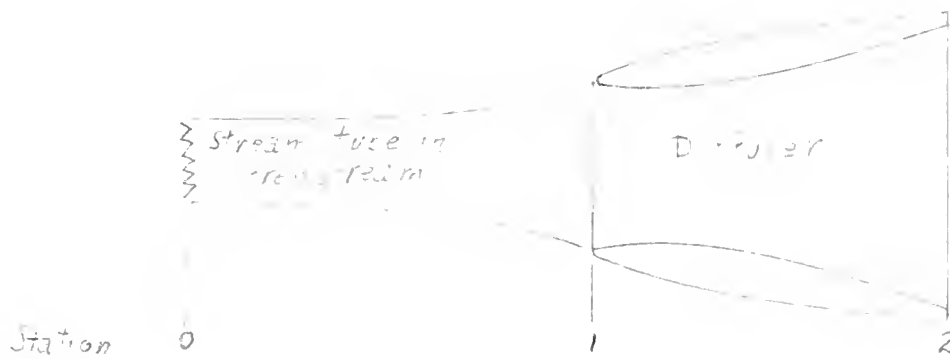
CHAPTER II

PERFORMANCE OF A DIFFUSER

1. Characteristics of Diffuser Flow.

Recognizing the advantages to be gained by efficient air induction into a turbojet engine, the mechanics of the air induction process will be investigated. For purposes of analysis it will be assumed that the engine is fixed in space and the air is flowing through and past it with an undisturbed free stream velocity equal to the flight velocity of the airplane. The velocity of flow at the entrance to the diffuser will not be the same as the undisturbed free stream velocity except at one flight velocity. The volume of airflow through the engine is a function of the engine speed. The flow velocity at the diffuser entrance depends upon this volume flow and the entrance area of the diffuser. Therefore, some process will occur before the air enters the diffuser. At low speeds, the air expands and accelerates into the diffuser; at high speeds, the air is compressed and decelerates into the diffuser. This process occurring before the air enters the diffuser is assumed to be isentropic.

The following equations can be used to determine the state of the air at the entrance to the diffuser.



$$\frac{A_0}{A_1} = \frac{M_1}{M_0} \left(\frac{1 + \frac{\gamma-1}{2} M_0^2}{1 + \frac{\gamma-1}{2} M_1^2} \right)^{\frac{\gamma+1}{2(\gamma-1)}}$$

$$\frac{P_0}{P_1} = \left(\frac{1 + \frac{\gamma-1}{2} M_1^2}{1 + \frac{\gamma-1}{2} M_0^2} \right)^{\frac{\gamma}{\gamma-1}} \quad P_0^0 = P_1^0 \text{ (Isentropic flow)}$$

$$\frac{T_0}{T_1} = \left(\frac{1 + \frac{\gamma-1}{2} M_1^2}{1 + \frac{\gamma-1}{2} M_0^2} \right) \quad T_0^0 = T_1^0 \text{ (Adiabatic flow)}$$

To consider the nature of the flow within the diffuser, let us write the following equations:

Euler's equation for one dimensional frictionless flow:

$$VdV + \frac{dp}{\rho} = 0 \quad (a)$$

Continuity equation:

$$\frac{d\rho}{\rho} + \frac{dA}{A} + \frac{dV}{V} = 0 \quad (b)$$

Definition of the speed of sound:

$$a^2 = \frac{dp}{d\rho} \quad (c)$$

$$\frac{1}{2} \frac{d}{dt} \left(\frac{1}{2} \frac{d^2}{dt^2} \right) = \frac{1}{2} \frac{d^3}{dt^3}$$

$$\frac{1}{2} \frac{d}{dt} \left(\frac{1}{2} \frac{d^2}{dt^2} \right) = \frac{1}{2} \frac{d^3}{dt^3}$$

$$\frac{1}{2} \frac{d}{dt} \left(\frac{1}{2} \frac{d^2}{dt^2} \right) = \frac{1}{2} \frac{d^3}{dt^3}$$

$$\frac{1}{2} \frac{d}{dt} \left(\frac{1}{2} \frac{d^2}{dt^2} \right) = \frac{1}{2} \frac{d^3}{dt^3}$$

$$\frac{1}{2} \frac{d}{dt} \left(\frac{1}{2} \frac{d^2}{dt^2} \right) = \frac{1}{2} \frac{d^3}{dt^3}$$

$$\frac{1}{2} \frac{d}{dt} \left(\frac{1}{2} \frac{d^2}{dt^2} \right) = \frac{1}{2} \frac{d^3}{dt^3}$$

$$\frac{1}{2} \frac{d}{dt} \left(\frac{1}{2} \frac{d^2}{dt^2} \right) = \frac{1}{2} \frac{d^3}{dt^3}$$

$$\frac{1}{2} \frac{d}{dt} \left(\frac{1}{2} \frac{d^2}{dt^2} \right) = \frac{1}{2} \frac{d^3}{dt^3}$$

$$\frac{1}{2} \frac{d}{dt} \left(\frac{1}{2} \frac{d^2}{dt^2} \right) = \frac{1}{2} \frac{d^3}{dt^3}$$

Substituting eq. (c) in (a), and combining eqs. (a) and (b), we arrive at the following expression:

$$\frac{dV}{V} (1-M^2) = - \frac{dA}{A} \quad (d)$$

This equation reveals that, for subsonic flow, velocity decreases with an increase in area; the reverse is true for supersonic flows. To decelerate a supersonic flow isentropically to subsonic would require a converging channel, followed by a diverging section. The velocity at the throat would be sonic.

However, the flow in a channel is not isentropic, but it is essentially adiabatic, therefore the result of an entropy increase can be determined from the definition of entropy increase as given in Ref. 2, p. 11.

$$ds = c_p \frac{dT}{T} - R \frac{dp}{p}$$

$$T^0 = T \left(1 + \frac{\gamma-1}{2} M^2 \right)$$

$$p^0 = p \left(1 + \frac{\gamma-1}{2} M^2 \right)^{\frac{\gamma}{\gamma-1}}$$

$$\frac{ds}{T} = \frac{\gamma}{\gamma-1} \frac{dT^0}{T^0} - \frac{dp^0}{p^0}$$

And since the process is adiabatic, $ds = 0$, and

$$\frac{dT^0}{T^0} = - \frac{dp^0}{p^0}$$

$$\frac{p_2^0}{p_1^0} = e^{-\frac{\Delta s}{R}}$$

The quantities p^0 and T^0 are defined as total pressure and total temperature. They are the values which would be obtained if the flow were slowed isentropically until it had zero velocity. Since according to the second law of thermodynamics, $ds > 0$, then $p_1^0 > p_2^0$, or in a non-isentropic process a decrease in total pressure accompanies an entropy increase. The conditions of flow at the diffuser exit are given by the following equations, M_2 being found as an implicit function of the entrance conditions.

$$\frac{M_2}{\left(1 + \frac{\gamma-1}{2} M_2^2\right)^{\frac{\gamma+1}{2(\gamma-1)}}} = \frac{A_1}{A_2} \frac{p_1^0}{p_2^0} \frac{M_1}{\left(1 + \frac{\gamma-1}{2} M_1^2\right)^{\frac{\gamma+1}{2(\gamma-1)}}}$$

$$\frac{p_2}{p_1} = \frac{p_2^0}{p_1^0} \left(\frac{1 + \frac{\gamma-1}{2} M_1^2}{1 + \frac{\gamma-1}{2} M_2^2} \right)^{\frac{\gamma}{\gamma-1}}$$

$$\frac{T_2}{T_1} = \left(\frac{1 + \frac{\gamma-1}{2} M_1^2}{1 + \frac{\gamma-1}{2} M_2^2} \right)$$

The above equations show that diffuser losses have the effect of increasing the exit Mach number for a given area ratio, and decreasing the static pressure recovery. Where the diffuser is being designed for a given exit Mach number, suitable for use in the compressor, the effect of the loss is to require use of a larger area ratio, increasing the diffuser length or increasing the rate of pressure recovery.

THE
JOURNAL
OF
THE
ROYAL
ANTHROPOLOGICAL
INSTITUTE
VOLUME
LXXV
PART I
1905

CONTENTS

THE
JOURNAL
OF
THE
ROYAL
ANTHROPOLOGICAL
INSTITUTE

1905

2. Diffuser Efficiency.

Diffuser efficiency is defined in many different ways. Some of these definitions have advantages in defining a particular aspect of diffuser performance, others may be more applicable to low velocity flows. In general, for the definition to be suitable it should fulfill certain requirements. Ref. 1 lists the following requirements for a diffuser efficiency parameter:

1. It should be readily measured.
2. Have a maximum value of unity to indicate the best possible diffuser performance, no pressure loss.
3. Remain essentially constant for the subsonic speed range (provided there are no energy losses due either to shock formation or separation resulting from changes in Reynold's number).

The third requirement mentioned above might be subjected to the criticism that we are interested not only in a device for energy conversion in subsonic flows, but also for use with supersonic flows. Also, why is it necessary that it remain constant? What interests us most in evaluating the diffuser is what is the relative energy remaining in the flow at the exit compared to the energy available in the flow ahead of the diffuser. More than one efficiency parameter may satisfy these requirements. Since no standard definition

of diffuser efficiency has been decided upon, it is best to be acquainted with the various definitions which may be encountered.

Ram recovery ratio. This has been discussed previously in connection with the improved performance of a turbojet engine with efficient pressure recovery. This parameter was chosen by the authors of Ref. 1 as best fulfilling the requirements which they set forth for a satisfactory diffuser efficiency parameter. It is defined as follows:

$$\text{Ram recovery ratio} = \frac{P_2^0 - P_0}{P_0^0 - P_0}$$

Exponential form. This form of expressing diffuser efficiency has more appeal to the thermodynamicist or mathematician. This parameter expresses the fraction of the kinetic energy increment which is converted into pressure. Ref. 2, p. 43, presents the development of this definition in the following manner.

$$\eta_D V dV = - \frac{dp}{\rho} \quad (a)$$

From the energy equation:

$$V dV = - c_p dT = \frac{-\gamma}{\gamma-1} d \left(\frac{P}{\rho} \right) \quad (b)$$

Combining eq. (a) and (b), and integrating produces:

$$\frac{p_2}{p_0} = \left(\frac{p_2}{p_0}\right)^{1 - \frac{\gamma-1}{\eta \gamma}} \quad (c)$$

$$\text{or } \left(\frac{p_2}{p_0}\right)^{\eta \frac{\gamma}{\gamma-1}} = \frac{p_2}{p_0} \quad (d)$$

Since the process is polytropic, and the pressure-temperature relationship for a polytropic process is:

$$\left(\frac{T_2}{T_0}\right)^{\frac{\eta}{\eta-1}} = \frac{p_2}{p_0} \quad (e)$$

Then,

$$\eta_D = \frac{\eta/\eta-1}{\gamma/\gamma-1} \quad (f)$$

For incompressible flow:

$$\eta_D = \frac{p_2 - p_0}{\Delta q}$$

Dynamic pressure recovery ratio. This quantity is defined in the following manner:

$$\text{Dynamic pressure recovery ratio} = \frac{p_2^0 - p_0}{q_0}$$

$$= \text{Ram recovery ratio} \times (1 + \eta)$$

$$(1 + \eta) = 1 + \frac{M^2}{4} + \frac{M^4}{40} + \frac{M^6}{160} + \dots$$

At low subsonic Mach numbers this parameter is the same as ram recovery ratio, but since it ignores the compressibility factor $(1 + \eta)$, it diverges rapidly as Mach number increases. With very high efficiency of pressure recovery it can exceed one, and so it is not desirable for measuring the efficiency of a compressible flow.

2.

10

11

12

13

14

15

16

17

18

19

20

21

22

23

24

25

26

27

28

29

30

31

32

33

34

35

36

37

38

39

40

41

42

43

44

45

46

47

48

49

50

51

52

53

54

55

56

57

58

59

60

61

62

63

64

65

66

67

68

69

70

71

72

73

74

75

76

77

78

79

80

81

82

83

84

85

86

87

88

89

90

91

92

93

94

95

96

97

98

99

100

101

102

103

104

105

106

107

108

109

110

111

112

113

114

115

116

117

118

119

120

121

122

123

124

125

126

127

128

129

130

131

132

133

134

135

136

137

138

139

140

141

142

143

144

145

146

147

148

149

150

151

152

153

154

155

156

157

158

159

160

161

162

163

164

165

166

167

168

169

170

171

172

173

174

175

176

177

178

179

180

181

182

183

184

185

186

187

188

189

190

191

192

193

194

195

196

197

198

199

200

201

202

203

204

205

206

207

208

209

210

211

212

213

214

215

216

217

218

219

220

221

222

223

224

225

226

227

228

229

230

231

232

233

234

235

236

237

238

239

240

241

242

243

244

245

246

247

248

249

250

251

252

253

254

255

256

257

258

259

260

261

262

263

264

265

266

267

268

269

270

271

272

273

274

275

276

277

278

279

280

281

282

283

284

285

286

287

288

289

290

291

292

293

294

295

296

297

298

299

300

301

302

303

304

305

306

307

308

309

310

311

312

313

314

315

316

317

318

319

320

321

322

323

324

325

326

327

328

329

330

331

332

333

334

335

336

337

338

339

340

341

342

343

344

345

346

347

348

349

350

351

352

353

354

355

356

357

358

359

360

361

362

363

364

365

366

367

368

369

370

371

372

373

374

375

376

377

378

379

380

381

382

383

384

385

386

387

388

389

390

391

392

393

394

395

396

397

398

399

400

401

402

403

404

405

406

407

408

409

410

411

412

413

414

415

416

417

418

419

420

421

422

423

424

425

426

427

428

429

430

431

432

433

434

435

436

437

438

439

440

441

442

443

444

445

446

447

448

449

450

451

452

453

454

455

456

457

458

459

460

461

462

463

464

465

466

467

468

469

470

471

472

473

474

475

476

477

478

479

480

481

482

483

484

485

486

487

488

489

490

491

492

493

494

495

496

497

498

499

500

501

502

503

504

505

506

507

508

509

510

511

512

513

514

515

516

517

518

519

520

521

522

523

524

525

526

527

528

529

530

531

532

1. $\frac{1}{2}$ 2. $\frac{1}{3}$ 3. $\frac{1}{4}$ 4. $\frac{1}{5}$ 5. $\frac{1}{6}$ 6. $\frac{1}{7}$ 7. $\frac{1}{8}$ 8. $\frac{1}{9}$ 9. $\frac{1}{10}$ 10. $\frac{1}{11}$ 11. $\frac{1}{12}$ 12. $\frac{1}{13}$ 13. $\frac{1}{14}$ 14. $\frac{1}{15}$ 15. $\frac{1}{16}$ 16. $\frac{1}{17}$ 17. $\frac{1}{18}$ 18. $\frac{1}{19}$ 19. $\frac{1}{20}$ 20. $\frac{1}{21}$ 21. $\frac{1}{22}$ 22. $\frac{1}{23}$ 23. $\frac{1}{24}$ 24. $\frac{1}{25}$ 25. $\frac{1}{26}$ 26. $\frac{1}{27}$ 27. $\frac{1}{28}$ 28. $\frac{1}{29}$ 29. $\frac{1}{30}$ 30. $\frac{1}{31}$ 31. $\frac{1}{32}$ 32. $\frac{1}{33}$ 33. $\frac{1}{34}$ 34. $\frac{1}{35}$ 35. $\frac{1}{36}$ 36. $\frac{1}{37}$ 37. $\frac{1}{38}$ 38. $\frac{1}{39}$ 39. $\frac{1}{40}$ 40. $\frac{1}{41}$ 41. $\frac{1}{42}$ 42. $\frac{1}{43}$ 43. $\frac{1}{44}$ 44. $\frac{1}{45}$ 45. $\frac{1}{46}$ 46. $\frac{1}{47}$ 47. $\frac{1}{48}$ 48. $\frac{1}{49}$ 49. $\frac{1}{50}$ 50. $\frac{1}{51}$ 51. $\frac{1}{52}$ 52. $\frac{1}{53}$ 53. $\frac{1}{54}$ 54. $\frac{1}{55}$ 55. $\frac{1}{56}$ 56. $\frac{1}{57}$ 57. $\frac{1}{58}$ 58. $\frac{1}{59}$ 59. $\frac{1}{60}$ 60. $\frac{1}{61}$ 61. $\frac{1}{62}$ 62. $\frac{1}{63}$ 63. $\frac{1}{64}$ 64. $\frac{1}{65}$ 65. $\frac{1}{66}$ 66. $\frac{1}{67}$ 67. $\frac{1}{68}$ 68. $\frac{1}{69}$ 69. $\frac{1}{70}$ 70. $\frac{1}{71}$ 71. $\frac{1}{72}$ 72. $\frac{1}{73}$ 73. $\frac{1}{74}$ 74. $\frac{1}{75}$ 75. $\frac{1}{76}$ 76. $\frac{1}{77}$ 77. $\frac{1}{78}$ 78. $\frac{1}{79}$ 79. $\frac{1}{80}$ 80. $\frac{1}{81}$ 81. $\frac{1}{82}$ 82. $\frac{1}{83}$ 83. $\frac{1}{84}$ 84. $\frac{1}{85}$ 85. $\frac{1}{86}$ 86. $\frac{1}{87}$ 87. $\frac{1}{88}$ 88. $\frac{1}{89}$ 89. $\frac{1}{90}$ 90. $\frac{1}{91}$ 91. $\frac{1}{92}$ 92. $\frac{1}{93}$ 93. $\frac{1}{94}$ 94. $\frac{1}{95}$ 95. $\frac{1}{96}$ 96. $\frac{1}{97}$ 97. $\frac{1}{98}$ 98. $\frac{1}{99}$ 99. $\frac{1}{100}$ 100. $\frac{1}{101}$ 101. $\frac{1}{102}$ 102. $\frac{1}{103}$ 103. $\frac{1}{104}$ 104. $\frac{1}{105}$ 105. $\frac{1}{106}$ 106. $\frac{1}{107}$ 107. $\frac{1}{108}$ 108. $\frac{1}{109}$ 109. $\frac{1}{110}$ 110. $\frac{1}{111}$ 111. $\frac{1}{112}$ 112. $\frac{1}{113}$ 113. $\frac{1}{114}$ 114. $\frac{1}{115}$ 115. $\frac{1}{116}$ 116. $\frac{1}{117}$ 117. $\frac{1}{118}$ 118. $\frac{1}{119}$ 119. $\frac{1}{120}$ 120. $\frac{1}{121}$ 121. $\frac{1}{122}$ 122. $\frac{1}{123}$ 123. $\frac{1}{124}$ 124. $\frac{1}{125}$ 125. $\frac{1}{126}$ 126. $\frac{1}{127}$ 127. $\frac{1}{128}$ 128. $\frac{1}{129}$ 129. $\frac{1}{130}$ 130. $\frac{1}{131}$ 131. $\frac{1}{132}$ 132. $\frac{1}{133}$ 133. $\frac{1}{134}$ 134. $\frac{1}{135}$ 135. $\frac{1}{136}$ 136. $\frac{1}{137}$ 137. $\frac{1}{138}$ 138. $\frac{1}{139}$ 139. $\frac{1}{140}$ 140. $\frac{1}{141}$ 141. $\frac{1}{142}$ 142. $\frac{1}{143}$ 143. $\frac{1}{144}$ 144. $\frac{1}{145}$ 145. $\frac{1}{146}$ 146. $\frac{1}{147}$ 147. $\frac{1}{148}$ 148. $\frac{1}{149}$ 149. $\frac{1}{150}$ 150. $\frac{1}{151}$ 151. $\frac{1}{152}$ 152. $\frac{1}{153}$ 153. $\frac{1}{154}$ 154. $\frac{1}{155}$ 155. $\frac{1}{156}$ 156. $\frac{1}{157}$ 157. $\frac{1}{158}$ 158. $\frac{1}{159}$ 159. $\frac{1}{160}$ 160. $\frac{1}{161}$ 161. $\frac{1}{162}$ 162. $\frac{1}{163}$ 163. $\frac{1}{164}$ 164. $\frac{1}{165}$ 165. $\frac{1}{166}$ 166. $\frac{1}{167}$ 167. $\frac{1}{168}$ 168. $\frac{1}{169}$ 169. $\frac{1}{170}$ 170. $\frac{1}{171}$ 171. $\frac{1}{172}$ 172. $\frac{1}{173}$ 173. $\frac{1}{174}$ 174. $\frac{1}{175}$ 175. $\frac{1}{176}$ 176. $\frac{1}{177}$ 177. $\frac{1}{178}$ 178. $\frac{1}{179}$ 179. $\frac{1}{180}$ 180. $\frac{1}{181}$ 181. $\frac{1}{182}$ 182. $\frac{1}{183}$ 183. $\frac{1}{184}$ 184. $\frac{1}{185}$ 185. $\frac{1}{186}$ 186. $\frac{1}{187}$ 187. $\frac{1}{188}$ 188. $\frac{1}{189}$ 189. $\frac{1}{190}$ 190. $\frac{1}{191}$ 191. $\frac{1}{192}$ 192. $\frac{1}{193}$ 193. $\frac{1}{194}$ 194. $\frac{1}{195}$ 195. $\frac{1}{196}$ 196. $\frac{1}{197}$ 197. $\frac{1}{198}$ 198. $\frac{1}{199}$ 199. $\frac{1}{200}$ 200. $\frac{1}{201}$ 201. $\frac{1}{202}$ 202. $\frac{1}{203}$ 203. $\frac{1}{204}$ 204. $\frac{1}{205}$ 205. $\frac{1}{206}$ 206. $\frac{1}{207}$ 207. $\frac{1}{208}$ 208. $\frac{1}{209}$ 209. $\frac{1}{210}$ 210. $\frac{1}{211}$ 211. $\frac{1}{212}$ 212. $\frac{1}{213}$ 213. $\frac{1}{214}$ 214. $\frac{1}{215}$ 215. $\frac{1}{216}$ 216. $\frac{1}{217}$ 217. $\frac{1}{218}$ 218. $\frac{1}{219}$ 219. $\frac{1}{220}$ 220. $\frac{1}{221}$ 221. $\frac{1}{222}$ 222. $\frac{1}{223}$ 223. $\frac{1}{224}$ 224. $\frac{1}{225}$ 225. $\frac{1}{226}$ 226. $\frac{1}{227}$ 227. $\frac{1}{228}$ 228. $\frac{1}{229}$ 229. $\frac{1}{230}$ 230. $\frac{1}{231}$ 231. $\frac{1}{232}$ 232. $\frac{1}{233}$ 233. $\frac{1}{234}$ 234. $\frac{1}{235}$ 235. $\frac{1}{236}$ 236. $\frac{1}{237}$ 237. $\frac{1}{238}$ 238. $\frac{1}{239}$ 239. $\frac{1}{240}$ 240.

5:4

Total pressure ratio. This parameter has direct application in turbojet performance calculations. It is the ratio of the total pressure at the diffuser outlet to the free stream total pressure. It is important because it is a direct measure of the entropy increase in the compression process. It is considerably affected by the mach number of the flow.

$$\text{Total pressure ratio} = \frac{p_2^0}{p_0^0} = e^{-\frac{\Delta S}{R}}$$

Pressure ratio. This parameter is given in most turbojet engine performance manuals and is directly applicable for the computation of net thrust, air flow, and specific fuel consumption. It is the ratio of the total pressure at the diffuser outlet to the free stream static pressure. Since it will be almost always greater than one, it is not too useful as a measure of the diffuser efficiency.

$$\text{Pressure ratio} = \frac{p_2^0}{p_0}$$

Energy ratio. This efficiency parameter is defined as the kinetic energy recovered by the air induction system, divided by the kinetic energy available in the airstream. It is derived in the following manner:

From the energy equation

$$c_p T_0 + \frac{V_0^2}{2gJ} = c_p T_2^0$$

and the pressure temperature relationship

$$\frac{T_0}{T_0^0} = \left(\frac{p_0}{p_0^0} \right)^{\frac{\gamma-1}{\gamma}}$$

the following expression for the kinetic energy available is obtained,

$$\frac{V_0^2}{2gJ} = c_p \left[T_0^0 - T_0 \left(\frac{p_0}{p_0^0} \right)^{\frac{\gamma-1}{\gamma}} \right]$$

As the exit from the diffuser the total pressure is p_2^0 and the total temperature is T_2^0 . If these quantities are reconverted to free stream conditions where the free stream static pressure is p_0 , and the air velocity V_0' is less than V_0 because of the pressure losses involved, then

$$\frac{(V_0')^2}{2gJ} = c_p \left[T_2^0 - T_2 \left(\frac{p_0}{p_2^0} \right)^{\frac{\gamma-1}{\gamma}} \right]$$

The above equation represents the kinetic energy which was recovered from the airstream. Since the process is adiabatic, T_0^0 equals T_2^0 , and the energy ratio equation can be written:

$$\text{Energy ratio} = \frac{T_2^0 - T_2 \left(\frac{p_0}{p_2^0} \right)^{\frac{\gamma-1}{\gamma}}}{T_0^0 - T_0 \left(\frac{p_0}{p_0^0} \right)^{\frac{\gamma-1}{\gamma}}}$$

or

$$\text{Energy ratio} = 1 - \frac{2}{(\gamma-1) p_0^0} \left[\left(\frac{p_0^0}{p_2^0} \right)^{\frac{\gamma-1}{\gamma}} - 1 \right]$$

Y = 100

[100]

[100]

Y = 100

[100]

Power Ratio. This definition of diffuser efficiency is used in Ref. 3, and is the ratio of the power transformed to pressure energy to the power supplied for transformation.

Power supplied for transformation =

$$\int_{A_1} \frac{1}{2} \rho w^2 u dA - \int_{A_2} \frac{1}{2} \rho w^2 u dA$$

u - axial flow velocity.

w - air stream velocity.

$$\text{Power transformed} = \int_{A_2} p u dA - \int_{A_1} p u dA$$

If the airflow is axial only, and the flow is one-dimensional, then

$$\text{Power ratio} = \frac{P_2 u_2 A_2 - P_1 u_1 A_1}{\frac{1}{2} \rho u_1^3 A_1 - \frac{1}{2} \rho u_2^3 A_2}$$

For incompressible flow, $u_1 A_1 = u_2 A_2$, and the power ratio can be written,

$$\text{Power ratio} = \frac{P_2 - P_1}{\frac{1}{2} \rho u_1^2 \left(1 - \frac{P_2 u_2^2}{P_1 u_1^2}\right)} = \frac{P_2 - P_1}{\rho_1 \left(1 - \left(\frac{A_1}{A_2}\right)^2\right)}$$

Since this definition of diffuser efficiency is based upon the assumption of incompressible flow, it is of little value for the types of flow which will be considered.

Diffuser efficiency based on static pressure rise.

This definition of diffuser efficiency is the ratio of

1. *Chlorophyll a* and *Chlorophyll b* were determined by the method of Lichtenthal and Whistler (1973). The total chlorophyll content was determined by the method of Arar and Cook (1977). The carotenoid content was determined by the method of Lichtenthal and Whistler (1973). The total carotenoid content was determined by the method of Arar and Cook (1977). The total protein content was determined by the method of Lowry et al. (1951). The total lipid content was determined by the method of Bligh and Dyer (1959). The total carbohydrate content was determined by the method of Dubois and Gilles (1950). The total nucleic acid content was determined by the method of Burton (1956). The total ash content was determined by the method of AOAC (1970). The total water-soluble carbohydrate content was determined by the method of Dubois and Gilles (1950). The total water-soluble protein content was determined by the method of Lowry et al. (1951). The total water-soluble lipid content was determined by the method of Bligh and Dyer (1959). The total water-soluble nucleic acid content was determined by the method of Burton (1956). The total water-soluble ash content was determined by the method of AOAC (1970).

Figure 1 consists of two line graphs. The left graph shows a positive relationship between the number of fish in a school (x-axis) and the probability of a predator attack (y-axis). The curve starts at the origin and increases at an increasing rate. The right graph shows a negative relationship between the number of fish in a school (x-axis) and the probability of a predator attack (y-axis). The curve starts at a high probability for small schools and decreases as the number of fish increases, approaching the x-axis.

1. *Chlorophyll a* (Chl a) and *Chlorophyll b* (Chl b) are the primary photosynthetic pigments in green plants. They are responsible for capturing light energy and converting it into chemical energy through the process of photosynthesis. Chl a is the most abundant pigment, while Chl b is present in smaller amounts. Both pigments absorb light most efficiently in the blue and red regions of the visible spectrum.

9

the static pressure rise obtained to the sum of the static pressure rise obtained plus the total pressure loss in the diffuser.

$$\eta_D = \frac{P_2 - P_0}{(P_2 - P_0) - (P_0^0 - P_2^0)}$$

This definition of diffuser efficiency is not unlike ram recovery ratio, which may be written in the following manner:

$$\text{ram recovery ratio} = \frac{(P_2^0 - P_0) - (P_0^0 - P_2^0)}{P_2^0 - P_0}$$

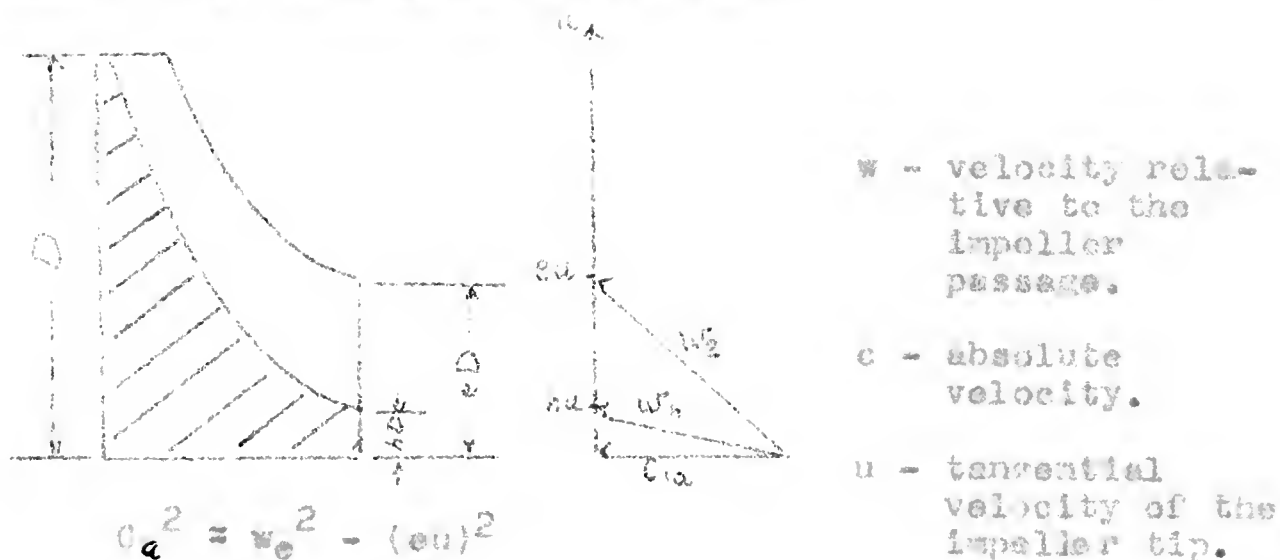
Ram recovery ratio when written in this manner is the ratio of the maximum possible pressure rise less the total pressure loss in the diffuser to the maximum possible pressure rise. The simplicity of ram recovery ratio would make it preferable to the diffuser efficiency, based on static pressure rise if the selection of a definition were a matter of choice.

3. Diffuser Discharge Limitations.

The main air intake duct of a turbojet engine is designed as a diffuser because at present flight velocities the velocity of the incoming air must be reduced before the air is introduced into the compressor. The desired velocity of the air at the diffuser exit depends upon the compressor design. Present types of compressors operate with subsonic velocities because their capacity and efficiency would fall if supersonic relative

velocities are attained and shock waves develop within the compressor. Compressors which take advantage of this phenomenon are in the process of development, but are not yet in actual use. Since we are concerned primarily with present designs, and since information on supersonic compressors is restricted, nothing further will be said about them.

From ref. 4, the entrance velocity diagram for a centrifugal compressor is as shown.



According to ref. 4, Ma_e , the Mach number corresponding to w_e , should not exceed 0.75 approximately, and eu should not exceed 0.650. If we assume these maximum values, and assume the impeller tip velocity to be sonic, the Mach number corresponding to the axial velocity is 0.371. This seems to be a fairly high value, and certainly it should be much lower than that if a double faced impeller is used. With the double faced impeller the airflow must turn through 180 degrees to enter the rear side, and the head loss resulting from this reversal would be high with such a large flow velocity.

4. External Drag Considerations.

The design of an efficient diffuser entails a two-fold consideration. First, the design must be such that the pressure recovery within the diffuser must be accomplished with a minimum loss; second, the flow over the outside surfaces in the vicinity of the diffuser inlet must not be disturbed to such an extent that the drag is increased. It is due to this latter consideration that a lower limit on velocity ratio is imposed.

In subsonic flows the total drag of a body shape can be considered to be composed of two components, skin friction drag and wake drag. The two components are inter-related and have their counterparts in the internal diffuser flow. In the consideration of drag we are more concerned with the resistance of the air to the motion of the body through it; with internal flow we are more concerned with the pressure loss in the flow.

A body in a subsonic, non-viscous, ideal flow has zero drag forces acting on it. The flow comes to a stagnation point on the leading edge of the body with the kinetic energy of the flow being transformed into pressure. As the flow continues around the body it is accelerated up to the widest dimension with the pressure decreasing as the velocity increases. Beyond the widest dimension the flow decelerates to a rear stagnation point. A summation of the pressure forces in the direction of flow is zero.

The real flow of a subsonic, viscous fluid tries to follow the pattern of the ideal flow, but viscosity causes some deviations. Due to viscous forces a boundary layer is formed, a thin layer of fluid at the surface of the body where a strong velocity gradient normal to the body surface exists. This velocity gradient is the result of viscous interaction, friction, between the body and the fluid. Friction tends to impede the progress of the body through the fluid. The drag due to friction is usually rather small, but with streamline bodies it may be the most significant component of the total drag.

The second component of drag is the one which causes most concern. As the flow progresses around the body the boundary layer grows. In the positive pressure gradient at the rear of the body the boundary layer is unstable and the flow tends to separate from surface. When the flow separates there is a pressure loss. The summation of the pressure forces about the body is no longer zero and a drag due to the unbalanced pressure forces results. Pressure drag increases with forward movement of the separation point. With poorly designed shapes the pressure or wake drag can amount to several times the skin friction drag. This is comparable with the separation loss which may occur in the internal flow through the diffuser. At low velocity ratios separation of the flow over the outside surface of

the diffuser is more likely to occur with attendant high drag losses.

Further complications are introduced with supersonic flows, and subsonic flows near the sonic velocity. For a body in a supersonic flow, a drag force exists even in a perfect fluid. The drag with which we are concerned, however, is not this form drag, but the added drag resulting from the appearance of a shock wave on the surface of the body.

The critical Mach number of a body is defined as that Mach number at which a Mach number of one appears in the flow around the body. When the flow is at a Mach number greater than the critical, there is always the possibility of a shock wave existing on the body. Since a shock wave causes an abrupt change in the flow with a high degree of turbulence in the vicinity of the shock, the results of this disturbance are transmitted to the boundary layer. The boundary layer is thickened and the added turbulence increases the likelihood of early flow separation and wake drag.

When evaluating diffuser performance the effects of drag increase due to a particular configuration must be balanced against the gain in engine performance resulting from the improved internal flow. This is probably an important factor in the choice of the flush type air inlet for some present high speed airplane designs.

CHAPTER III

DIFFUSER LOSSES

We have seen that the purpose of a diffuser is to reduce the velocity of the incoming air to a level suitable for use in the engine compressor, and, further, to recover as much as possible of the kinetic energy of the airstream and convert it into pressure energy. It was shown that when the ram recovery ratio was high the performance of the jet engine increased. Let us now investigate some of the factors which decrease the diffuser efficiency. If we appreciate what things affect diffuser performance, we can incorporate into our diffuser design features which minimize these effects.

The principal types of losses encountered in diffuser flow are:

1. Shock loss.
2. Entrance loss.
3. Yawing effect.
4. Expansion loss.
5. Friction loss.
6. Turning loss.
7. Obstructions in the flow.
8. Leakage loss.
9. Exit loss.

Some of these losses can be approximated by simple analysis while others are so complex and dependent upon the conditions of a particular installation that only general rules for evaluating their magnitude can be given. The losses listed above are discussed in the following paragraphs.

1. The first part of the document discusses the importance of maintaining accurate records of all transactions and activities. It emphasizes that proper record-keeping is essential for transparency and accountability, particularly in financial matters. The text suggests that organizations should implement robust systems to track and document every aspect of their operations.

2. The second part of the document addresses the challenges associated with data management and security. It highlights the need for strong cybersecurity measures to protect sensitive information from unauthorized access and breaches. The author argues that investing in advanced security technologies and training personnel is crucial for ensuring the integrity and confidentiality of data.

3. The third part of the document focuses on the role of technology in improving operational efficiency. It explores various digital tools and platforms that can streamline processes, reduce errors, and enhance communication within an organization. The text encourages the adoption of innovative solutions to stay competitive in a rapidly changing market.

4. The fourth part of the document discusses the importance of continuous learning and development for the workforce. It suggests that organizations should provide regular training and professional development opportunities to their employees. This not only helps in keeping the workforce up-to-date with the latest industry trends but also fosters a culture of innovation and growth.

5. The fifth part of the document concludes by summarizing the key points discussed and reiterating the importance of a holistic approach to organizational management. It stresses that success is achieved through a combination of effective record-keeping, robust security measures, efficient use of technology, and a commitment to employee development.

1. Shock Loss.

The shock loss is a problem which is peculiar to supersonic speeds. A shock wave is a region across which sudden and finite changes in pressure, density and velocity of the flow occur. It is a non-isentropic compression. The pressure and density increase while the velocity decreases. Since the shock wave is accompanied by an entropy increase, there is a decrease in total pressure. This loss increases with increase of flow Mach number before the shock wave. The width of the shock wave in the direction of flow is very small. Shock waves may be classified into two categories, normal and oblique. These descriptions specify the orientation of the wave with respect to the flow direction. The normal shock is characterized by a jump from supersonic to subsonic velocity; the oblique shock, on the other hand, may cause a velocity jump from supersonic to a lesser supersonic, or subsonic velocity. The velocity jump from supersonic to a lesser supersonic velocity is more likely. The total head loss across a normal shock wave is greater than that across an oblique shock wave.

The relationships across either type of shock wave are given by the following equations.

β - angle between the direction of flow and the shock wave, 90° for a normal shock.

Subscripts:

x - condition before a shock.

y - condition after the shock.

$$M_y^2 = \frac{1 + \frac{\gamma-1}{2} M_x^2}{\gamma M_x^2 \sin^2 \beta - \frac{\gamma-1}{2}} - \frac{M_x^2 \cos^2 \beta}{1 + \frac{\gamma-1}{2} M_x^2 \sin^2 \beta}$$

$$\frac{P_0^y}{P_0^x} = \left[\frac{2\gamma}{\gamma+1} M_x^2 \sin^2 \beta - \frac{\gamma-1}{\gamma+1} \right]^{\frac{1}{\gamma-1}} \\ \times \left[\frac{(\gamma-1) M_x^2 \sin^2 \beta + 2}{(\gamma+1) M_x^2 \sin^2 \beta} \right]^{\frac{\gamma}{\gamma-1}}$$

$$\frac{P_y}{P_x} = \frac{2\gamma}{\gamma+1} M_x^2 \sin^2 \beta - \frac{\gamma-1}{\gamma+1}$$

Further information on shock waves can be found in ref. 2, and the relationships across the shock wave can be found in ref. 5.

Shockless compression from supersonic speed to subsonic speed is theoretically possible. The diffuser shape for such a flow would be that of a reversed Laval nozzle designed for one particular inlet mach number. With such shockless compression occurring, the mach number at the diffuser throat is one, and the mass flow is a maximum. Now, consider a slight variation in the mach number of the incoming flow. If it is less than the design mach number, the mass flow will be less than maximum, the throat mach number will have to be less than one, but isentropic compression from supersonic to subsonic flow demands sonic velocity at the diffuser throat. The flow becomes unstable and a detached shock

forms ahead of the diffuser entrance. Flow through the diffuser becomes wholly subsonic. On the other hand, if the entrance mach number is greater than the design value, the value of the throat mach number will never get as low as one. Supersonic flow will start into the diverging part of the diffuser and transition to subsonic flow can only occur through a shock wave in the diverging part of the diffuser.

We have considered what happens when variations in flow occur with a reversed Laval nozzle flowing full. Actually, we should consider what happens when we have subsonic flow through such a diffuser, and the entrance mach number is increased to supersonic values. At entrance mach numbers below the design value a detached shock occurs ahead of the diffuser because a mach number of one tries to occur in the converging part of the diffuser, an unstable flow condition. At some flow mach number, the contraction ratio of the converging part of the diffuser is such that a mach number of one occurs in the diffuser throat. This contraction ratio can be determined from the following relationship:

Contraction ratio for sonic velocity at diffuser

throat = area ratio for isentropic deceleration
of flow to sonic velocity at the throat

$$= p_2^0 / p_1^0$$

At this point the diffuser is able to swallow the detached shock, supersonic flow starts into the diffuser,

and the shock forms in the diverging part of the diffuser, its location dependent upon the pressure ratios across the diffuser. We can see, therefore, that shockless diffusion is impossible, but we can move the detached shock into the diverging part of the diffuser.

In Ref. 6 the theoretical maximum efficiency attainable with the type of diffuser described above is given, as well as the results of actual experiments. This data is shown in Fig. 4. Actually, with an adjustable throat one hundred per cent efficiency is theoretically possible. If, after supersonic flow has started through the diffuser throat, the throat area is reduced, then the throat Mach number becomes one. By adjusting the pressure ratio across the diffuser the position of the shock wave can be moved into the throat of the diffuser, and there is no loss when the Mach number at the throat is one. Such a procedure presupposes that conditions across the diffuser can be closely controlled. In the evaluation of the theoretical maximum efficiencies of Fig. 4, the shock had been located in the diffuser throat by adjusting the pressure ratios across the diffuser. However, the pressure ratio across the diffuser depends upon the ambient pressure, in this case, and the volume flow through the compressor, a function of compressor speed. It is not advisable to vary the compressor speed over too wide a range, because the efficiency of the engine will decrease. Also, the

mechanical difficulties of an adjustable throat would not be offset by the improved diffuser performance which would result. A third objection to this diffuser design is that for flight mach numbers greater than that for which the diffuser was designed, the volume flow through the diffuser increases with the mach number. To accommodate this flow the compressor speed would have to increase which would affect the overall engine performance.

As the free stream mach number increases, the losses occurring through a detached shock wave increase very rapidly, as can be seen in Fig. 5. Ref. 7 presents an analytical study of one method of reducing these shock losses. Since the losses through an oblique shock are less than those through a normal shock, it was proposed to reduce the initial mach number of the flow through a series of oblique shocks, and finally through a normal shock wave. The results of this analysis, shown in Fig. 6, would seem to indicate that pressure recovery would be considerably improved over that possible with one normal shock, particularly at high mach numbers.

From the foregoing discussion it would appear that shock free compression from supersonic to subsonic velocities is unlikely. Some shock system will occur, either normal or oblique, and located either within or external to the diffuser. Even though the shock

may be external to the diffuser proper it is only right that the losses incurred across the shock be attributed to the diffuser. In all our discussion of diffuser flow we have referred to free stream conditions of flow with the subscript "o"; with a shock located ahead of the diffuser entrance, this condition will be that on the downstream side of the shock.

The detached shock ahead of a diffuser entrance is of a complicated structure. In the region of the stream tube which ultimately enters the diffuser entrance, it is essentially a normal shock, or at least the assumption of a normal shock will give a reasonable approximation of the conditions downstream of the shock. Proceeding outward, normal to the direction of flow, the shock progresses through the whole family of strong and weak oblique shocks, and finally degenerates into a mach line. This complicates the flow pattern around the outside of the diffuser because of the resulting velocity gradient normal to the direction of flow. Also, the location of the shock wave ahead of the diffuser is difficult to determine, except when the mach number immediately downstream of the shock wave corresponds to the entrance mach number of the diffuser as determined by the volume flow and diffuser geometry. In this latter case, the shock wave will probably attach itself to the entrance lip of the diffuser.

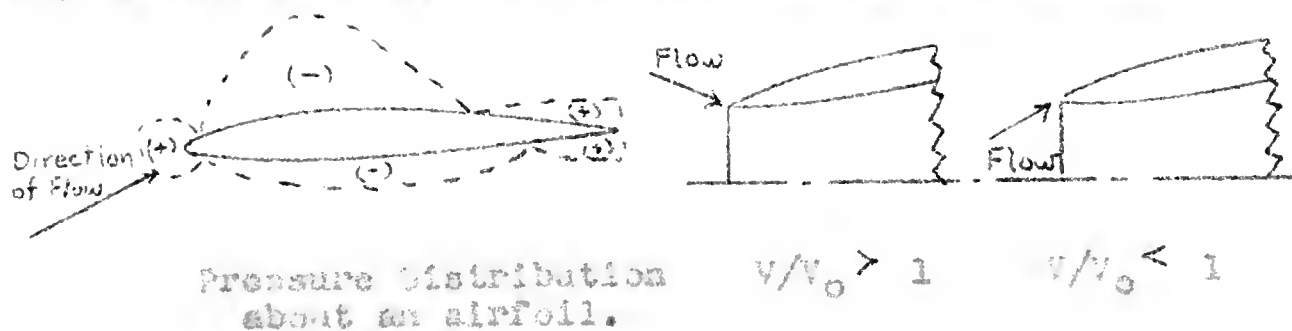
In some respects the detached shock wave is advantageous. It will accommodate a wider range of flow conditions through the diffuser. At relatively low supersonic Mach numbers the loss occurring through the shock wave is not excessive, and additional compression of the flow can be made before the flow enters the diffuser. Further, the flow turbulence occasioned by the shock can be wholly or partially damped out before the flow enters the diffuser. That this turbulence caused by the shock wave is of some importance can be seen from Fig. 7, which shows the loss in pressure recovery occasioned by increasing the exit cone angle of the diffuser from 3 degrees to 5 degrees. For a diffuser without shock the optimum exit cone angle of the diffuser is about 3 degrees. This indicates that the pressure recovery within the diffuser must be more gradual because of this shock induced turbulence. Although the internal flow within a diffuser benefits from a detached shock wave, the effect of the external flow on the drag of the engine nacelle may be seriously increased. This particular problem merits experimental investigation.

2. Entrance Loss.

The importance of the entrance conditions of a diffuser is not due to any particular loss occurring in the diffuser itself, but the effect of the entrance

conditions on other diffuser losses. For example, one turbojet engine manufacturer specifies that the engine performance is not guaranteed unless the airflow variation across the compressor inlet is less than five per cent. The plane using this engine achieves this result by having constant velocity head at the diffuser entrance. Obtaining uniform flow conditions at the diffuser entrance may be complicated by some entrance duct locations.

If we can conceive the idea that the lip of the diffuser entrance is an airfoil shape, we can picture what happens as the airflow approaches and passes it. Assume that the external surface of the diffuser is the top of the airfoil, and the internal surface is the



bottom. With a velocity ratio (V/V_0) greater than one the diffuser airfoil shape is at a negative angle of attack, a negative pressure area due to this flow forms inside the diffuser. The lowest pressure will occur at the throat of the diffuser. The flow in the diverging part of the diffuser is progressing against a positive pressure gradient due to the diffuser design. This increased negative pressure at the diffuser throat increases the pressure gradient and makes separation of the internal flow more likely.

1891-1892

1892-1893

1893-1894

1894-1895

1895-1896

1896-1897

1897-1898

1898-1899

1899-1900

1900-1901

1901-1902

1902-1903

1903-1904

1904-1905

1905-1906

1906-1907

1907-1908

1908-1909

1909-1910

1910-1911

1911-1912

1912-1913

1913-1914

1914-1915

1915-1916

1916-1917

1917-1918

1918-1919

1919-1920

1920-1921

With a velocity ratio less than one the diffuser lip is at a positive angle of attack. The increased negative pressure area occurs external to the diffuser. Some limiting velocity ratio will be attained where the entrance lip stalls, and the flow separates from the outside surface of the diffuser with external drag increasing accordingly.

If a sharp leading edge had been selected for the diffuser lip, the effects described above would have been aggravated, considering subsonic flow at the diffuser entrance. A sharp nosed airfoil stalls at lower angles of attack than those with rounded leading edges due to the difficulty of the flow around such a corner. With supersonic flow into the diffuser a sharp edged profile might prove beneficial because supersonic flow can change direction sharply in following contours. Where the normal shock is located at the diffuser entrance, and there is subsonic flow in the diffuser and supersonic flow outside, a sharp leading edge would be preferable because it would have less effect on the external flow, and no effect on the internal flow because the velocity ratio in this case is one. However, at conditions other than that at which the shock sits on the nose of the diffuser, the sharp leading edge would be detrimental.

In the entrance of a diffuser with a rounded leading edge, there is a region where the flow will be

expanding. A point of minimum diffuser cross-sectional area will occur. This region of contraction has its advantages and disadvantages. It provides a region of favorable pressure gradient where stream turbulence, such as that following a shock wave, may be damped out. On the other hand, the flow is accelerating in this region and more compression is required in the diverging part of the diffuser. At entry mach numbers near one it does not require much of a change in area ratio to cause considerable change in flow mach number. Some reasonable compromise must be effected.

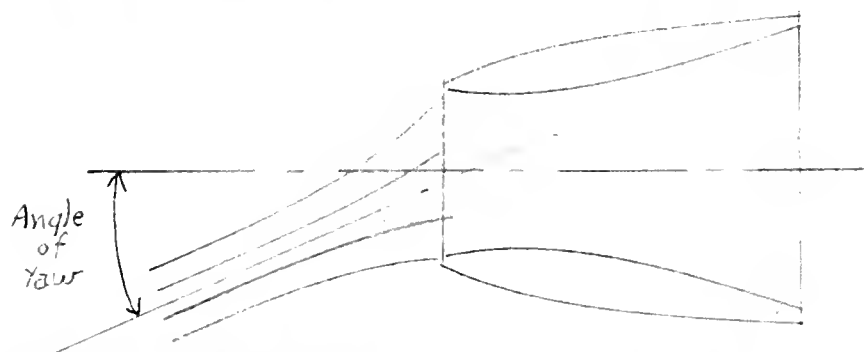
Because the flow at the entrance to the diffuser is not parallel to the diffuser axis, some question may arise as to what is the effective entrance area of the diffuser. The stagnation point of the flow, from which the boundary layer starts, will tend to move into the diffuser as velocity ratio decreases below one. It will move to the outside of the diffuser for velocity ratios increasing above one. This will affect the contraction ratio to the diffuser throat which may reach measurable magnitude with high subsonic entrance mach numbers.

Realizing the effect of the diffuser entrance on the internal flow through the diffuser, it should be carefully designed to cause the least disturbance possible. In this case the only loss in the diffuser entrance will be the friction loss which should be very

small. If the diffuser entrance is poorly designed the internal losses in the diffuser will be increased. Although this additional loss is directly attributable to the diffuser entrance it is difficult to assess the extent of the loss so occasioned.

3. Yawing Effect.

Closely allied with entrance loss is the loss occasioned when the axis of the diffuser is not parallel to the axis of the initial airflow. Under such



circumstances the flow at the diffuser inlet will be complex. Such a condition could occur with yawing or pitching motion of an aircraft, or when landing and a high angle of attack results. Some aircraft designers allow for this last case by extending the upper lip of the air entrance duct. A good example of this configuration is the air entrance duct of the F-86.

In the plane containing the duct axis and the maximum yawing angle, this effect is greatest. The duct lip will have a higher angle of attack than normally on one side, and a lower angle of attack on the other side. Since the volume of airflow through the duct is a

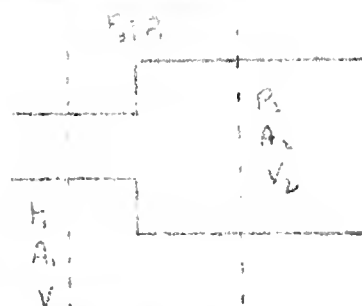
function of the engine speed, the average air velocity across the face of the duct, parallel to the duct axis will be unaffected by this condition. The velocity distribution across the face of the duct will not be uniform, however. The lip in the direction of the flow will have a lower pressure internally than the lip away from the direction of flow. A higher velocity will accompany the lower pressure to satisfy the flow equilibrium. This will be the maximum velocity across the face of the duct. Diametrically opposite a minimum velocity will occur. In other radial planes around the duct entrance the flow will vary from a maximum at one lip to a minimum at the other, except that there will be a lesser degree of difference. In a bend in a duct, which is not unlike the situation in this case, it has been found that a secondary flow in a plane normal to the main flow axis sometimes occurred. This could also take place in this instance. The net result of the yawing effect is a disturbed entrance flow into the diffuser which may result in sufficient turbulence to cause a loss in pressure potential, and will result in decreased diffuser performance. Since the resulting flow will vary in all three dimensions, and vorticity will be introduced, it will be difficult to analyze.

4. Expansion Loss.

It has been recognized that diffuser flow is unstable by its very nature. In the diverging part of a

diffuser the flow is advancing against a positive pressure gradient, and it has been found that if this gradient is too severe the flow will separate from the diffuser wall. The result of this separation is a sudden expansion from the point of separation to the end of the diffuser. The loss caused by a sudden expansion is calculated in Ser. 3.

The loss due to a sudden expansion yields to analysis in the following manner:



From Bernoulli's equation:

$$\frac{p_1}{\rho} + \frac{V_1^2}{2g} = \frac{p_2}{\rho} + \frac{V_2^2}{2g} + h_f \quad (a)$$

h_f - head loss due to sudden enlargement.

$$h_f = \frac{V_1^2 - V_2^2}{2g} - \frac{(p_2 - p_1)}{\rho} \quad (b)$$

Now, the momentum principle states that the resulting force acting on a body equals the change of momentum of the body per second.

$$\text{Rate of change of momentum} = \frac{\rho A_2 V_2}{\gamma} (V_1 - V_2)$$

$$\text{Force acting} = (p_2 - p_1) A_2$$

$$(p_2 - p_1) A_2 = \frac{\rho A_2 V_2}{\gamma} (V_1 - V_2) \quad (c)$$

$$\frac{p_2 - p_1}{\rho} = \frac{V_2}{g} (V_1 - V_2) \quad (d)$$

Substituting in eq. (b) yields:

$$h_f = \frac{(V_1 - V_2)^2}{2g}$$

In our case V_1 will be the velocity at the point of separation, and V_2 , the velocity with which the flow re-establishes itself. It is evident that the loss will be least if the point of flow separation is near the exit of the diffuser, increasing as the point of separation moves toward the throat. An incompressible flow analysis was made in this instance, and is acceptable because it is hoped that the flow will be slowed to the point where it can be considered incompressible before separation occurs. If such is not the case the diffuser is much too inefficient.

The next points to be considered are the cause of flow separation, how the point of flow separation can be determined, and what experimental results have been obtained. The cause of flow separation is linked with the growth of the boundary layer, and some characteristics of the boundary layer must be reviewed first.

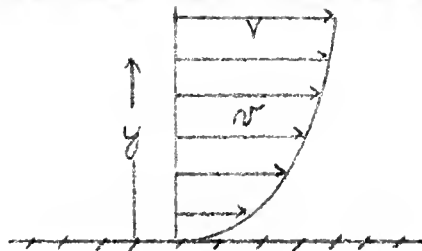
A. Boundary layer in a diffuser.

The boundary layer is a region in a fluid flow adjacent to a solid surface where strong velocity gradients normal to the surface exist. It is caused

100

1980

by friction, the viscous reaction of a fluid at the solid surface. At the point of contact of the fluid with the surface the velocity of the flow is zero, increasing normal to the surface until it reaches the free stream velocity. A typical velocity pattern would be:

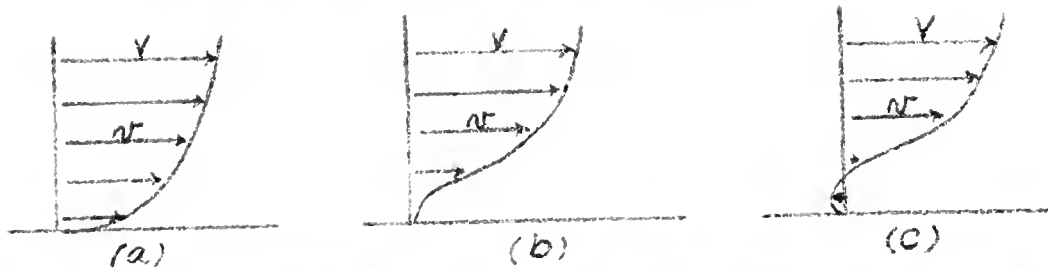


V - free stream velocity.

v - Velocity at any point in the boundary layer.

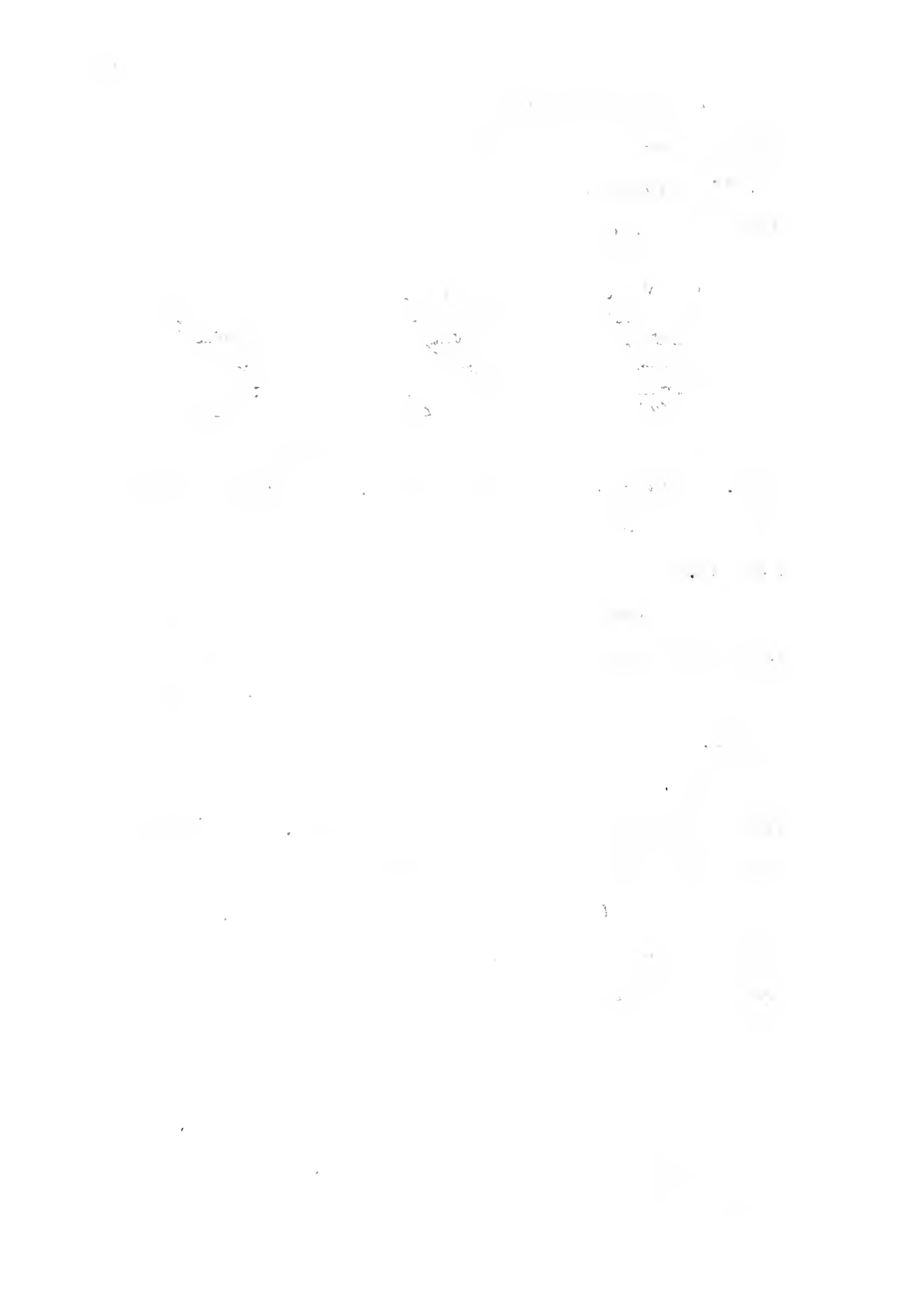
Generally, boundary layers may be classified into two types, the laminar and the turbulent boundary layers. The velocity distribution in these two types is quite different. In the laminar boundary layer there is no flow of the fluid particles normal to the main axis of the flow. In the turbulent boundary layer small velocity variations normal to the main flow do exist. Both types of boundary layer increase in thickness in the direction of flow, but at different rates. Boundary layer growth is a function not only of the axial distance in the direction of flow, but also of the pressure gradient which may exist in the flow. A boundary layer which is initially laminar may go through a transition point where laminar flow can no longer be maintained. The flow may even separate from the surface and re-establish itself downstream as a turbulent boundary layer.

As the turbulent boundary layer grows it loses some of the kinetic energy initially present due to friction losses. The development of the turbulent boundary layer can be visualized thus:



In state (c) a reversal of flow has started next to the wall. This condition is unstable. A vortex will develop and the flow will ultimately separate from the surface.

The development of the boundary layer in a diffuser is probably somewhat like the following pattern. At the entrance lip of the diffuser a stagnation point occurs. At this point the boundary layer has zero thickness. From this point to the throat of the diffuser a negative pressure gradient exists. A negative pressure gradient has a stabilizing effect on the boundary layer so it grows in the laminar fashion. In the diverging part of the diffuser a positive pressure gradient exists. A positive pressure gradient has a destabilizing effect on the boundary layer. The laminar boundary layer will persist for a short distance into this unfavorable pressure gradient, then transition to a turbulent boundary layer will occur. The turbulent boundary layer will continue to grow until a point



or the end of the diffuser if separation does not occur.

There is a considerable fund of information on both laminar and turbulent boundary layer growth, transition, and separation. Ref. 9 reviews the field and contains several pages of further references for those interested in pursuing the subject further. Most of the work done in boundary layer research is confined to two dimensional cases. The flow in a diffuser, or any duct for that matter, is further complicated by three dimensional effects. The flow outside the boundary layer in a duct is not uniform. It, too, may be either laminar or turbulent. Further complications in a duct of varying cross-section, like a diffuser, are added by the fact that the pressure recovery across any cross-section is not uniform.

For purposes of analysis some assumptions, however erroneous, are necessary. In this particular case it will be assumed that the main flow in the duct is one dimensional, and that the boundary layer behaves as it would in a simple two dimensional flow. This will probably be not too far from the truth if the boundary layer thickness remains small in comparison with the duct diameter.

B. Point of Laminar Separation.

Ref. 10 gives the following method of determining the point of separation of the laminar boundary layer.

CONTENTS

Original Articles—The Effect of the Diet on the Blood Pressure in Normal and Hypertensive Subjects

—The Effect of the Diet on the Blood Pressure in Normal and Hypertensive Subjects

—The Effect of the Diet on the Blood Pressure in Normal and Hypertensive Subjects

—The Effect of the Diet on the Blood Pressure in Normal and Hypertensive Subjects

—The Effect of the Diet on the Blood Pressure in Normal and Hypertensive Subjects

—The Effect of the Diet on the Blood Pressure in Normal and Hypertensive Subjects

—The Effect of the Diet on the Blood Pressure in Normal and Hypertensive Subjects

—The Effect of the Diet on the Blood Pressure in Normal and Hypertensive Subjects

—The Effect of the Diet on the Blood Pressure in Normal and Hypertensive Subjects

—The Effect of the Diet on the Blood Pressure in Normal and Hypertensive Subjects

—The Effect of the Diet on the Blood Pressure in Normal and Hypertensive Subjects

—The Effect of the Diet on the Blood Pressure in Normal and Hypertensive Subjects

—The Effect of the Diet on the Blood Pressure in Normal and Hypertensive Subjects

—The Effect of the Diet on the Blood Pressure in Normal and Hypertensive Subjects

—The Effect of the Diet on the Blood Pressure in Normal and Hypertensive Subjects

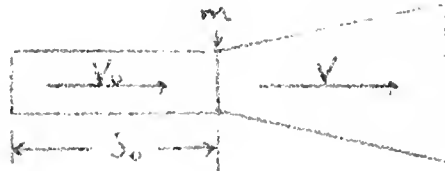
—The Effect of the Diet on the Blood Pressure in Normal and Hypertensive Subjects

—The Effect of the Diet on the Blood Pressure in Normal and Hypertensive Subjects

—The Effect of the Diet on the Blood Pressure in Normal and Hypertensive Subjects

—The Effect of the Diet on the Blood Pressure in Normal and Hypertensive Subjects

—The Effect of the Diet on the Blood Pressure in Normal and Hypertensive Subjects



$$\text{Velocity gradient} = F = \frac{s_0}{V_0} \frac{dV}{ds} = \frac{-s_0}{2(1+fm)} \frac{dV}{ds}$$

s_0 = equivalent flat plate length from the entrance of the duct to the point at which the adverse pressure gradient is applied
 $= s_1 + s_2$

$$s_1 = 0.376 s_m \left(\frac{\Delta p}{q_m} \right)^{-0.164}$$

s_2 = the distance from s_m to the point at which an adverse gradient is applied.

s_m = point of minimum pressure.

$$F = \text{pressure coefficient} = \frac{(p - p_\infty)}{q}$$

p = static pressure at any point.

p_∞ = free stream static pressure.

q_m = dynamic pressure at s_m .

$\frac{dp}{ds}$ = slope of line approximating the pressure distribution back of the point of minimum pressure.

$$\Delta p = \frac{(p_{s_m} - p_{s_e})}{2}$$

The permissible velocity decrement with a given velocity gradient is shown in Fig. 5.

5

C. Mixing Length.

After the separation of the laminar boundary layer there exists a transition region in which the flow in the boundary layer is neither laminar nor turbulent. According to Ref. 11 the extent of this region has been experimentally determined to be:

$$\frac{x}{c} = \frac{70,000}{c} \frac{\nu}{V_\infty}$$

x = the extent of the transition region, the distance from the point of laminar separation to the point at which a fully developed turbulent profile is observed.

V_∞ = velocity outside the boundary layer at the laminar separation point.

ν = Kinematic viscosity at the point of laminar separation

c = a characteristic length, in this case, the length of the diffuser.

D. Point of Separation of the Turbulent Boundary Layer.

A method of determining the point of separation of the turbulent boundary layer is given in Ref. 12. It was found that the variables controlling the development of the turbulent boundary layer were (1) the ratio of the non-dimensional pressure gradient, expressed in terms of the local dynamic pressure outside the boundary layer and boundary layer thickness, to the local skin friction coefficient,

is devoted to

the study of the properties of the

operator T defined by

$Tf(x) = \int_0^x f(t) dt$ for $f \in L^1$.

It is shown that T is a bounded operator

$$\|Tf\|_1 \leq \|f\|_1$$

and that T is

self-adjoint.

The second part of the

paper

is devoted to the study of the

operator S defined by

$$Sf(x) = \int_0^x f(t) dt$$

for $f \in L^1$. It is shown that S is a

bounded operator

and that S is

self-adjoint. The third part of the

paper is devoted to the study of the

operator R defined by

$$Rf(x) = \int_0^x f(t) dt$$

and (2) the shape of the boundary layer. An empirical equation was developed in terms of these variables which, when used with the momentum equation and the skin friction relation, makes it possible to trace the development of the turbulent boundary layer to the separation point.

At this point it is well to review some definitions which will be used subsequently. Boundary layer thickness, δ , is the distance normal to a solid boundary in a fluid flow in which a velocity gradient exists. For a laminar boundary layer, Ref. 13 gives the equation for this thickness.

$$\delta = 5.48 \sqrt{\frac{\nu x_0}{V}}$$

Other references give essentially the same equation with some variations in the numerical factor.

The velocity distribution in the laminar boundary layer, according to Ref. 14 is:

$$\frac{v}{V} = 2\left(\frac{y}{\delta}\right) - 2\left(\frac{y}{\delta}\right)^3 + \left(\frac{y}{\delta}\right)^4 \quad (\text{Prandtl-Blassius Equation})$$

This equation for velocity distribution is satisfactory if the stream turbulence is low and the Reynolds number is less than 500,000.

The actual boundary layer thickness is difficult to determine, however, and other characteristic parameters are used. One of these is the displacement thickness which is defined as the amount the external flow is

displaced outward by the boundary layer. It may be written

$$\delta^* = \int_0^\delta \left(1 - \frac{v}{V}\right) dy$$

Another boundary layer thickness parameter is the momentum thickness. The difference between the actual flow of momentum in the boundary layer, and that of the same quantity of fluid flowing with velocity V is $\rho V^2 \theta$. From this relation momentum thickness gets its name. It is defined as:

$$\theta = \int_0^\delta \frac{v}{V} \left(1 - \frac{v}{V}\right) dy$$

This definition is quite frequently used in boundary layer calculations. It should be noted that, although boundary layer thickness does change in transition from laminar to turbulent flow, momentum thickness does not, according to Ref. 15.

Another parameter which takes an appearance in boundary layer calculations is the shape parameter. This is defined as the ratio of the displacement thickness to the momentum thickness

$$H = \frac{\delta^*}{\theta}$$

The equation that gives the rate of change of the momentum in a boundary layer, originally derived by von Karman, may be written in the following form for two dimensional flow:

11/11/11
 11/11/11

$$b \rightarrow c + \delta$$

11/11/11

11/11/11

11/11/11

$$b \rightarrow c + \delta$$

$$\frac{b}{c}$$

$$\frac{d\theta}{dx} + \frac{(H+2)}{2} \frac{\theta}{q} \frac{dq}{dx} = \frac{\tau_0}{2q}$$

$$\frac{\tau_0}{q} = \text{local skin friction coefficient.}$$

$$\frac{\theta}{q} \frac{dq}{dx} = \text{non-dimensional pressure gradient.}$$

The value of the skinfriction coefficient was determined by the Schlichting and Young formula (Ref. 16), which states:

$$\frac{2\theta}{\tau_0} = \left[5.470 \log_{10} (4.775 R_\theta) \right]^2$$

$$R_\theta = \frac{\rho q \theta}{\mu}$$

This skin friction formula gives good agreement with experimental results on airfoils.

The variation of the shape parameter, H , along the surface was determined by von Doenhoff and Tetervin to be:

$$H = \frac{d\theta}{dx} = e^{1.030 (H - 2.775)} \left[-\frac{\theta}{q} \frac{dq}{dx} \frac{2\theta}{\tau_0} - 2.035 (H - 1.246) \right]$$

To calculate the characteristics of the turbulent boundary layer, it is always required to know the initial values of θ and δ , the pressure distribution, and the Reynolds number. With this information and the three equations above a solution can be obtained. Separation may be considered to have occurred when H reaches a value of 8.0. According to Ref. 17 the calculation is better in a region where the ratio of the non-dimensional

27

+

+

+

27

27

1

1

1

27

1

1

1

pressure coefficient to the skin friction coefficient is very small or positive, the boundary layer is not very sensitive to the initial value of H . For example, if dq/dx is zero, H will eventually have the value of 1.236 regardless of its initial value.

Some criticism of the above method of determining the point of separation of the turbulent boundary layer is given in Ref. 15. These criticisms are:

1. To determine the separation point within 4 per cent of the chord, the value of H immediately after transition must be known within ± 0.05 .
2. There is evidence that skin friction increases violently through the adverse pressure gradient preceding separation.
3. The empirical equation is derived entirely from data at low Reynolds number, $0.35 - 4.13 \times 10^6$. It may be proved ultimately that certain constants in the equation may vary appreciably with Reynolds number.
4. The mean value of H after transition is nearer 1.1. In von Karman's momentum equation ($H = 1.1$) would be better than ($H = 1.236$).

Means of Delaying Separation.

Ref. 17 suggests the following methods of artificially delaying separation:

1. Provide suction of the whole boundary in the direction of the stream.

1000 - 2000 - 3000

1000 - 2000 - 3000

1000 - 2000 - 3000

1000 - 2000 - 3000

1000 - 2000 - 3000

1000 - 2000 - 3000

1000 - 2000 - 3000

1000 - 2000 - 3000

1000 - 2000 - 3000

1000 - 2000 - 3000

1000 - 2000 - 3000

1000 - 2000 - 3000

1000 - 2000 - 3000

1000 - 2000 - 3000

1000 - 2000 - 3000

1000 - 2000 - 3000

1000 - 2000 - 3000

1000 - 2000 - 3000

1000 - 2000 - 3000

1000 - 2000 - 3000

1000 - 2000 - 3000

1000 - 2000 - 3000

1000 - 2000 - 3000

1000 - 2000 - 3000

1000 - 2000 - 3000

1000 - 2000 - 3000

1000 - 2000 - 3000

2. Increase the momentum of the retarded fluid by jets.

3. Prevent the accumulation of retarded fluid by suction.

The first method of delaying separation suggested is impractical in a duct. The shape of a diffuser does not lend itself to such a device, and secondly, the additional mechanism involved would cause more serious penalties in performance than the expected loss due to separation. The idea is of purely academic interest.

The second method is a decided possibility and Ref. 3 claims that the expansion loss can be reduced 40 to 50 per cent at expansion angles greater than 50° by the use of deflectors. These deflectors essentially provide a jet in the boundary layer region by reducing the pressure gradient near the wall, or even accelerating the flow in that region. Such large divergence angles



are not necessary for a diffuser to be used as the entrance duct of a jet engine, however. If a jet discharging into the boundary layer from an outside source is contemplated, the additional power required to furnish the jet must be accounted for in the computation of diffuser efficiency. Also, the increased mass flow must be allowed for in the calculation of diffuser performance.

The third method of preventing boundary layer separation seems the most inviting. ref. 3 claims that diffuser efficiencies of the order of 80 per cent, based on power ratios, are possible with divergence angles greater than 50 degrees. Some results of experiments using this principle are shown in Fig. 9. The definition of efficiency is corrected for the power expended in raising the pressure of the fluid removed to the diffuser exit pressure, assuming a pump efficiency of 75 per cent.

$$\eta_s = \frac{p_2 - p_1}{\frac{1}{2} \rho u_1^2 \left[1 - \left(\frac{A_1}{A_2} \right)^2 \right] + \frac{\Delta p_s}{.75}}$$

Q_s = quantity of fluid sucked away per unit time.

Δp_s = required increase in pressure from the section exit to p_2 , diffuser discharge pressure.

Still a fourth method of reducing expansion loss is suggested in ref. 3. In this method a solid body rotation is imposed on the flow by curved vanes at the diffuser entrance. This action has the effect of decreasing the rate of compression by increasing the mean distance travelled by the flow through the diffuser. Other methods of reducing the rate of compression suggested by the same article are the use of a circular duct and the use of a dividing vane in the flow. In

100 100 100 100

100 100 100 100

100 100 100 100

100 100 100 100

100 100 100 100

100 100 100 100

100 100 100 100

100 100 100 100

100 100 100 100

100 100 100 100

100 100 100 100

100 100 100 100 100 100

100 100 100 100

100 100 100 100

100 100 100 100

100 100 100 100

100 100 100 100

100 100 100 100

100 100 100 100

100 100 100 100

100 100 100 100

100 100 100 100

100 100 100 100

100 100 100 100

100 100 100 100

100 100 100 100

100 100 100 100

100 100 100 100

100 100 100 100

100 100 100 100

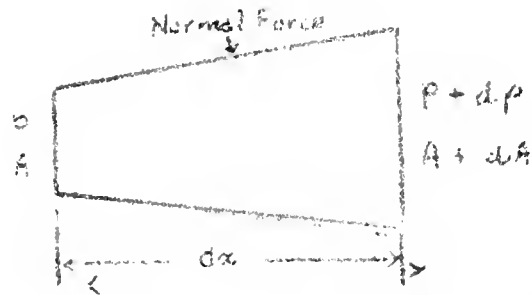
both of these latter cases the divergence angle is decreased with the same diffuser length. In ref. 18 it was found that the use of the dividing vane in a flow reduced the losses in wide angled diffusers, but the efficiency was not as high as for a longer diffuser with the same divergence angle as each of the separate passages into which the shorter diffuser was divided.

5. Friction Loss.

Skin friction is one of the major losses encountered in the flow of a viscous fluid over a surface. Prandtl in 1904 introduced the concept of the boundary layer, a region of small thickness near the surface of an object immersed in a fluid stream, or moving through a fluid, within which the speed of the fluid relative to the surface rises within a comparatively short distance from zero at the surface to a value comparable to the relative speed of the body and the fluid at a great distance. The frictional force exerted by the body on the fluid is proportional to the velocity gradient normal to the body and can be expressed:

$$\tau_0 = \mu \frac{dv}{dy} \quad (1)$$

The effect of skin friction is such as to cause a pressure drop in the fluid in the direction of flow. Considering a filament of flow upon which frictional forces are acting:



$$\text{Pressure force} = pA - (p + dp)(A + dA) = -Adp - p dA \quad (2)$$

$$\text{Normal force} = (p + \frac{dp}{2})(A + dA - A) = p dA \quad (3)$$

$$\text{Friction force} = -\tau_0 \pi (r + \frac{dr}{2})(v + dv) dt \quad (4)$$

According to Newton's law of motion:

$$dp = dm \, dv/dt \quad (5)$$

Now, summing the forces in the direction of motion:

$$F = \text{Pressure force} + \text{normal force component} + \text{friction force} \quad (6)$$

$$dp = -Adp - p dA + p dA - \tau_0 \pi (r dt + \frac{dr}{2} dt + \frac{v dt}{2}) \quad (7)$$

$$dm = \rho A dx / v \quad (8)$$

Substituting in the equation of motion:

$$-Adp - \tau_0 \pi r dt = \frac{\rho}{g} A dx \frac{dv}{dt}$$

$$-dp - \frac{\tau_0 \pi r}{A} \frac{dx}{v} = \frac{\rho}{g} \frac{dx}{dt} \quad (9)$$

$$-dp - \frac{1}{4} \tau_0 \frac{dx}{r} = \frac{\rho}{g} v dv \quad (10)$$

This equation has also been written:

$$v + \frac{\rho}{g} d(v^2) + \frac{\rho}{g} \frac{1}{2} r \frac{dx}{v} = 0 \quad (11)$$



To find the friction loss in terms of total pressure:

$$\frac{dp}{\rho} + \frac{1}{2} \frac{d(v^2)}{g \frac{\rho}{\rho}} + 4 \frac{\tau_0}{\rho} \frac{dx}{D} = 0 \quad (11)$$

$$v^2 = K \gamma M^2 H^2$$

$$d(v^2) = 2 \gamma M^2 dH^2 + 2 \gamma H^2 dM^2 \quad (12)$$

$$\frac{p_0}{p} = 1 + \frac{\gamma-1}{2} M^2$$

$$\frac{dp_0}{p_0} = \frac{dp}{p} + \frac{\frac{\gamma-1}{2} d(v^2)}{1 + \frac{\gamma-1}{2} M^2}$$

$$dp_0 = 0 \text{ (Adiabatic process)}$$

$$dp = - \frac{\frac{\gamma-1}{2} \tau_0 d(v^2)}{1 + \frac{\gamma-1}{2} M^2} \quad (13)$$

$$\frac{p_0}{p} = (1 + \frac{\gamma-1}{2} M^2)^{\frac{\gamma}{\gamma-1}}$$

$$\frac{dp}{p} = \frac{dp_0}{p_0} - \frac{\frac{\gamma}{2} d(v^2)}{1 + \frac{\gamma-1}{2} M^2} \quad (14)$$

Substituting eq. 13 in eq. 12, and eqs. 12 and 14 in eq. 11 gives:

$$\frac{dp_0}{p_0} + \frac{1}{F} \frac{\tau_0}{\rho} \frac{dx}{D} = 0 \quad (15)$$

$$\ln \frac{p_2^0}{p_1^0} + \int_1^2 \frac{\tau_0}{\rho} \frac{dx}{D} = 0 \quad (16)$$

$$\ln \frac{p_2^0}{p_1^0} + \int_1^2 \frac{2}{\gamma} \frac{\tau_0}{\rho} \gamma M^2 \frac{dx}{D} = 0 \quad (17)$$

The skin friction coefficient for the laminary boundary layer on a thin flat plate is: (Ref. 13.)

$$x^2 + y^2 = 1 \quad (1)$$

$$x^2 + y^2 = 1 \quad (2)$$

$$x^2 + y^2 = 1$$

$$x^2 + y^2 = 1$$

$$x^2 + y^2 = 1$$

$$x^2 + y^2 = 1$$

$$x^2 + y^2 = 1$$

$$x^2 + y^2 = 1$$

$$x^2 + y^2 = 1$$

$$x^2 + y^2 = 1$$

$$x^2 + y^2 = 1$$

$$x^2 + y^2 = 1$$

$$x^2 + y^2 = 1$$

$$\frac{\tau_0}{q} = 0.730 \sqrt{\frac{\nu}{Vx}}$$

For the turbulent boundary layer, the skin friction coefficient is given by the Squire and Young formula (Ref. 16.) previously given:

$$\frac{\tau_0}{q} = \frac{2}{[5.48 \log (4.375 R_e)]^2}$$

Although neither one of these skin friction coefficient equations have been obtained for flow in a duct, it is believed that they will be reasonably accurate if the boundary layer thickness remains small compared with the duct diameter.

6. Turning Loss.

In a turbojet installation it is not always feasible to duct the airflow from the diffuser entrance to the compressor without the use of bends in the ducting. A loss of head results from this change in the direction of the airflow, but with proper design the loss can be kept to a very low value. The loss of head in a turn is caused by the tendency of the flow to separate from the inside wall of the bend. At the entrance to the bend, the velocities in the duct are rectilinear. After entering the bend, the velocities distribution tends to change. The flow on the inside of the bend, turning through a shorter radius, is accelerated faster than the flow on the outside of the turn. Conditions become

189

189

189

189

189

189

189

189

189

189

189

189

189

189

189

189

189

189

189

189

189

189

189

189

189

189

189

189

189

189

189

189

189

189

189

189

189

similar to those for a free vortex, and the pressure on the inside of the turn is less than that on the outside. This redistribution of velocity results in increased turbulence throughout the bend. Upon leaving the bend, conditions are reversed, and the approximate free vortex motion established in the bend must be changed back to rectilinear flow. For a 90° turn the length of duct following the corner should be about $\frac{1}{4}$ x the diameter of the duct.

According to Ref. 1), the turning loss is a function of the following:

1. the radius ratio, the ratio of the radius of curvature of the duct (r) to the diameter or width of the duct (d), measured in the same plane as θ .
2. the aspect ratio, or ratio of the height of the duct (h) to its width (b).
3. the angle (θ) through which the air is deflected by the corner.
4. the local Reynold's number.

The pressure loss involved in turning the airflow can be expressed in the form of a resistance coefficient:

$$K_c = \frac{\Delta h_c}{\frac{1}{2} \rho V^2}$$

Fig. 1 shows the effect of radius ratio on deflection angle upon the resistance coefficient. It should also be realized that the turning loss is proportional to the

1. The first part of the paper is devoted to the study of the

properties of the function $f(x) = \sum_{n=0}^{\infty} \frac{x^n}{n!}$.

2. In the second part, we consider the function $f(x) = \sum_{n=0}^{\infty} \frac{x^n}{n!}$.

3. The third part of the paper is devoted to the study of the

properties of the function $f(x) = \sum_{n=0}^{\infty} \frac{x^n}{n!}$.

4. In the fourth part, we consider the function $f(x) = \sum_{n=0}^{\infty} \frac{x^n}{n!}$.

5. The fifth part of the paper is devoted to the study of the

properties of the function $f(x) = \sum_{n=0}^{\infty} \frac{x^n}{n!}$.

6.

7.

8.

9.

10.

11. The first part of the paper is devoted to the study of the

properties of the function $f(x) = \sum_{n=0}^{\infty} \frac{x^n}{n!}$.

12. In the second part, we consider the function $f(x) = \sum_{n=0}^{\infty} \frac{x^n}{n!}$.

13. The third part of the paper is devoted to the study of the

properties of the function $f(x) = \sum_{n=0}^{\infty} \frac{x^n}{n!}$.

14. In the fourth part, we consider the function $f(x) = \sum_{n=0}^{\infty} \frac{x^n}{n!}$.

15. The fifth part of the paper is devoted to the study of the

properties of the function $f(x) = \sum_{n=0}^{\infty} \frac{x^n}{n!}$.

16.

square of the velocity. Some representative values of the resistance coefficient for various duct shapes and turning angles are given below. In this particular series of tests the Reynolds number was between 10^5 and 10^6 based upon duct diameter.



$\theta = 30^\circ$	$k_0 = 0.15$	0.10	0.02
$\theta = 60^\circ$	1.10	0.40	0.05
$\theta = 90^\circ$	1.60	1.05	0.20

The advantage of the circular duct without too small a value of radius ratio and with small turning angles is readily apparent from the above listed values of resistance coefficient. However, the efficiency of the rectangular duct can be made to approach that of the circular duct by increasing the aspect ratio, a/b . The influence of aspect ratio with varying radius ratio to give a resistance coefficient of 0.15 is shown in Fig. 11.

Sharp bends may also be improved by the use of curved vanes in the bend. These have the effect of creating high aspect ratio passages. The gap/chord ratio, s/c , of these vanes is important as shown in Fig. 12. Resistance coefficient reduces to a minimum at a gap/chord ratio of about 4.3, and then increases as the gap/chord ratio is raised or lowered. This data

was obtained in a 90 degree bend with vanes shaped as quarter circles. The angle of incidence of the flow was 45 degrees, and the Reynolds number based on the chord of the vane was between 10^4 and 10^5 . It was also found that the angle of incidence was not particularly critical as long as the vanes did not stall. The primary requisite of the vanes is to have the flow parallel to the duct wall when it leaves the vanes. The angle of incidence of the vanes is defined as the angle which the chord of the vane makes with the direction of the incoming flow.

Some data on the losses involved when a turn is made in an expanding entry was obtained from def. 20 and is shown in Fig. 13. In this test the duct was rectangular with two diverging and two parallel walls. It was found that fairly high resistance coefficients were encountered particularly with increasing expansion ratios. Since the loss occurring in a bend involves flow separation from the wall, and since the danger of separation is always encountered in the diffusion process with increasing area ratios, it might be expected that the combination of these two unstable flow processes would result in fairly high losses.

7. Obstructions in the Flow.

It would be desirable to eliminate all obstructions from air intake ducts, but it is not always possible. In

many cases the diffuser is not a simple conical shape, but may be an annular duct with a central cone. The central cone must be supported in some manner, usually by struts to the outer cone structure. The central cone may also house apparatus requiring leads from the outside of the engine. In some instances, screens may be placed in the duct ahead of the compressor inlet to prevent the entry of foreign matter into the engine. All of these obstructions are potential sources of pressure loss due to turbulent flow about them. The magnitude of the loss depends upon the location and shape of the obstruction. It would be impossible to give general rules covering all possible cases, but some estimate of the loss may be made for a particular case.

Let us consider one of the worst cases, an obstruction which is not streamlined. The loss occasioned by this shape can be considered to be caused by a sudden contraction, followed by a sudden expansion of the flow. Ref. 3 gives the general form of these losses.

Loss due to a sudden contraction:

$$\Delta p = \frac{k P V_b^2}{2g}$$

b/c_d	0.6	0.7	0.8	0.9	1.0
k	0.28	0.21	.1	0.06	0.0

Loss due to a sudden expansion:

$$\Delta p = \frac{P(V_b - V_e)^2}{2g}$$

Subscripts:

a - position ahead of obstruction.

b - position of minimum cross-sectional area.

c - Position after obstruction.

Loss due to an obstruction:

Assume that $V_a = V_c$

$$\Delta p = k \frac{\rho V_b^2}{2g} + \frac{\rho (V_b - V_a)^2}{2g}$$

$$\Delta p = q_b \left(k + \left(1 - \frac{V_a}{V_b} \right)^2 \right)$$

Assume that the flow is incompressible in the vicinity of the obstruction. This assumption is justified because the obstruction will probably be located in a region in which the flow has already been considerably slowed down. Since the loss is a function of the square of the velocity it would not be logical to have an obstruction in the high speed flow region.

$$V_a/V_b = A_b/A_a = (q_b/q_a)^2$$

$$\Delta p = q_b \left(k + \left(1 - A_b/A_a \right)^2 \right)$$

Now the loss coefficient of sudden contraction is based on flow from a larger pipe to a smaller one, but let us assume that the same coefficient is satisfactory based on area ratios, then a new loss coefficient based on area ratios can be calculated.

$$\Delta p = q_b$$

2-10-11

9 + 9 = 18

4 + 4 = 8

1000 - 100 = 900

1000 - 1000 = 0

1000 - 1000 = 0

1000 - 1000 = 0

1000 - 1000 = 0

4 + 4 = 8

where $C = k + (1 - A_p/A_n)^2$

This new coefficient is plotted in Fig. 14 for various area ratios.

If the obstruction is large, the losses will be large, but for most obstructions which might be encountered the loss is low, but of significant magnitude when trying to keep efficiency high. The loss due to an obstruction in the flow can be further reduced by the use of a fairing or streamline shape around the obstruction. In this case the only loss to be expected would be that due to friction which should be very small.

8. Leakage Loss.

At the exit of a diffuser the internal pressure may be considerably above the pressure of the surrounding air. Unless care has been taken in making the joints, particularly where the diffuser joins the compressor, the air will leak into the region of lower pressure. This consideration militates against the use of long ducts from the diffuser exit to the compressor entrance.

Depending upon the number and size of the leaks themselves, leakage can have a serious effect on diffuser efficiency. Leakage results in a two-fold loss. First, there is a loss in the mass flow into the compressor; and, secondly, there is a loss in pressure resulting from the loss in fluid. To make an estimate

... ..

... ..

... ..

... ..

... ..

... ..

... ..

of the extent of loss due to leakage would serve no useful purpose. Leakage is inexcusable, and if it should occur, the first thought should not be what is the effect of the loss, but how can the leak be stopped.

9. Exit Loss.

It has been found (Ref. 21 and Ref. 3) that complete pressure recovery does not occur entirely within the diffuser for a given diffuser area ratio. Ref. 21 was the source of Fig. 15 which shows the length of ducting necessary for a turbulent velocity profile to develop in the duct. The velocity profile leaving the diffuser proper is parabolic in shape due to the fact that pressure recovery is not uniform in a plane normal to the diffuser axis.

Ref. 3 claims that the required length of ducting following a diffuser can be reduced by suction slots in the vicinity of the diffuser exit, or inducing a solid body rotation in the flow in the diffuser. Suction slots, therefore, which were used to reduce the likelihood of flow separation now serve a two fold purpose and reduce the required length of exit ducting. The extent of rotation induced in the flow at the diffuser exit by the rotary motion of the compressor is not known, but it is felt that some rotation does occur. This, too, would have the beneficial effect of shortening the length of exit ducting required. Generally

speaking, an annular type diffuser has a more desirable exit velocity profile than does a plain conical diffuser and would require a shorter length of exit ducting for complete pressure recovery.

CHAPTER IV

GEOMETRIC CONSIDERATIONS

1. Inlet Duct Location.

The aircraft designer has the choice of many different locations for his engine air inlet, limited, of course, by the engine location which may be:

1. Submerged in the fuselage.
2. Partially submerged in the fuselage.
3. Submerged in the wing root.
4. Located in a nacelle in the wing structure.
5. Located in a nacelle supported by a pylon from the wing structure.

The air inlet may be located at a stagnation point in the flow about the airplane, or may be of the scoop type, with or without boundary layer control, or it may be a flush type opening in the fuselage. The choice of design is a compromise between internal flow considerations, external drag considerations, and structural considerations.

The stagnation point inlet has the advantage of giving a good velocity distribution across the inlet face without artificial flow control. When the stagnation point is the nose of the fuselage, however, long ducts are required to lead the flow back to the engine. At high speeds the pressure differential between the

inside and outside of the duct requires substantially constructed ducts with well sealed joints to prevent leakage. Valuable fuselage space is sacrificed to the ducting, and bends in the ducting are generally required to guide the flow around obstructions.

In multi-engine installations, the trend is to locate the jet engines in or supported from the wings. This type of engine installation permits stagnation point air inlet ducts with short diffusers required because of space limitations. Expansion angles greater than optimum may be required. Additional problems are also present. For supersonic plane designs the effect of the shock wave, originating at the fuselage nose, on the flow ahead of the air inlet must be considered, and may limit the engine location. The shock wave forming ahead of the air inlet duct itself will undoubtedly influence the flow over the wing of the plane, and may cause such a loss in the wing performance that such a configuration would not be permissible. For subsonic flows care must be taken where several air inlets are adjacent that the flow into one duct does not affect the velocity distribution across the face of another, or cause the critical Mach number of the wing to be lowered.

The scoop type of inlet has poor velocity distribution across the face of the duct because it is located next to a surface where a boundary layer exists. The

velocity distribution can be improved by boundary layer bleeds at the duct entrance until conditions comparable to the stagnation point inlet exist. The added feature of the boundary layer bleed and its control add to the design complexity, however. For scoop inlets to an engine submerged in the fuselage the flow must negotiate two turns and join in a Y-duct at the compressor entrance in most instances. This problem is not unique to the scoop type of inlet, though. Many designs with the inlet in the nose of the fuselage have a similar configuration where the ducting is divided at the nose of the airplane, and the ducts follow the sides of the fuselage and meet at the engine entrance.

The scoop type of inlet has advantages also. Shorter lengths of ducting are required which mean a weight saving and reduce the probability of leakage loss. Less fuselage space is required for the ducting, and improved visibility for the pilot due to more desirable nose shapes results. For military aircraft better armament arrangement can be obtained when there is no ducting in the nose of the fuselage. Here the scoop is located at the wing-fuselage juncture the critical Mach number of this section can be improved. This particular point is also a source of drag which may be reduced considerably by the inlet and exit duct location there.

With the coming of supersonic plane designs several examples of the flush type of air inlet duct have

appeared. The flush air inlet located at some point on the fuselage sacrifices ram compression ahead of the air inlet and has an entrance velocity distribution problem, but the decrease in resulting drag and small effect on the flow around the fuselage contour must offer greater benefits than the reduced performance due to incomplete ram recovery.

The inlet ducts under discussion are the main air inlet ducts for high speed operation. Some aircraft have auxiliary air inlet ducts for low speed operation and take-off conditions. At low speeds the velocity ratio is so high that diffuser performance suffers. Ram recovery is not of much significance at these low speeds, and so the auxiliary air inlets provide a means of getting a large volume of air to the engine in the quickest possible manner. These auxiliary ducts are usually spring loaded doors opening directly into the plenum chamber at the compressor entrance. When the pressure in the plenum chamber is below atmospheric the auxiliary air inlet opens; when the pressure gets up to atmospheric the auxiliary air inlet closes due to the spring action, and a flush exterior surface results.

The choice of air inlet duct location is subject to many compromises. It would be impossible to reach a definite conclusion as to which is unreservedly better than any other. Present airplane designs show a great variety of inlet duct locations and types of entrances,

some of these particular instances will be discussed later. It appears that in some cases the location of the entrance duct was a result of the airframe configuration; in other cases it would appear that the airframe configuration resulted from a choice in the location of the air entrance duct. In the future it is believed that the latter approach will be more prevalent.

2. Area Ratios and Diffuser Length.

If a diffuser exit mach number is assumed, the required area ratio to obtain it can be computed for various entrance mach numbers and diffuser efficiencies. An exit mach number of 0.3 will be assumed, which is a reasonable value for the airflow to be supplied to the compressor. A range of entrance mach numbers from 0.3 to 1.0 will be investigated. Mach numbers greater than one will not occur in the diffuser because it is preferable to have the shock wave located outside the diffuser. Instead of diffuser efficiency the variation of area ratio and diffuser length with total pressure ratio, which is a measure of diffuser efficiency, will be investigated.

First, the area ratio necessary to accelerate a flow isentropically from its present mach number to a mach number of one can be determined from continuity considerations.

$$\frac{p_{01}}{T} = \frac{p^* A^*}{\sqrt{\gamma}} \frac{1}{M^*}$$

$$\frac{A}{A^*} = \frac{M^*}{M} \frac{p^*}{p} \left(\frac{T}{T^*} \right)^{\frac{\gamma}{\gamma-1}}$$

$$M^* = 1$$

$$\frac{p^*}{p} = \left(\frac{1 + \frac{\gamma-1}{2} M^2}{\frac{\gamma+1}{2}} \right)^{\frac{\gamma}{\gamma-1}}$$

$$\frac{T}{T^*} = \left(\frac{1 + \frac{\gamma-1}{2} M^2}{\frac{\gamma+1}{2}} \right)^{-1}$$

$$\frac{A}{A^*} = \frac{1}{M} \left(\frac{1 + \frac{\gamma-1}{2} M^2}{\frac{\gamma+1}{2}} \right)^{\frac{\gamma+1}{2(\gamma-1)}}$$

If the process is isentropic, $A_1^* = A_2^*$

$$\frac{A_2}{A_1} = \frac{A_2/A_2^*}{A_1/A_1^*} = \frac{M_1}{M_2} \left(\frac{1 + \frac{\gamma-1}{2} M_2^2}{1 + \frac{\gamma-1}{2} M_1^2} \right)^{\frac{\gamma+1}{2(\gamma-1)}}$$

If the process is adiabatic, but non-isentropic

$$\frac{A_2}{A_1} = \frac{A_2^*}{A_1^*} \frac{M_1}{M_2} \left(\frac{1 + \frac{\gamma-1}{2} M_2^2}{1 + \frac{\gamma-1}{2} M_1^2} \right)^{\frac{\gamma+1}{2(\gamma-1)}}$$

$$\frac{A_2^*}{A_1^*} = \frac{p_1}{p_2} \frac{A_1}{A_2}$$

$$\frac{A_2}{A_1} = \frac{p_1}{p_2} \frac{M_1}{M_2} \left(\frac{1 + \frac{\gamma-1}{2} M_2^2}{1 + \frac{\gamma-1}{2} M_1^2} \right)^{\frac{\gamma+1}{2(\gamma-1)}}$$

The required area ratios to accomplish compression to an exit Mach number of 0.3 with various entrance Mach numbers and total pressure ratios are shown in Fig. 10.

If a conical diffuser with a divergence angle of θ deg. is assumed, the resultant ^{ing} diffuser length is a function of the mass flow to be directed and the area ratios previously determined.

1

2

3

4

5

6

7

8

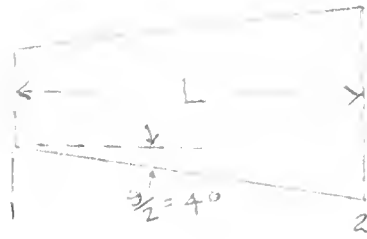
9

$$w = P \Delta V = 44.1 P \Delta V \sqrt{T}$$

$$\sigma = P/P_{SL} \quad \phi = w/P_{SL}$$

$$A_1 = \frac{\pi}{4} D_1^2 = \frac{w}{49.1 P_{SL} \sqrt{T_{SL}}}$$

$$D_1 = \sqrt{\frac{w/\sqrt{T}}{67 P}}$$



$$\tan \frac{\alpha}{2} = \frac{1/2 - 1/2}{L}$$

$$L = \frac{D_1 (\sqrt{A_2/A_1} - 1)}{2 \tan \frac{\alpha}{2}}$$

Fig. 17 shows the variation of diffuser length with different values of the weight flow parameter and total pressure ratios for various entrance Mach numbers.

Figure 18 reveals that relatively small area ratios will reduce any expected diffuser entrance Mach number to an exit Mach number of 0.3, even with large internal losses in the diffuser. Large internal losses in the diffuser are not to be expected, however, with such small area ratios. Ref. 3 shows high diffuser efficiencies with small area ratios, and a diffuser divergence angle of 6 to 8 deg.

In Fig. 17 the effect of entrance Mach number and weight flow upon the diffuser length can be seen with an exit Mach number of 0.3 and a diffuser divergence angle of 6 degrees. It is interesting to note that the shortest

7 9 1 1 9 1 1
12/9 1 0

0 0 1
1 2

0 0 1
1 2

0 0 1
1 2

diffuser length does not occur with the largest diffuser entrance mach number, but occurs at an entrance mach number of about 0.82. This is due to the small change in area ratio required at these high entrance mach numbers in comparison to the change in entrance area required to maintain the given weight flow. As was to be expected, diffuser length increases with increased mass flow and decreased diffuser efficiency.

Whether these diffuser lengths are tolerable depends upon the engine location and the size of the airplane. For an engine located in the fuselage, and with the diffuser entrance located in the nose, it is hardly likely that such diffuser lengths would be critical even with large weight flows. The weight flow of 150 pounds of air per second, using the thumb rule that one pound of air per second corresponds to 50 pounds of thrust, would be the equivalent of a 7,500 pound thrust unit. For an engine installation in the wing, or in a pylon attached to the wing, such diffuser lengths as have been calculated might be impractical. These lengths could be decreased by increasing the divergence angle, but reduced diffuser performance could be expected since the divergence angle used in the computations is just about the optimum. Such problems, however, should be considered in the selection of an engine and its installation.

3. Velocity ratio.

A. Effect of velocity ratio on a diffuser.

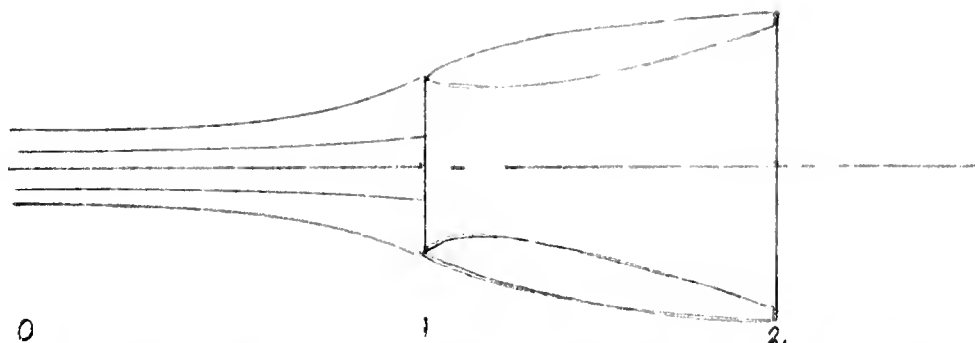
Velocity ratio is defined as the ratio of the diffuser entrance velocity to the free stream velocity of the airflow. For subsonic flows NACA has determined experimentally that this ratio should be within the range of 0.3 to 0.6 for optimum performance. It was found that at very low velocity ratios the flow tended to separate from the outside lip of the diffuser and increase the external drag of the engine nacelle. At higher velocity ratios the flow tended to separate from the diffuser wall and the pressure recovery and diffuser efficiency decreased.

The volume flow through a turbojet tends to remain constant for a given engine speed, and so, at any one flight velocity, the required inlet area for a diffuser is a function of the velocity ratio.

$$A_1 = \frac{Q}{V_0}$$

Therefore, a bigger entrance area is required for low velocity ratios than for high velocity ratios.

At flight velocities greater than the diffuser inlet velocity a stream tube ahead of the diffuser inlet starts expanding. The flow velocity in the stream tube is decelerated to the desired inlet velocity and in the process is compressed isentropically.



At the lower velocity ratios more of the compression is accomplished outside the diffuser than at higher velocity ratios.

Since compression outside the diffuser is accomplished at greater efficiency than compression in the diffuser, it would seem to be more practical to keep the velocity ratio as low as possible. However, it should be noted that as the flow approaches the diffuser entrance it has a velocity component normal to the diffuser axis. This is equivalent to increasing the angle of attack of the diffuser lip in the air stream. At very low velocity ratios the diffuser lip stalls and the flow separates from the outside surface of the diffuser increasing the drag of the nacelle. For this reason, a lower limit of permissible velocity ratios is established.

At the higher velocity ratios more of the compression must be accomplished in the diffuser. For the same length of diffuser and exit velocity the pressure gradient is greater, and the danger of internal flow separation from the wall of the diffuser is increased. If the length of the diffuser is increased to permit the same pressure gradient as could be obtained with the lower

velocity ratio, the boundary layer has a greater distance in which to grow thicker. Generation of flow is also a function of the boundary layer thickness. In view of these reasons the upper limit on desirable velocity ratios is established.

D. Variation of velocity ratio with range of operation.

Once the geometry of a diffuser has been established for desirable operation at a particular design condition, the velocity ratio will vary with departure from the design point.

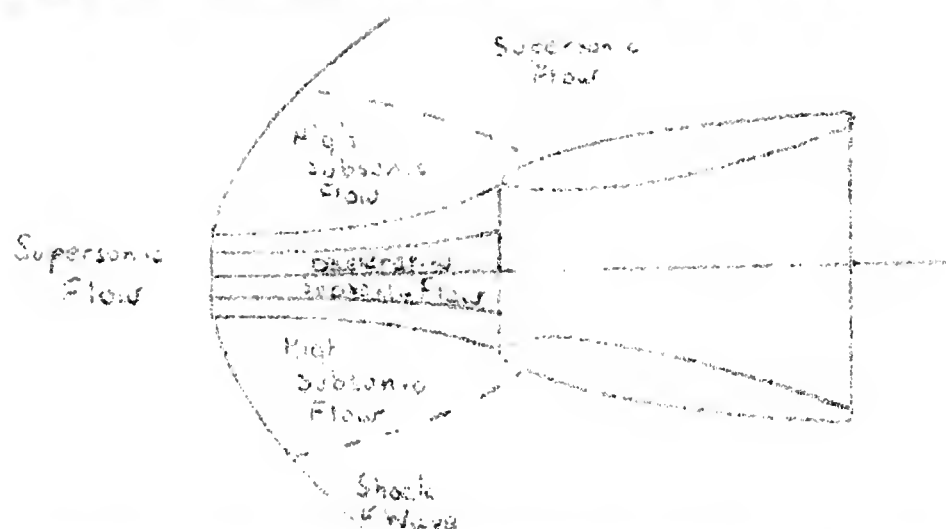
$$r = \frac{V_1}{V_0} = \frac{C}{49.1 A_1 M_0 \sqrt{T_0}}$$

This equation indicates that the velocity ratio varies inversely as the flight Mach number and the square root of the ambient temperature. It also varies directly with the volume of airflow. Particularly critical are the static thrust and take-off conditions. At the static thrust condition the velocity ratio is infinite, and at take-off velocity the velocity ratio is considerably greater than one for an entrance duct designed for efficient operation at high speed, unless auxiliary air inlets are provided into the plenum chamber.

E. Effect of supersonic speed on velocity ratio.

At supersonic speeds with a shock wave ahead of the diffuser entrance, the values of V_0 , C , and T_0

used in the computation of velocity ratio are the free stream conditions immediately following the shock wave. Other values would have little significance. Since it is assumed that a normal plane shock occurs in the region of flow through which the stream tube entering the diffuser passes, the conditions immediately following the shock are uniform. Whether or not the limits for velocity ratio which have been established for subsonic flow are applicable is a question of great importance. Although the stream velocity directly ahead of the diffuser inlet is subsonic, the adjacent flow is not. The velocities in the region about the diffuser entrance are of some such complicated pattern as shown.



Low velocity ratios will move the position of the shock wave to greater distances from the diffuser inlet. The effect of this position of the shock wave on the inlet drag, and the exact position of the shock wave is not known. It would seem likely that positioning the shock wave on the diffuser lip with a velocity ratio of one would reduce the inlet drag. In this case, the external

flow field would be supersonic, and the internal flow subsonic. Of course, this would require a large percentage of the pressure recovery to be effected by the diffuser, and diffuser efficiency decreases with increased demands upon the diffuser. A further complication introduced by positioning the shock on the diffuser lip is the effect on the boundary layer.

The deceleration of flow through a shock wave is accomplished with some degree of turbulence accounting for the entropy increase through the shock. With a detached shock this turbulence tends to be damped out in the free stream flow. If the shock is positioned on the diffuser lip, the ensuing turbulence is transmitted to the boundary layer. Up to the throat of the diffuser there is a favorable negative pressure gradient tending to damp the turbulence, and establish laminar flow conditions in the boundary layer. This favorable region is of very short length, however, and the turbulence may carry over into the unfavorable positive pressure gradient region in the divergent part of the diffuser, and hasten flow separation, seriously affecting the diffuser efficiency. This should be thoroughly investigated.

Thus, we are confronted with a situation where a decision must be made as to which is the more critical factor, the powerplant performance or the aerodynamic performance of the airplane. Before a decision can be

reached, the magnitude of the effects of shock wave position must be determined.

CHAPTER V

TYPICAL DIFFUSER DESIGN

1. The Geometry of the Diffuser.

The first consideration in the design of a diffuser is its size and shape. The size is controlled by the desired volume of airflow through the diffuser, and its shape by the desired characteristics of the internal flow. An infinite number of shapes and sizes could be considered, but for practical reasons only one configuration will be analyzed. It is hoped that the method of analysis used will be applicable to other designs with necessary modifications.

A representative modern turbo-jet engine develops 4,000 pounds of static thrust with an airflow of 73 pounds of air per second. The compressor of this engine will consume a constant volume of air for a given engine speed. The turbo-jet engine is characterized by giving its best performance at its design engine speed which is 100 per cent RPM. The volumetric capacity of the given engine can then be calculated from the continuity equation, and the diffuser will be designed accordingly. The density of the entering airflow will be assumed to be that of the standard sea level atmosphere.

$$w = \rho AV = 73 \text{ lb./sec.}$$

$$Q = AV = \frac{W}{\rho} = \frac{73}{.0705} = 103.2 \text{ cu. ft./sec.}$$

w = weight flow, lb./sec.

Q = volume flow, cu. ft./sec.

A = cross-sectional area of flow, sq. ft.

V = flow velocity, ft./sec.

ρ = specific weight of fluid, lb./cu.ft.

The three critical design conditions of a turbo-jet powered airplane are the static thrust condition, take-off and maximum speed. In the first two conditions a diffuser is of little use, and it would be better if some device was used to bypass the diffuser. The condition of maximum speed, however, is the point at which diffuser performance is desired. The design operating condition of the diffuser is then decided upon. Our selection is a flight Mach number of 1.5 at 40,000 feet altitude.

The diffuser will be conical with a rounded entrance lip to reduce entrance losses. The velocity ratio desired is 0.5. For flight Mach numbers greater than one a detached normal shock will occur ahead of the diffuser, and the total pressure loss accompanying this shock will be accepted. Where shock occurs, the free stream velocity fall with the shock will be used to determine the velocity ratio of the diffuser. The velocity of flow from the exit of the diffuser will be that corresponding to a Mach number of 0.5. It

1990

4. 5. 6. 7. 8. 9. 10. 11. 12. 13. 14. 15. 16. 17. 18. 19. 20. 21. 22. 23. 24. 25. 26. 27. 28. 29. 30. 31. 32. 33. 34. 35. 36. 37. 38. 39. 40. 41. 42. 43. 44. 45. 46. 47. 48. 49. 50. 51. 52. 53. 54. 55. 56. 57. 58. 59. 60. 61. 62. 63. 64. 65. 66. 67. 68. 69. 70. 71. 72. 73. 74. 75. 76. 77. 78. 79. 80. 81. 82. 83. 84. 85. 86. 87. 88. 89. 90. 91. 92. 93. 94. 95. 96. 97. 98. 99. 100. 101. 102. 103. 104. 105. 106. 107. 108. 109. 110. 111. 112. 113. 114. 115. 116. 117. 118. 119. 120. 121. 122. 123. 124. 125. 126. 127. 128. 129. 130. 131. 132. 133. 134. 135. 136. 137. 138. 139. 140. 141. 142. 143. 144. 145. 146. 147. 148. 149. 150. 151. 152. 153. 154. 155. 156. 157. 158. 159. 160. 161. 162. 163. 164. 165. 166. 167. 168. 169. 170. 171. 172. 173. 174. 175. 176. 177. 178. 179. 180. 181. 182. 183. 184. 185. 186. 187. 188. 189. 190. 191. 192. 193. 194. 195. 196. 197. 198. 199. 200. 201. 202. 203. 204. 205. 206. 207. 208. 209. 210. 211. 212. 213. 214. 215. 216. 217. 218. 219. 220. 221. 222. 223. 224. 225. 226. 227. 228. 229. 230. 231. 232. 233. 234. 235. 236. 237. 238. 239. 240. 241. 242. 243. 244. 245. 246. 247. 248. 249. 250. 251. 252. 253. 254. 255. 256. 257. 258. 259. 260. 261. 262. 263. 264. 265. 266. 267. 268. 269. 270. 271. 272. 273. 274. 275. 276. 277. 278. 279. 280. 281. 282. 283. 284. 285. 286. 287. 288. 289. 290. 291. 292. 293. 294. 295. 296. 297. 298. 299. 300. 301. 302. 303. 304. 305. 306. 307. 308. 309. 310. 311. 312. 313. 314. 315. 316. 317. 318. 319. 320. 321. 322. 323. 324. 325. 326. 327. 328. 329. 330. 331. 332. 333. 334. 335. 336. 337. 338. 339. 340. 341. 342. 343. 344. 345. 346. 347. 348. 349. 350. 351. 352. 353. 354. 355. 356. 357. 358. 359. 360. 361. 362. 363. 364. 365. 366. 367. 368. 369. 370. 371. 372. 373. 374. 375. 376. 377. 378. 379. 380. 381. 382. 383. 384. 385. 386. 387. 388. 389. 390. 391. 392. 393. 394. 395. 396. 397. 398. 399. 400. 401. 402. 403. 404. 405. 406. 407. 408. 409. 410. 411. 412. 413. 414. 415. 416. 417. 418. 419. 420. 421. 422. 423. 424. 425. 426. 427. 428. 429. 430. 431. 432. 433. 434. 435. 436. 437. 438. 439. 440. 441. 442. 443. 444. 445. 446. 447. 448. 449. 450. 451. 452. 453. 454. 455. 456. 457. 458. 459. 460. 461. 462. 463. 464. 465. 466. 467. 468. 469. 470. 471. 472. 473. 474. 475. 476. 477. 478. 479. 480. 481. 482. 483. 484. 485. 486. 487. 488. 489. 490. 491. 492. 493. 494. 495. 496. 497. 498. 499. 500. 501. 502. 503. 504. 505. 506. 507. 508. 509. 510. 511. 512. 513. 514. 515. 516. 517. 518. 519. 520. 521. 522. 523. 524. 525. 526. 527. 528. 529. 530. 531. 532. 533. 534. 535. 536. 537. 538. 539. 540. 541. 542. 543. 544. 545. 546. 547. 548. 549. 550. 551. 552. 553. 554. 555. 556. 557. 558. 559. 560. 561. 562. 563. 564. 565. 566. 567. 568. 569. 570. 571. 572. 573. 574. 575. 576. 577. 578. 579. 580. 581. 582. 583. 584. 585. 586. 587. 588. 589. 590. 591. 592. 593. 594. 595. 596. 597. 598. 599. 600. 601. 602. 603. 604. 605. 606. 607. 608. 609. 610. 611. 612. 613. 614. 615. 616. 617. 618. 619. 620. 621. 622. 623. 624. 625. 626. 627. 628. 629. 630. 631. 632. 633. 634. 635. 636. 637. 638. 639. 640. 641. 642. 643. 644. 645. 646. 647. 648. 649. 650. 651. 652. 653. 654. 655. 656. 657. 658. 659. 660. 661. 662. 663. 664. 665. 666. 667. 668. 669. 670. 671. 672. 673. 674. 675. 676. 677. 678. 679. 680. 681. 682. 683. 684. 685. 686. 687. 688. 689. 690. 691. 692. 693. 694. 695. 696. 697. 698. 699. 700. 701. 702. 703. 704. 705. 706. 707. 708. 709. 710. 711. 712. 713. 714. 715. 716. 717. 718. 719. 720. 721. 722. 723. 724. 725. 726. 727. 728. 729. 730. 731. 732. 733. 734. 735. 736. 737. 738. 739. 740. 741. 742. 743. 744. 745. 746. 747. 748. 749. 750. 751. 752. 753. 754. 755. 756. 757. 758. 759. 760. 761. 762. 763. 764. 765. 766. 767. 768. 769. 770. 771. 772. 773. 774. 775. 776. 777. 778. 779. 780. 781. 782. 783. 784. 785. 786. 787. 788. 789. 790. 791. 792. 793. 794. 795. 796. 797. 798. 799. 800. 801. 802. 803. 804. 805. 806. 807. 808. 809. 810. 811. 812. 813. 814. 815. 816. 817. 818. 819. 820. 821. 822. 823. 824. 825. 826. 827. 828. 829. 830. 831. 832. 833. 834. 835. 836. 837. 838. 839. 840. 841. 842. 8

100

1990

100

this information the size of the diffuser can be determined.

First, the conditions across the shock front have to be determined. The initial conditions are for the standard atmosphere, and the conditions across the normal shock are found in ref. 5, Table 4.3. It is then assumed that the flow is slowed isentropically from the free stream condition to the condition at the diffuser entrance. This gives the following conditions:

| Station | M | T , °R | a -ft/sec | p -lb/ft ² | ρ -slugs/ft ³ |
|---------|-------|----------|-------------|-------------------------|-------------------------------|
| x | 1.5 | 392.4 | 970.7 | 391.9 | .000512 |
| x/x | | 1.320 | | 2.453 | 1.4021 |
| y | .7011 | 517 | 1117.5 | 767.5 | .001094 |

| Station | M | M^2 | V |
|---------|-------|-------|-------|
| y | .7011 | .491 | 743.6 |
| 1 | .409 | .167 | 470 |

a - velocity of sound, ft./sec.

p - static pressure, lb./sq.ft.

T - static temperature, deg. R.

M - Mach number, V/a .

x - condition before the shock.

y - condition after the shock.

1 - diffuser entrance.

2 - diffuser throat.

3 - diffuser exit.

* - reference state where mach number is one.

Knowing the velocity at the entrance of the diffuser, and knowing the volume rate of flow the area of the diffuser entrance can be calculated.

$$V_1 = 0.6 \times V_y = 470 \text{ ft./sec.}$$

$$A_1 = \frac{Q}{V_1} = \frac{954.2}{470} = 2.025 \text{ sq. ft.}$$

$$D_1 = 1.605 \text{ ft.} = 19.25 \text{ in.}$$

$$A_3 = A_1 \times \frac{A_3/A^*}{A_1/A^*} = 2.025 \times \frac{2.0351}{1.563} = 2.635 \text{ sq. ft.}$$

$$D_3 = 1.83 \text{ ft.} = 21.95 \text{ in.}$$

A_3 was calculated from Table 30 of the "Gas Tables", knowing the desired exit mach number, and assuming an isentropic process. This assumption will be corrected later to allow for the fact that the process will not be isentropic. Next, with a contraction ratio of 1.184 between the diffuser entrance and throat, and rounding the entrance lip, the mach number at the throat was found to be 0.51, throat area - 1.71 sq. ft., throat diameter - 17.75 in. A divergence angle of 3 deg. from the throat to the exit was assumed, and the diffuser length determined. The dimensions of the diffuser are now known and the shape is as shown in the accompanying figures.

$$r = \frac{21.95 - 17.75}{2 \times \sin 40^\circ} = 30.1 \text{ in.}$$

2. Conditions of Internal Flow.

Now that the geometry of the diffuser has been determined, the character of the internal flow can be determined for any given condition of inflow. The volume rate of flow for the design operating condition of the engine has been calculated, and the velocity at the diffuser entrance has been established. The compression or expansion of the flow from the free stream condition to the condition at the diffuser entrance has been assumed to be an isentropic process, except across the shock front when such occurs. The compression of the flow within the diffuser will also be assumed to be isentropic, and when the diffuser losses have been determined, the geometry of the diffuser will be corrected accordingly to allow for variation from the isentropic condition.

The character of the internal flow can be determined from Table 30 of the Gas Tables, and the resulting flow for the design operating condition of a flight mach number of 1.5 at 40,000 feet altitude is shown in Table I, and Fig. 20.

3. Separation of Laminar Flow.

Since a diffuser in a free stream has a boundary layer of zero thickness at the stagnation point of the

flow, and since the rounded entrance lip has the effect of producing a favorable pressure gradient up to the point of the diffuser throat, the initial boundary layer in the entrance of the diffuser will be laminar. Due to the adverse pressure gradient in the diverging part of the diffuser, however, this laminar boundary layer will separate, there will be a transition zone, and then a turbulent boundary layer will establish itself if the pressure gradient is not too great. The point of separation of the laminar boundary layer can be determined by the method of Ref. 10, previously mentioned.

$$\text{Velocity gradient} = P = \frac{-s_0}{2(1 + \frac{1}{n})} \frac{dp}{ds}$$

$$s_0 = s_1 + s_2$$

$$s_1 = 0.376 s_m \frac{(p_{sm}/2 - p_{sm})^{-0.164}}{Q_m}$$

$$s_1 = 0.376 \times 1.9 \times \frac{(1137.5 - 1116)}{20} = 1.105 \text{ in.}$$

$$s_2 = 0$$

$$s_0 = 1.105 \text{ in.}$$

$$P_m = -0.523$$

$$\frac{dp}{ds} = 0.0594$$

$$P = -0.041$$

$$\frac{V_m - V_s}{V_s} = 0.055 \text{ (From Fig. 6)}$$

$$V_s = 53.9 \text{ ft./sec. at } x/c = 0.1325$$

4. Mixing Length.

After the separation of the laminar boundary layer, there exists a transition region in which the flow in the boundary layer is neither laminar nor turbulent. Ref. 11 gives this length as:

$$x/c = \frac{70,000}{c} \frac{\nu}{V_s}$$

For the particular condition under investigation separation occurred at $x/c = .1325$ where the following conditions existed:

$$V_s = 553.7 \text{ ft./sec.}$$

$$c = 32.03 \text{ in.}$$

$$\nu = .000297 \text{ ft.}^2/\text{sec.}$$

$$\text{Mixing length} = x/c = .01405$$

This indicates that turbulent flow is established soon after laminar separation at $x/c = .1466$.

5. Separation of the Turbulent Boundary Layer.

The possibility of separation of the turbulent boundary layer was investigated by the method of von Doenhoff and Tetarvin described in Ref. 12, and previously discussed. Since it was found that laminar separation would occur very soon after the flow progressed into the region of positive pressure gradient, it was believed that it should be satisfactory to assume that the turbulent boundary was established at the point

...
...
...
...

...
...
...

...

...
...
...
...

...
...
...

...
...
...

...

...

...

of the diffuser. An initial value of the shape parameter β was assumed as 1.296 because at the throat the pressure gradient would be zero. The initial value of momentum thickness, θ , was computed in the following manner. The boundary layer thickness at the throat was computed, and using the Prandtl - Blasius equation, which was previously given, for the velocity distribution in the boundary layer, the momentum thickness of the boundary layer was computed. This momentum thickness does not change when there is a transition from laminar to turbulent flow in the boundary layer, and so this value is suitable for the initial momentum thickness of the turbulent boundary layer.

$$\delta = 5.2 \sqrt{\frac{\nu x_2}{V}}$$

$$\delta = 5.2 \sqrt{\frac{3.615 \times 10^{-7} \times 1.105}{1.235 \times 10^{-3} \times 581 \times 12}} = .001135 \text{ ft.}$$

$$\frac{V}{V_\infty} = 2\left(\frac{y}{\delta}\right) - 2\left(\frac{y}{\delta}\right)^3 + \left(\frac{y}{\delta}\right)^4$$

$$\theta = \int_0^\delta \frac{V}{V_\infty} \left(1 - \frac{V}{V_\infty}\right) dy$$

$$\theta = .118\delta = .000134 \text{ ft.}$$

$$Re_\theta = \frac{V_\infty \theta}{\nu} = \frac{581 \times .000134}{3 \times 10^{-4}} = 260$$

The initial boundary layer conditions have been established, and the correlation for the growth of the turbulent boundary layer is shown in Table II. From the correlations it appears that the boundary layer will not separate.

1. The first part of the paper is devoted to the study of the

properties of the function $f(x)$ defined by the equation

$$f(x) = \int_0^x \frac{1}{1+t^2} dt$$

and to the study of the function $F(x)$ defined by the equation

$$F(x) = \int_0^x \frac{1}{1+t^2} dt$$

and to the study of the function $G(x)$ defined by the equation

$$G(x) = \int_0^x \frac{1}{1+t^2} dt$$

and to the study of the function $H(x)$ defined by the equation

$$H(x) = \int_0^x \frac{1}{1+t^2} dt$$

and to the study of the function $I(x)$ defined by the equation

$$I(x) = \int_0^x \frac{1}{1+t^2} dt$$

and to the study of the function $J(x)$ defined by the equation

$$J(x) = \int_0^x \frac{1}{1+t^2} dt$$



$$x + y = 1$$



$$x^2 + y^2 = 1$$

$$x^2 + y^2 = 1$$

The displacement thickness of the boundary layer at the exit of the diffuser can be determined from the relation between it, the momentum thickness and the shape parameter.

$$\text{Shape parameter} = \frac{\text{displacement thickness}}{\text{momentum thickness}}$$

$$\text{displacement thickness} = 1.536 \times .00101 = .001536 \text{ ft.}$$

The exit diameter of the diffuser will have to be increased by twice the displacement thickness to allow for the thickness of the boundary layer.

6. Skin Friction.

The skin friction in the diffuser will cause a pressure loss which can be calculated from the following equation which was developed earlier:

$$\ln \frac{p_2^0}{p_1^0} = - \int_0^1 \frac{\tau_0}{2c} \frac{dc}{p}$$

The skin friction coefficient was determined as previously explained. The pressure loss equation can be graphically integrated. A plot of the integrand is shown in Fig. 21. The graphical integration yields the following result:

$$p_1^0/p_2^0 = e^{.0025} = 1.0025$$

$$p_1^0 - p_2^0 = 3.33 \text{ lb./sq.ft.}$$

These computations show the loss due to friction to be very small which might have been expected with such a

1. *Chlorophyll a* (Chl *a*)

1. The first group of variables includes the demographic characteristics of the respondents, such as age, gender, and education level. These variables are used to control for potential confounding factors that may influence the relationship between the independent and dependent variables.

1. *Chlorophyll a* and *Chlorophyll b* were determined by the method of Arar and Collins (1971).

1. The first part of the document is a list of names and titles, including "The Hon. Mr. Justice" and "The Hon. Mr. Justice".

small L/D ratio as the duct was. Since this was the only loss which could be attributed to the internal flow in the diffuser, the exit area of the diffuser must be increased by a factor of 1.0625 to achieve the desired exit conditions.

We have been able to make estimates of the shock loss, the separation loss and the friction loss in a typical diffuser. For the particular configuration chosen, it was found that the pressure loss across the shock wave was considerable, but was accompanied by a considerable pressure recovery, and speed decrease which facilitated the work of further compression. It was found that separation did not occur for the particular symmetric configuration selected, and the expansion loss was non-existent. The loss due to friction was very small because of the short length of diffuser required. Further frictional losses in the ducting between the exit of the diffuser and the compressor entrance are shown in Fig. 22.

The method of obtaining the pressure loss due to friction in the length of constant area duct between the diffuser exit and the entrance to the compressor was the following:

Conditions at diffuser exit.

$$V = 313 \text{ ft./sec.} \quad \rho = 1.2 \text{ lb./cu.ft.}$$

$$P = 1.316 \times 10^{-3} \text{ slugs/ft.}^3$$

$$\mu = 3.71 \times 10^{-7} \text{ lb.sec./ft.}^2$$

D (uncorrected) = 1.83 ft.

Boundary layer displacement thickness = .00035 ft.

D (corrected) = $(1.83 + (2 \times .00035)) \times (1.0025)^{1/2} = 1.843$ ft.

Reynolds number = 2.27×10^6

The friction factor, f , for the length of ducting was obtained from the Moody equation which is:

$$f = .0055 \left(1 + \left(20,000 \frac{\epsilon}{D} + \frac{10^6}{Re} \right)^{1/3} \right)$$

$\epsilon = .00015$ ft.

$f = .0125$

$\Delta p = f \rho L/V^2 = .79$ lb./sq.ft.

If we assume an exit length equal to three times the exit diameter which should assure complete pressure recovery, then we can make an estimate of the pressure recovery ratio of the diffuser under investigation.

Total pressure loss due to the shock wave.

$$p_0 = 391.9 \text{ lb./sq.ft.}$$

$$p_0^* = 1437 \text{ lb./sq.ft.}$$

$$p_0^*/p_0 = .273$$

$$p_0^* - p_0 = 1045.1 \text{ lb./sq.ft.}$$

Total pressure loss due to friction in the diffuser.

$$\Delta p^* = 3.33 \text{ lb./sq.ft.}$$

Total pressure loss due to friction in the convergent area and throat of the diffuser.

1. The first part of the paper

is devoted to the study of the

properties of the

operator

defined by the

and

the

operator is defined by the

operator is defined by the

operator

operator is defined by the

operator is defined by the

operator

operator

operator

operator is defined by the

operator is defined by the

operator

operator is defined by the

operator

operator is defined by the

$$\Delta p = 2.97 \text{ lb./sq.ft.}$$

$$\frac{\Delta p}{p} \sim \frac{\Delta p^0}{p^0} \quad (\text{at low subsonic Mach numbers.})$$

$$\Delta p^0 = 3.17 \text{ lb./sq.ft.}$$

$$p_2^0 = 1.37 - 10.7 - 3.33 - 3.17 = 1330 \text{ lb./sq.ft.}$$

$$\text{Ram recovery ratio} = \frac{p_2^0 - p_0}{p_0^0 - p_0} = \frac{1330 - 391.2}{1437 - 391.9} = .898$$

It appears that the ram recovery ratio of the chosen diffuser configuration is fairly high, and that the principal pressure loss occurs through the shock wave. No attempt was made to assess entrance loss, yawing loss, turning loss, loss due to obstructions, exit loss or leakage loss because these are factors which can be minimized with proper design. It would appear from this analysis that ram recovery ratio can be kept to a reasonable value even through a normal shock proceeding the entrance of the flow into the diffuser.

Fig. 23 shows the variation of velocity ratio with flight Mach number. As is to be expected, velocity ratio decreases with increasing flight Mach number up to the sonic velocity. Due to a shock occurring in the flow ahead of the diffuser, velocity ratio increases with increasing supersonic flight velocities since the strength of the shock and the velocity decrease across

$$f(x) = \frac{1}{x} \quad \Delta$$

$$\frac{1}{x} \Delta \approx \frac{1}{x} \Delta$$

$$f(x) = \frac{1}{x} \quad \Delta$$

$$f(x) = \frac{1}{x} \quad \Delta$$

$$\frac{1}{x} \Delta \approx \frac{1}{x} \Delta$$

$$\Delta$$

$$\Delta$$

$$\Delta \approx \frac{1}{x} \Delta$$

$$\Delta \approx \frac{1}{x} \Delta$$

$$\Delta \approx \frac{1}{x} \Delta$$

$$\Delta \approx \frac{1}{x} \Delta$$

$$\Delta \approx \frac{1}{x} \Delta$$

$$\Delta \approx \frac{1}{x} \Delta$$

$$\Delta \approx \frac{1}{x} \Delta$$

$$\Delta$$

$$\Delta$$

$$\Delta$$

$$\Delta$$

$$\Delta$$

$$\Delta \approx \frac{1}{x} \Delta$$

$$\Delta$$

$$\Delta$$

the shock increase with increasing Mach number. Velocity ratio increases with altitude as flight mach number increases because of the variation of Mach number with temperature. Temperature decreases with altitude, sonic velocity decreases, and a lesser flight velocity gives the same Mach number.

Fig. 24 shows the increase of density ratio with flight mach number. This ratio is also a measure of the mass flow through the engine. The entrance area and entrance velocity are fixed. The former is fixed due to diffuser design; the latter due to the engine speed and permissible volume flow. The mass flow through the engine, therefore, with a fixed engine speed varies directly with the flow density at the diffuser entrance. Entrance density increases with flight Mach number because of the recovery of ram pressure ahead of the diffuser entrance. The reduction in entrance density with increasing altitude is due to the reduced ambient air density at altitude.

CHAPTER VI

PRESENT AIR INLET DESIGN FEATURES

Whereas a few short years ago the idea of driving an aircraft with anything except a propeller would have been scoffed at, now dozens of practical jet propelled bombers and fighter planes are available. A survey of the field will reveal a wide variation of entrance duct designs, and air inlet locations. It must be remembered, however, that the majority of these airplanes were designed for subsonic speeds, although several experimental designs for transonic and supersonic flight are also available.

Designs which feature fuselage engine installations are confined to fighter types. The air entrance duct locations vary with the different designs. Examples of the nose inlet ducts are the Republic P-84, the North American P-86, the Republic XF-91, and the McDonnell XF-85. One thing common to all these models is an axial flow turbojet engine.

The P-84 had serious duct trouble in its development. The inlet duct is divided into two rectangular ducts aft of the circular nose inlet. The ducts extend along the side of the fuselage to a Y inlet assembly at the face of the engine. The ducts are fifteen feet long and considerable leakage occurred in the early

models. Losses in the Y duct were reduced by the use of sealing compound and a decrease in fastener spacing. To clear the pressurized portion of the fuselage the ducts extend down along the side and then rise upward. To eliminate losses due to duct bends, the engine was tipped down four degrees to permit a straight connection with the air inlet ducts. This requires a similar four degree bend aft of the engine at the tail cone splice. Auxiliary air inlets near the compressor inlet for low speed flight were considered, but the complexity outweighed the thrust saving which would have amounted to four per cent gain in static thrust. Present development of an improved model of the F-84 envisages a flush type air inlet instead of the stagnation point inlet

The F-86, present holder of the world's air speed record, differs from the F-84 in that the air entrance duct is not divided but passes directly rearward to the compressor inlet. The cockpit floor is located above the air duct. The nose air inlet features an extended upper lip to furnish adequate air to the engine at high angles of attack. The latest version of the F-86, the XF-88, will feature flush type air inlets.

The XF-91, a new high speed, high altitude interceptor reputed to be capable of supersonic speed, has a divided air inlet duct with a four to five foot sting projecting out of it. It is not known if this sting is to function as an Oswatitch type diffuser (Ref. 7) or not.

The XF-85, the parasite fighter, features an annular type nose air inlet. The air inlet duct leads directly to the face of the compressor of the Westinghouse J-34 axial flow turbojet.

Examples of fighter designs employing wing-fuselage junction air inlets to engines installed in the fuselage are the Chance-Vought XF6U and the F7U, the Grumman F9F, the McDonnell XF-88, and the following British designs, the Hawker H. 7/46 and Gloster G. 1/44. Both axial flow and centrifugal flow type engines are represented in these airplanes.

The XF6U has semi-circular shaped air inlets, the semi-circles projecting below the wing. No information seems to be available on this configuration which is unique, but the change in the orientation of the duct entrance on the F7U would indicate that the first installation was not entirely satisfactory. Semi-circular shaped entrance ducts are also used on the F7U, but the semi-circle now appears as a scoop extending out of the fuselage. To improve the velocity distribution across the face of the air inlet, a boundary layer suction slot is provided adjacent to the fuselage. Information about the duct problems with these aircraft is not available, but some information on the design principles can be gleaned from Ref. 22 which was written by a member of the Chance Vought engineering staff. In this reference the author recommends a velocity ratio of 0.7 at the

maximum speed flight condition with a flow velocity at the compressor inlet of about 200 miles per hour. A good duct six feet long, with a gentle curvature of five to ten degrees gives about a one per cent total pressure loss, equivalent to a 1.7 - 2.0 per cent loss in thrust. An S-shaped duct with two gentle bends having a total curvature of sixty degrees gives a three to four per cent total pressure loss corresponding to a five to eight per cent loss in thrust. The air entrance duct configuration of the F70 and the Gloster 4.1/46 are very similar, semi-circular in shape with a boundary layer bleed next to the fuselage. Internally some difference must exist since the F70 has two J-34 engines while the S. 1/46 has a single Rolls-Royce "Gene".

The P9F, the XF-88 and the Hawker S. 7/46 have triangular shaped air entrance ducts with the base of the triangle adjacent to the fuselage. Whether boundary layer suction slots are used at the fuselage is not evident from pictures of the installations. The air inlet of the P9F is normal to the direction of flow. The air inlets of the XF-88 and the S. 7/46 have an angularity in plan view. The upper lip of the S. 7/46 also extends beyond the lower lip. McDonnell must have solved the problem of lateral flow across the face of the duct which caused velocity distribution problems on a similar configuration in the XF-1. On the XF-1 of which the XF-88 was a prototype the orientation of the

face of the duct entrance was changed to be normal to the air flow direction. The $K_7/46$ features four auxiliary blower doors opening directly into the plenum chamber for low speed and ground operation of the engine. The ducting of the $K_7/46$ is unique in that having two air intakes in the wing root, it also has two exhaust outlets in the wing trailing edge at the fuselage. A single engine is located in the fuselage. The Hawker air inlet design must have proven satisfactory because it is retained on the new Hawker P.1052.

Fighters have ^{ing}scoop type air entrance ducts to engine installations in the fuselage are the Lockheed P-30, TP-30, and XF-90, the Northrop XP-39, and the Vickers-Armstrong "Attacker". The air inlet ducts of the P-30 and TP-30 are nostril shaped on either side of the fuselage ahead of the wing root. Ref. 23 gives an explanation of the choice of entrance duct location and reveals some of the problems encountered with this design. It was found that unstable duct flow resulted at low flow ratios due to flow breakdown and boundary layer separation. The flow separation gave a loud duct "rumble" which could be heard for miles. Directional "shaking" of the aircraft could also be traced to this source. During ground operation flow reversal occurred in the ducts, flow coming in the duct on one side and out the duct on the opposite side. Introduction of a boundary layer ahead of the duct entrances cured the

difficulties at a cost of two to three miles per hour in airspeed. The final result was a net ram at high speed equal to seventy per cent of the available adiabatic compression ratio. Spring loaded doors behind the pilot supply air to the compressor at low speeds and for ground operation.

The XF-90 was originally reported to have a flush type air inlet duct, but pictures show ducts similar to those employed on the F-80. The XF-90, however, has two axial flow turbojets in the fuselage whereas the F-80 had one centrifugal flow engine. The XF-89 has two engines slung semi-externally from the lower part of the fuselage. Semi-circular air inlet ducts lead directly to the two J-35 engines. It would seem that a uniform flow at the compressor entrance would be difficult with this design. The "Attacker" has air inlet ducts in the shape of circular arcs, less than semi-circles. The inlets project from the fuselage forward of the wing. Boundary layer slots are located adjacent to the fuselage at the duct entrances. The flow through the boundary layer slots exhausts through louvred openings in the fuselage skin aft of the duct entrance. The main air ducts follow aft on both sides of the fuselage and dump into a plenum chamber at the forward face of the engine. An auxiliary air intake on top of the fuselage provides air to the engine for ground operation.

Three fighter designs which have engine installations in the wings are the McDonnell F4U-1, and F2H-1 and the Curtiss P-57. The McDonnell models are similar in appearance with similar engine installations and air inlet ducts. The F4U-1 is equipped with two Westinghouse 19XB axial flow jet engines; the F2H-1 is equipped with two J-34 engines. The engines are located in the wing roots and a triangular shaped air inlet is used. It is claimed that this configuration gives a constant velocity distribution across the inlet face, and the ram pressure recovery is 99 per cent of that available. The design is said to be free from internal flow separation at any velocity ratio to be expected in normal operation. Due to the fact that the upper and lower portions of the powerplant section act as two thin airfoils, the critical Mach number of the wing root is higher than that of the outer wing panel. To cool the powerplant section and bleed off the boundary layer adjacent to the fuselage, a boundary layer suction slot is provided at the air inlet. The air from the suction slot flows through the accessory compartment and thence into the air stream. A reverse flow through the boundary layer suction slot occurs in ground operation, but no adverse effects are noticed with this flow reversal.

The P-57 is powered by four J-34 engines. The engines are installed in nacelles in the wings, two engines to each nacelle. The engine nacelles are about

ten feet long so that the air entrance duct must necessarily be short. A single rectangular shaped air inlet provides air to the two engines in each nacelle, the flow dividing just aft of the entrance. The air intake ducts are protected to prevent icing or water entering during heavy rain. The extent or nature of this protection was not made known.

The bomber types almost all have engines installed in the wings, or attached to the wings. The air inlets, therefore, are of the stagnation point type. Representative installations are those on the Consolidated XB-46, Boeing XB-47, Martin XB-48 and the Northrop YB-49. The XB-46 has four engines contained in two engine nacelles slung below the wing. One elliptical air inlet provides flow to both engines in the same nacelle. The air inlet duct is divided just aft of the entrance. The XB-47 holds the transcontinental flight record, crossing the U.S. in 3 hours and 46 minutes and averaging 607.2 miles per hour. It has six engines supported by pylons extending down from the wing, two engines mounted on each of the inboard pylons and one engine on each of the outboard pylons. The air inlet ducts are annular, one for each engine. On the inboard pylons where the engines are located adjacent to each other, the segments of the outer cones common to both engines extend further forward than the remainder of the inlet rim to prevent interaction of the individual flows to

each engine. The XB-47 also has six engines, three on each wing in a common nacelle. The air entrance ducts to each engine are annular in form, and tunnels through the nacelle are provided between adjacent engines to keep the critical Mach number over the wings as high as possible. The YB-49 has four engines located side by side in each wing. The air inlet to the engines is located in the wing leading edge. The air inlet is wide and narrow with internal partitions to divide the flow to each engine.

The Martin P4M-1 is an example of a hybrid installation. Its main motive power is two reciprocating engines with two jet engines for additional power when needed. One reciprocating engine and one jet engine are mounted in a common nacelle projecting below the wing. When the jet engine is in operation air is provided through a scoop which opens forward and down from the nacelle. When the jet engine is not operating the scoop retracts and its bottom provides the lower forward face of the nacelle. Since the top speed of the P4M-1 is not very high, ram recovery is not a serious problem and careful duct design is not critical.

The experimental planes designed to investigate flight at or near the sonic velocity are not unlike the latest fighter designs. The Douglas D558-1 designed for high subsonic velocities features a circular nose inlet with the ducting dividing just aft of the inlet.

1. The first part of the paper is devoted to the

study of the properties of the function

$$f(x) = \sum_{n=0}^{\infty} \frac{x^n}{n!}$$

and its derivatives. It is shown that

the function $f(x)$ is entire and that

$$f(x) = e^x \quad \text{for all } x \in \mathbb{C}.$$

Moreover, it is proved that

$$f(x) = \lim_{n \rightarrow \infty} \left(1 + \frac{x}{n} \right)^n$$

for all $x \in \mathbb{C}$. This result is known as

$$e^x = \lim_{n \rightarrow \infty} \left(1 + \frac{x}{n} \right)^n$$

and is one of the most important properties

of the exponential function. It is also

shown that the function $f(x)$ satisfies the

$$f(x+y) = f(x)f(y) \quad \text{for all } x, y \in \mathbb{C}.$$

This property is characteristic of the

$$f(x) = e^x \quad \text{and is used to prove that}$$

$$f(x) = e^x \quad \text{for all } x \in \mathbb{C}.$$

The second part of the paper is devoted

to the study of the function

$$g(x) = \sum_{n=0}^{\infty} \frac{x^n}{n!} \quad \text{for } x \in \mathbb{R}.$$

It is shown that the function $g(x)$ is

$$g(x) = e^x \quad \text{for all } x \in \mathbb{R}.$$

The third part of the paper is devoted

to the study of the function

$$h(x) = \sum_{n=0}^{\infty} \frac{x^n}{n!} \quad \text{for } x \in \mathbb{C}.$$

It is shown that the function $h(x)$ is

$$h(x) = e^x \quad \text{for all } x \in \mathbb{C}.$$

The split duct rejoins just forward of the J-33 jet engine. The ducting and air inlet are similar to the installation on the P-64.

The Douglas D558-II, a combination rocket and turbo-jet powered airplane, is designed for supersonic speeds. It features two flush air inlets on either side of the lower, forward fuselage. Few details on these air inlets are available. NACA was responsible for the design. Pictures show nothing projecting beyond the contour of the fuselage.

The Consolidated 7002 research plane, powered by a J-33 engine, has a circular air inlet in the nose of the fuselage. A sting projects forward out of the center of the air inlet. It is reported that this sting is an Oswatitsch type diffuser (Ref. 7). Further details on the air inlet ducting are not available.

The Northrop X-4, designed to investigate the transonic speed range, Mach numbers 0.8 - 1.2, is powered by two Westinghouse 19XB engines installed at the wing-fuselage junction. Scoop type air inlet ducts supply the engine air. The shape of the duct entrances is not unlike that of the P-60.

The Armstrong-Whitworth 52, a British design to test the potentialities of the flying wing, is powered by two Rolls-Royce "Nene" engines, located in separate nacelles projecting below the wing. The air inlet duct entrance to each is elliptical with an overhanging upper

... ..

... ..

... ..

... ..

... ..

... ..

... ..

... ..

... ..

... ..

... ..

... ..

... ..

... ..

... ..

... ..

... ..

... ..

... ..

... ..

... ..

... ..

... ..

... ..

... ..

lip. A novel feature of the air inlet ducting is the auxiliary source of air at low speeds. A boundary layer suction slot on the wing near the tip at the fifty per cent chord point supplies air directly to the plenum chamber at low speed flight. This serves a dual purpose. In addition to supplying additional air to the engine, it delays wing tip stall. It would seem that such a system would have great possibility.

This resume of the types and locations of engine air inlet ducts on some representative modern airplanes reveals the variations in design which have been successful in the past. The trend in experimental aircraft is just as varied. The results of flights with the experimental aircraft may show that one type of installation is superior to another, but more than likely it will only show that the final design must still be a compromise.

1. The first part of the paper discusses the importance of the study.

2. The second part of the paper discusses the methodology used.

3. The third part of the paper discusses the results of the study.

4. The fourth part of the paper discusses the conclusions of the study.

5. The fifth part of the paper discusses the implications of the study.

6. The sixth part of the paper discusses the limitations of the study.

7. The seventh part of the paper discusses the future research.

8. The eighth part of the paper discusses the acknowledgments.

9. The ninth part of the paper discusses the references.

10. The tenth part of the paper discusses the appendices.

11. The eleventh part of the paper discusses the index.

12. The twelfth part of the paper discusses the glossary.

13. The thirteenth part of the paper discusses the bibliography.

14. The fourteenth part of the paper discusses the list of figures.

15. The fifteenth part of the paper discusses the list of tables.

16. The sixteenth part of the paper discusses the list of abbreviations.

17. The seventeenth part of the paper discusses the list of symbols.

18. The eighteenth part of the paper discusses the list of equations.

19. The nineteenth part of the paper discusses the list of formulas.

20. The twentieth part of the paper discusses the list of diagrams.

21. The twenty-first part of the paper discusses the list of charts.

22. The twenty-second part of the paper discusses the list of graphs.

23. The twenty-third part of the paper discusses the list of maps.

24. The twenty-fourth part of the paper discusses the list of photographs.

25. The twenty-fifth part of the paper discusses the list of illustrations.

26. The twenty-sixth part of the paper discusses the list of figures.

27. The twenty-seventh part of the paper discusses the list of tables.

28. The twenty-eighth part of the paper discusses the list of abbreviations.

29. The twenty-ninth part of the paper discusses the list of symbols.

30. The thirtieth part of the paper discusses the list of equations.

CHAPTER VII

CONCLUSIONS AND RECOMMENDATIONS

In this report an attempt has been made to investigate analytically the performance of a diffuser for use in a turbo-jet engine at transonic flight speeds. The factors which detract from diffuser performance have been explored, and means to minimize these losses have been discussed. Convenient methods of determining the magnitude of these losses analytically have been suggested, but final corroboration of these methods will depend upon future experimental verification.

It was found that the internal diffuser flow was not affected greatly by the presence of a shock wave ahead of the diffuser entrance. With such a situation, the internal flow in the diffuser was not materially different from that resulting at subsonic flight speeds. The losses encountered across such a shock wave were not found to penalize the diffuser performance greatly at flight mach numbers below 1.5. Of course, the validity of these findings, and the advisability of allowing a detached shock to form ahead of the diffuser entrance are open to question.

It is believed that the key to the advisability of utilizing a shock ahead of the diffuser entrance to assist in ram pressure recovery, lies in the extent of

the influence of this shock on the drag of the airplane. It is also believed that the drag of the airplane will be affected by the velocity ratio of the airflow entering the diffuser. The limits of velocity ratio, particularly the lower limit, found suitable for subsonic flight will not necessarily be satisfactory for supersonic flight. Experimental investigation of this problem is warranted. It may be found that the lower limit of allowable velocity ratio is raised so high that it complicates the internal flow of the diffuser.

Other problems which are associated with the detached shock wave, and which should be investigated experimentally are the location of the shock wave ahead of the diffuser entrance, and the persistence of turbulence induced in the flow by the shock wave. The location of the shock wave is of interest primarily in that it might explain the limits of permissible velocity ratios, and might be a measure of the shock induced turbulence entering the diffuser. The persistence of the shock induced turbulence is of interest because it will have great influence on the internal diffuser flow if it persists beyond the throat of the diffuser. This shock induced turbulence if it is transmitted to the boundary layer in the region of positive pressure gradient will limit the rate of pressure recovery, or may cause internal flow separation.

Two dimensional effects at the entrance and exit of the diffuser section are not explained clearly in any of the literature dealing with flow in a diffuser, although hints are given in Refs. 3 and 21 when it is suggested that extra lengths of constant area ducting following the diverging section are necessary for complete pressure recovery. It would be interesting to investigate experimentally the velocity profile across the face of the diffuser at various velocity ratios, for both subsonic and supersonic flows. The velocity profile at the diffuser exit would be of even greater interest, particularly its variation with diffuser length and divergence angle, and the effect of suction slots and induced rotation on the velocity profile. This latter effect, induced flow rotation, is not mentioned in any of the literature on diffuser flow encountered to date. The advantages of a flow with rotation are set forth in Ref. 3. With rotating flow in a diffuser, separation is delayed and more complete pressure recovery is obtained in the diffuser proper. Since the diffuser exhausts to the compressor, a rotating machine, it is reasonable to believe that rotation of flow in the diffuser will be induced by the compressor rotation. The strength of the rotation and the region of flow affected would be useful design information.

Finally, the development of the boundary layer in a diffuser is worthy of investigation. The method of

analysis suggested in Ref. 12 is not strictly applicable to flow in a duct, and it also entails considerable computation. An experimental investigation involving variation of rates of pressure recovery and diffuser lengths, with necessary corrections for variation of the Reynolds number, could speed the problem of diffuser analysis and fill a gap in the study of diffuser performance. Past investigations of permissible diffuser divergence angles have neglected the effect of diffuser length, and have been conducted at area ratios such higher than those necessary for a turbo-jet engine air inlet duct.

It is not felt that these suggestions for future investigation exhaust the possibilities for diffuser research. It is believed that they include the more immediately important items, those topics neglected in the past which may influence diffuser performance at transonic speeds. Other subjects, equally interesting, will probably be suggested by discussions in the body of the report. Undoubtedly, ideas on diffuser performance and analysis different from those included in this report will arise, and errors in reasoning may be found, but if this report stimulates thought on diffuser problems, then it has fulfilled its purpose.

APPENDIX I

SYMBOLS

- a - speed of sound.
- A - cross-sectional area.
- c_p - specific heat at constant pressure.
- c_v - specific heat at constant volume.
- M - Mach number, V/a .
- n - exponent for a polytropic process, $pv^n =$
constant.
- p - static pressure.
- p^0 - total pressure.
- q - dynamic pressure, $\frac{1}{2} \rho V^2$.
- R - gas constant, 1545/molecular weight.
- ds - change in entropy.
- T - static temperature.
- T^0 - total temperature.
- V - velocity.
- γ - ratio of specific heats.
- η_0 - diffuser efficiency.
- $1+\eta$ - compressibility factor.
- μ - coefficient of viscosity.
- ν - kinematic viscosity, μ/ρ .
- ρ - density.

where symbols other than the above are used in the text, they are defined where used.

1. The first part of the paper is devoted to the study of the properties of the function $f(x)$ defined by the equation $f(x) = \sum_{n=0}^{\infty} a_n x^n$, where a_n are the coefficients of the power series. It is shown that the function $f(x)$ is analytic in the disk $|x| < 1$ and that it satisfies the functional equation $f(x) = x f(x^2) + g(x)$, where $g(x)$ is a certain function.

2. In the second part, the properties of the function $f(x)$ are studied in more detail. It is shown that the function $f(x)$ is bounded in the disk $|x| < 1$ and that it has a certain symmetry property. It is also shown that the function $f(x)$ is not identically zero.

3. In the third part, the properties of the function $f(x)$ are studied in more detail. It is shown that the function $f(x)$ is not identically zero and that it has a certain symmetry property. It is also shown that the function $f(x)$ is bounded in the disk $|x| < 1$.

REFERENCES

1. Hanson, Frederick H., Jr. and Vossman, Emmet A.: Effect of Pressure Recovery on the Performance of a Jet Propelled Airplane. NACA TN No. 1695, September, 1948.
2. Leipmann, H. W., and Puckett, A. E.: Introduction to the Aerodynamics of a Compressible Fluid. Third Printing, 1948. John Wiley and Sons, New York.
3. Patterson, G. N.: Modern Diffuser Design. Aircraft Engineering, Vol. 10, September 1938.
4. Zucrow, M. J.: Principles of Jet Propulsion and Gas Turbines. 1948. John Wiley and Sons, New York.
5. Kenan, J. H., and Kaye, J.: Gas Tables. 1948. John Wiley and Sons, New York.
6. Kantrowitz, A., and Donaldson, C. duP.: Preliminary Investigations of Supersonic Diffusers. NACA ACR L5D20, May 1945.
7. Oswatitsch, K.: Pressure Recovery for Missiles with Reaction Propulsion at High Supersonic Speeds. NACA TN No. 1140, June 1947.
8. Cox, S. M. and Germano, P. J.: Fluid Mechanics. Third printing, 1946. D. van Nostrand and Company, New York.
9. Dryden, H. L.: Some Recent Contributions to the Study of Transition and Turbulent Boundary Layers, NACA TN No. 1168, April 1947.
10. von Doenhoff, A. E.: A Method of Rapidly Estimating the Position of the Laminar Separation Point. NACA TN No. 671, October 1933.
11. von Doenhoff, A. E.: A Preliminary Investigation of Boundary Layer Transition along a Flat Plate with Adverse Pressure Gradient. NACA TN No. 639, 1933.
12. von Doenhoff, A. E., and Tetervin, E.: Determination of General Relations for the Behavior of Turbulent Boundary Layers. NACA TN No. 772, 1943.

13. Dodge, R. A. and Thompson, W. J.: Fluid Mechanics. 1937. First Edition, McGraw-Hill Book Co., New York.
14. Squire, H. B.: A Note on Boundary Layer Flow. British A.R.C., R. & M. No. 1664.
15. Garner, H. G.: The Development of Turbulent Boundary Layers. British A.R.C., R. & M. No. 2133, June 1944.
16. Squire, H. B., and Young, A. D.: The Calculation of the Profile drag of Airfoils. British A.R.C., R. & M. No. 1438, 1938.
17. Goldstein, S.: Modern Developments in Fluid Dynamics, Vol. I. Oxford, Clarendon Press. 1938.
18. Young, A. D., and Green, S. L.: Tests of High Speed Flow in Diffusers of Rectangular Cross-Section. British A.R.C., R. & M. No. 2201, July 1944.
19. Patterson, G. H.: Corner Losses in Ducts. Aircraft Engineering, Vol. IX, August 1937.
20. Patterson, G. H.: The Design of Aeroplane Ducts. Aircraft Engineering, Vol. XI, July 1939.
21. Peters, H.: Conversion of Energy in Cross-Sectional Divergences under Different Conditions of Inflow, NACA Tech. No. 737, 1934.
22. Jordan, T. J.: Design of Turbo-jet Installations, Part I. Aero Digest, October 1943.
23. Johnson, C. L.: Development of the Lockheed P-30A Jet Fighter Airplane. Journal of the Aeronautical Sciences, December 1947.

... ..

... ..

... ..

... ..

... ..

... ..

... ..

... ..

... ..

... ..

... ..

... ..

TABLE I

HYDRODYNAMIC CONDITIONS IN THE HYPERBOLIC

$M_0 = 1.5$

$n = 40,000 \text{ feet}$

| x | x/c | $1/Dt$ | A/A_t | p
lb/ft^2 | P
$\frac{slugs}{ft^3}$ | σ_H | v
ft/sec | q
$\frac{lb}{ft^2}$ | dq/dx |
|------|-------|--------|---------|------------------|-----------------------------|------------|-----------------|--------------------------|---------|
| .409 | 0 | 1.03 | 1.114 | 1139 | 1.261×10^{-3} | 550 | 470 | 139.5 | |
| .43 | .0065 | 1.005 | 1.133 | 1174 | 1.250 | 548 | 494 | 152.5 | |
| .45 | .0137 | 1.010 | 1.097 | 1160 | 1.240 | 547 | 516 | 165.3 | |
| .47 | .0225 | 1.03 | 1.062 | 1145 | 1.230 | 545 | 538 | 177.3 | |
| .49 | .0349 | 1.014 | 1.03 | 1130 | 1.218 | 543 | 558 | 189 | |
| .51 | .0613 | 1.0 | 1.0 | 1116 | 1.205 | 541 | 581 | 204 | |
| .549 | .1175 | 1.01 | 1.03 | 1130 | 1.218 | 543 | 598 | 189 | -6.10 |
| .47 | .1350 | 1.03 | 1.062 | 1145 | 1.230 | 545 | 538 | 178 | -5.54 |
| .45 | .2520 | 1.066 | 1.097 | 1160 | 1.240 | 547 | 516 | 165 | -5.00 |
| .43 | .319 | 1.065 | 1.133 | 1174 | 1.250 | 548 | 494 | 153 | -4.52 |
| .41 | .603 | 1.036 | 1.180 | 1188 | 1.261 | 550 | 472 | 141 | -4.00 |
| .39 | .512 | 1.12 | 1.255 | 1207 | 1.276 | 553 | 439 | 122 | -3.53 |
| .35 | .700 | 1.16 | 1.348 | 1225 | 1.290 | 555 | 405 | 106 | -3.12 |
| .32 | .877 | 1.205 | 1.450 | 1241 | 1.301 | 557 | 371 | 90 | -2.78 |
| .30 | 1.000 | 1.24 | 1.541 | 1251 | 1.310 | 559 | 345 | 79 | -2.70 |

0 1 2 3 4 5 6 7 8 9

1997, 1998, 1999, 2000, 2001, 2002, 2003, 2004, 2005, 2006, 2007, 2008, 2009, 2010, 2011, 2012, 2013, 2014, 2015, 2016, 2017, 2018, 2019, 2020, 2021, 2022, 2023, 2024, 2025, 2026, 2027, 2028, 2029, 2030, 2031, 2032, 2033, 2034, 2035, 2036, 2037, 2038, 2039, 2040, 2041, 2042, 2043, 2044, 2045, 2046, 2047, 2048, 2049, 2050, 2051, 2052, 2053, 2054, 2055, 2056, 2057, 2058, 2059, 2060, 2061, 2062, 2063, 2064, 2065, 2066, 2067, 2068, 2069, 2070, 2071, 2072, 2073, 2074, 2075, 2076, 2077, 2078, 2079, 2080, 2081, 2082, 2083, 2084, 2085, 2086, 2087, 2088, 2089, 2090, 2091, 2092, 2093, 2094, 2095, 2096, 2097, 2098, 2099, 2100, 2101, 2102, 2103, 2104, 2105, 2106, 2107, 2108, 2109, 2110, 2111, 2112, 2113, 2114, 2115, 2116, 2117, 2118, 2119, 2120, 2121, 2122, 2123, 2124, 2125, 2126, 2127, 2128, 2129, 2130, 2131, 2132, 2133, 2134, 2135, 2136, 2137, 2138, 2139, 2140, 2141, 2142, 2143, 2144, 2145, 2146, 2147, 2148, 2149, 2150, 2151, 2152, 2153, 2154, 2155, 2156, 2157, 2158, 2159, 2160, 2161, 2162, 2163, 2164, 2165, 2166, 2167, 2168, 2169, 2170, 2171, 2172, 2173, 2174, 2175, 2176, 2177, 2178, 2179, 2180, 2181, 2182, 2183, 2184, 2185, 2186, 2187, 2188, 2189, 2190, 2191, 2192, 2193, 2194, 2195, 2196, 2197, 2198, 2199, 2200, 2201, 2202, 2203, 2204, 2205, 2206, 2207, 2208, 2209, 2210, 2211, 2212, 2213, 2214, 2215, 2216, 2217, 2218, 2219, 2220, 2221, 2222, 2223, 2224, 2225, 2226, 2227, 2228, 2229, 2230, 2231, 2232, 2233, 2234, 2235, 2236, 2237, 2238, 2239, 2240, 2241, 2242, 2243, 2244, 2245, 2246, 2247, 2248, 2249, 2250, 2251, 2252, 2253, 2254, 2255, 2256, 2257, 2258, 2259, 2260, 2261, 2262, 2263, 2264, 2265, 2266, 2267, 2268, 2269, 2270, 2271, 2272, 2273, 2274, 2275, 2276, 2277, 2278, 2279, 2280, 2281, 2282, 2283, 2284, 2285, 2286, 2287, 2288, 2289, 2290, 2291, 2292, 2293, 2294, 2295, 2296, 2297, 2298, 2299, 2300, 2301, 2302, 2303, 2304, 2305, 2306, 2307, 2308, 2309, 2310, 2311, 2312, 2313, 2314, 2315, 2316, 2317, 2318, 2319, 2320, 2321, 2322, 2323, 2324, 2325, 2326, 2327, 2328, 2329, 2330, 2331, 2332, 2333, 2334, 2335, 2336, 2337, 2338, 2339, 2340, 2341, 2342, 2343, 2344, 2345, 2346, 2347, 2348, 2349, 2350, 2351, 2352, 2353, 2354, 2355, 2356, 2357, 2358, 2359, 2360, 2361, 2362, 2363, 2364, 2365, 2366, 2367, 2368, 2369, 2370, 2371, 2372, 2373, 2374, 2375, 2376, 2377, 2378, 2379, 2380, 2381, 2382, 2383, 2384, 2385, 2386, 2387, 2388, 2389, 2390, 2391, 2392, 2393, 2394, 2395, 2396, 2397, 2398, 2399, 2400, 2401, 2402, 2403, 2404, 2405, 2406, 2407, 2408, 2409, 2410, 2411, 2412, 2413, 2414, 2415, 2416, 2417, 2418, 2419, 2420, 2421, 2422, 2423, 2424, 2425, 2426, 2427, 2428, 2429, 2430, 2431, 2432, 2433, 2434, 2435, 2436, 2437, 2438, 2439, 2440, 2441, 2442, 2443, 2444, 2445, 2446, 2447, 2448, 2449, 2450, 2451, 2452, 2453, 2454, 2455, 2456, 2457, 2458, 2459, 2460, 2461, 2462, 2463, 2464, 2465, 2466, 2467, 2468, 2469, 2470, 2471, 2472, 2473, 2474, 2475, 2476, 2477, 2478, 2479, 2480, 2481, 2482, 2483, 2484, 2485, 2486, 2487, 2488, 2489, 2490, 2491, 2492, 2493, 2494, 2495, 2496, 2497, 2498, 2499, 2500, 2501, 2502, 2503, 2504, 2505, 2506, 2507, 2508, 2509, 2510, 2511, 2512, 2513, 2514, 2515, 2516, 2517, 2518, 2519, 2520, 2521, 2522, 2523, 2524, 2525, 2526, 2527, 2528, 2529, 2530, 2531, 2532, 2533, 2534, 2535, 2536, 2537, 2538, 2539, 2540, 2541, 2542, 2543, 2544, 2545, 2546, 2547, 2548, 2549, 2550, 2551, 2552, 2553, 2554, 2555, 2556, 2557, 2558, 2559, 2560, 2561, 2562, 2563, 2564, 2565, 2566, 2567, 2568, 2569, 2570, 2571, 2572, 2573, 2574, 2575, 2576, 2577, 2578, 2579, 2580, 2581, 2582, 2583, 2584, 2585, 2586, 2587, 2588, 2589, 2590, 2591, 2592, 2593, 2594, 2595, 2596, 2597, 2598, 2599, 2600, 2601, 2602, 2603, 2604, 2605, 2606, 2607, 2608, 2609, 2610, 2611, 2612, 2613, 2614, 2615, 2616, 2617, 2618, 2619, 2620, 2621, 2622, 2623, 2624, 2625, 2626, 2627, 2628, 2629, 2630, 2631, 2632, 2633, 2634, 2635, 2636, 2637, 2638, 2639, 2640, 2641, 2642, 2643, 2644, 2645, 2646, 2647, 2648, 2649, 2650, 2651, 2652, 2653, 2654, 2655, 2656, 2657, 2658, 2659, 2660, 2661, 2662, 2663, 2664, 2665, 2666, 2667, 2668, 2669, 2670, 2671, 2672, 2673, 2674, 2675, 2676, 2677, 2678, 26

• • • • •

1 2 3 4 5 6 7 8 9 10 11 12 13 14 15 16 17 18 19 20 21 22 23 24 25 26 27 28 29 30 31 32

I • • • • • • •

1 2 3 4 5 6 7 8 9 10 11 12 13 14 15 16 17 18 19 20 21 22 23 24 25 26 27 28 29 30 31 32 33 34 35 36 37 38 39 40 41 42 43 44 45 46 47 48 49 50 51 52 53 54 55 56 57 58 59 60 61 62 63 64 65 66 67 68 69 70 71 72 73 74 75 76 77 78 79 80 81 82 83 84 85 86 87 88 89 90 91 92 93 94 95 96 97 98 99 100

TABLE II
COMPUTATION OF THE TYPICAL SEPARATION
OF THE TURBULENT BOUNDARY LAYER

$$M_0 = 1.5$$

$$h = 40,000 \text{ ft.}$$

$$c/q_0 = .1575$$

| x/c | R_0 | e/c | H | q/q_0 | $\frac{c}{q_0} \frac{dq}{dx}$ | $\tau_0/2q$ |
|-------|-------|------------------------|-------|---------|-------------------------------|-----------------------|
| .0613 | 260 | $.0501 \times 10^{-3}$ | 1.236 | 1 | 0 | 3.14×10^{-3} |
| .070 | 394 | $.0759 \times 10^{-3}$ | 1.236 | .99 | -1.025 | 2.41×10^{-3} |
| .09 | 635 | .1347 | 1.239 | .963 | -.995 | 2.43 |
| .20 | 2090 | .4267 | 1.305 | .850 | -.850 | 1.81 |
| .30 | 3210 | .6852 | 1.323 | .765 | -.735 | 1.71 |
| .40 | 4320 | .9657 | 1.343 | .690 | -.637 | 1.60 |
| .50 | 5490 | 1.275 | 1.365 | .633 | -.575 | 1.53 |
| .60 | 6350 | 1.623 | 1.390 | .572 | -.530 | 1.46 |
| .65 | 7350 | 1.423 | 1.405 | .545 | -.512 | 1.44 |
| .73 | 8310 | 2.271 | 1.431 | .505 | -.435 | 1.39 |
| .80 | 9910 | 2.630 | 1.459 | .475 | -.465 | 1.36 |
| .85 | 10720 | 2.920 | 1.483 | .445 | -.450 | 1.35 |
| .90 | 11630 | 3.242 | 1.510 | .427 | -.436 | 1.34 |
| .94 | 12400 | 3.527 | 1.536 | .411 | -.426 | 1.31 |
| .97 | 13060 | 3.760 | 1.559 | .400 | -.420 | 1.30 |
| 1.00 | 13750 | 4.010 | 1.560 | .389 | -.415 | 1.29 |

1/2

10

TABLE II (Continued)

| $\frac{n+2}{2}$ | $\frac{q}{q}$ | $\frac{dq}{dx}$ | $\frac{dq}{dx}$ | $\Delta q/c$ | $-\frac{q}{q} \frac{dq}{dx} \frac{2q}{q_0}$ | $\frac{2.035}{x}$
($n=1.236$) |
|-----------------|------------------|-----------------------|------------------------|--------------|---|------------------------------------|
| 0 | | 3.14×10^{-3} | $.0253 \times 10^{-3}$ | | 0 | 0 |
| -.129 | $\times 10^{-3}$ | 2.94 | .0588 | | .028 | 0 |
| -.229 | | 2.66 | .292 | | .0572 | .0057 |
| -.705 | | 2.535 | .2535 | | .2270 | .0386 |
| -1.095 | | 2.305 | .2305 | | .3350 | .0754 |
| 1.470 | | 3.090 | .3090 | | .5560 | .1160 |
| 1.955 | | 3.485 | .3485 | | .760 | .1610 |
| 2.55 | | 4.01 | .200 | | 1.03 | .211 |
| 2.91 | | 4.35 | .348 | | 1.19 | .242 |
| 3.74 | | 5.13 | .359 | | 1.57 | .295 |
| 4.45 | | 5.81 | .290 | | 1.89 | .352 |
| 5.09 | | 6.41 | .322 | | 2.16 | .401 |
| 5.80 | | 7.14 | .235 | | 2.46 | .456 |
| 6.46 | | 7.77 | .233 | | 2.79 | .509 |
| 7.03 | | 8.33 | .250 | | 3.04 | .555 |

| No. | Name | Age | Sex | Profession | Religion | Marital Status | Remarks |
|-----|--------------------|-----|-----|------------|--------------|----------------|---------|
| 1 | John A. Smith | 35 | M | Teacher | Methodist | Married | |
| 2 | James B. Jones | 42 | M | Farmer | Baptist | Married | |
| 3 | William C. Brown | 28 | M | Merchant | Presbyterian | Single | |
| 4 | Robert D. White | 55 | M | Physician | Episcopal | Married | |
| 5 | Elizabeth E. Green | 30 | F | Homemaker | Methodist | Married | |
| 6 | Thomas F. Black | 48 | M | Engineer | Baptist | Married | |
| 7 | Mary G. Gray | 25 | F | Teacher | Presbyterian | Single | |
| 8 | Charles H. Hall | 38 | M | Lawyer | Episcopal | Married | |
| 9 | Anna I. King | 40 | F | Homemaker | Methodist | Married | |
| 10 | David J. Lee | 50 | M | Farmer | Baptist | Married | |
| 11 | Sarah K. Miller | 22 | F | Student | Presbyterian | Single | |
| 12 | George L. Wilson | 33 | M | Merchant | Episcopal | Married | |
| 13 | Frances M. Moore | 27 | F | Homemaker | Methodist | Married | |
| 14 | Henry N. Taylor | 45 | M | Physician | Baptist | Married | |
| 15 | Isabel O. Young | 31 | F | Teacher | Presbyterian | Single | |
| 16 | John P. Adams | 52 | M | Engineer | Episcopal | Married | |
| 17 | Rebecca Q. Baker | 29 | F | Homemaker | Methodist | Married | |
| 18 | Samuel R. Clark | 41 | M | Lawyer | Baptist | Married | |
| 19 | Emily S. Evans | 24 | F | Student | Presbyterian | Single | |
| 20 | Frank T. Fisher | 36 | M | Merchant | Episcopal | Married | |
| 21 | Lucy U. Gibson | 26 | F | Homemaker | Methodist | Married | |
| 22 | William V. Hall | 49 | M | Physician | Baptist | Married | |
| 23 | Julia W. Harris | 32 | F | Teacher | Presbyterian | Single | |
| 24 | Richard X. Hill | 51 | M | Engineer | Episcopal | Married | |
| 25 | Martha Y. Jones | 28 | F | Homemaker | Methodist | Married | |
| 26 | Samuel Z. King | 43 | M | Lawyer | Baptist | Married | |
| 27 | Elizabeth A. Lee | 23 | F | Student | Presbyterian | Single | |
| 28 | George B. Miller | 34 | M | Merchant | Episcopal | Married | |
| 29 | Frances C. Moore | 27 | F | Homemaker | Methodist | Married | |
| 30 | Henry D. Taylor | 46 | M | Physician | Baptist | Married | |
| 31 | Isabel E. Young | 31 | F | Teacher | Presbyterian | Single | |
| 32 | John F. Adams | 53 | M | Engineer | Episcopal | Married | |
| 33 | Rebecca G. Baker | 29 | F | Homemaker | Methodist | Married | |
| 34 | Samuel H. Clark | 41 | M | Lawyer | Baptist | Married | |
| 35 | Emily I. Evans | 24 | F | Student | Presbyterian | Single | |
| 36 | Frank J. Fisher | 36 | M | Merchant | Episcopal | Married | |
| 37 | Lucy K. Gibson | 26 | F | Homemaker | Methodist | Married | |
| 38 | William L. Hall | 49 | M | Physician | Baptist | Married | |
| 39 | Julia M. Harris | 32 | F | Teacher | Presbyterian | Single | |
| 40 | Richard N. Hill | 51 | M | Engineer | Episcopal | Married | |
| 41 | Martha O. Jones | 28 | F | Homemaker | Methodist | Married | |
| 42 | Samuel P. King | 43 | M | Lawyer | Baptist | Married | |
| 43 | Elizabeth Q. Lee | 23 | F | Student | Presbyterian | Single | |
| 44 | George R. Miller | 34 | M | Merchant | Episcopal | Married | |
| 45 | Frances S. Moore | 27 | F | Homemaker | Methodist | Married | |
| 46 | Henry T. Taylor | 46 | M | Physician | Baptist | Married | |
| 47 | Isabel U. Young | 31 | F | Teacher | Presbyterian | Single | |
| 48 | John V. Adams | 53 | M | Engineer | Episcopal | Married | |
| 49 | Rebecca W. Baker | 29 | F | Homemaker | Methodist | Married | |
| 50 | Samuel X. Clark | 41 | M | Lawyer | Baptist | Married | |
| 51 | Emily Y. Evans | 24 | F | Student | Presbyterian | Single | |
| 52 | Frank Z. Fisher | 36 | M | Merchant | Episcopal | Married | |
| 53 | Lucy A. Gibson | 26 | F | Homemaker | Methodist | Married | |
| 54 | William B. Hall | 49 | M | Physician | Baptist | Married | |
| 55 | Julia C. Harris | 32 | F | Teacher | Presbyterian | Single | |
| 56 | Richard D. Hill | 51 | M | Engineer | Episcopal | Married | |
| 57 | Martha E. Jones | 28 | F | Homemaker | Methodist | Married | |
| 58 | Samuel F. King | 43 | M | Lawyer | Baptist | Married | |
| 59 | Elizabeth G. Lee | 23 | F | Student | Presbyterian | Single | |
| 60 | George H. Miller | 34 | M | Merchant | Episcopal | Married | |
| 61 | Frances I. Moore | 27 | F | Homemaker | Methodist | Married | |
| 62 | Henry J. Taylor | 46 | M | Physician | Baptist | Married | |
| 63 | Isabel K. Young | 31 | F | Teacher | Presbyterian | Single | |
| 64 | John L. Adams | 53 | M | Engineer | Episcopal | Married | |
| 65 | Rebecca M. Baker | 29 | F | Homemaker | Methodist | Married | |
| 66 | Samuel N. Clark | 41 | M | Lawyer | Baptist | Married | |
| 67 | Emily O. Evans | 24 | F | Student | Presbyterian | Single | |
| 68 | Frank P. Fisher | 36 | M | Merchant | Episcopal | Married | |
| 69 | Lucy Q. Gibson | 26 | F | Homemaker | Methodist | Married | |
| 70 | William R. Hall | 49 | M | Physician | Baptist | Married | |
| 71 | Julia S. Harris | 32 | F | Teacher | Presbyterian | Single | |
| 72 | Richard T. Hill | 51 | M | Engineer | Episcopal | Married | |
| 73 | Martha U. Jones | 28 | F | Homemaker | Methodist | Married | |
| 74 | Samuel V. King | 43 | M | Lawyer | Baptist | Married | |
| 75 | Elizabeth W. Lee | 23 | F | Student | Presbyterian | Single | |
| 76 | George X. Miller | 34 | M | Merchant | Episcopal | Married | |
| 77 | Frances Y. Moore | 27 | F | Homemaker | Methodist | Married | |
| 78 | Henry Z. Taylor | 46 | M | Physician | Baptist | Married | |
| 79 | Isabel A. Young | 31 | F | Teacher | Presbyterian | Single | |
| 80 | John B. Adams | 53 | M | Engineer | Episcopal | Married | |
| 81 | Rebecca C. Baker | 29 | F | Homemaker | Methodist | Married | |
| 82 | Samuel D. Clark | 41 | M | Lawyer | Baptist | Married | |
| 83 | Emily E. Evans | 24 | F | Student | Presbyterian | Single | |
| 84 | Frank F. Fisher | 36 | M | Merchant | Episcopal | Married | |
| 85 | Lucy G. Gibson | 26 | F | Homemaker | Methodist | Married | |
| 86 | William H. Hall | 49 | M | Physician | Baptist | Married | |
| 87 | Julia I. Harris | 32 | F | Teacher | Presbyterian | Single | |
| 88 | Richard J. Hill | 51 | M | Engineer | Episcopal | Married | |
| 89 | Martha K. Jones | 28 | F | Homemaker | Methodist | Married | |
| 90 | Samuel L. King | 43 | M | Lawyer | Baptist | Married | |
| 91 | Elizabeth M. Lee | 23 | F | Student | Presbyterian | Single | |
| 92 | George N. Miller | 34 | M | Merchant | Episcopal | Married | |
| 93 | Frances O. Moore | 27 | F | Homemaker | Methodist | Married | |
| 94 | Henry P. Taylor | 46 | M | Physician | Baptist | Married | |
| 95 | Isabel Q. Young | 31 | F | Teacher | Presbyterian | Single | |
| 96 | John R. Adams | 53 | M | Engineer | Episcopal | Married | |
| 97 | Rebecca S. Baker | 29 | F | Homemaker | Methodist | Married | |
| 98 | Samuel T. Clark | 41 | M | Lawyer | Baptist | Married | |
| 99 | Emily U. Evans | 24 | F | Student | Presbyterian | Single | |
| 100 | Frank V. Fisher | 36 | M | Merchant | Episcopal | Married | |

TABLE II (Continued)

| ϕ 4.68(H-2.975) | $\phi \frac{dH}{dx}$ | $\phi \frac{dH}{dx}$ | ΔH | $\Delta x/c$ |
|----------------------|------------------------|----------------------|------------|--------------|
| $.38 \times 10^{-3}$ | 0 | 0 | 0 | .0082 |
| $.38 \times 10^{-3}$ | $.0107 \times 10^{-3}$ | .140 | .0023 | .02 |
| .38 | .0196 | .145 | .0160 | .11 |
| .405 | .0763 | .179 | .0177 | .10 |
| .440 | .1363 | .199 | .0199 | .10 |
| .480 | .2110 | .219 | .0219 | .10 |
| .530 | .317 | .249 | .0249 | .10 |
| .600 | .491 | .303 | .0152 | .05 |
| .630 | .593 | .323 | .0263 | .03 |
| .700 | .692 | .393 | .0275 | .07 |
| .805 | 1.233 | .480 | .0249 | .05 |
| .900 | 1.585 | .543 | .0272 | .05 |
| 1.050 | 2.10 | .646 | .0253 | .04 |
| 1.20 | 2.74 | .778 | .0233 | .03 |
| 1.35 | 3.36 | .892 | .0261 | .03 |

TABLE III
COMPUTATION TABLE FOR FRICTION FACTORS IN DIFFUSER

$M_0 = 15$ $h = 40,000 \text{ ft.}$
LAMINAR INLET ZONE
 $\frac{\tau_0}{q} = 0.730 \sqrt{\frac{1}{R_x}}$
 $c = 2.67 \text{ ft.}$
 $\gamma \approx 2.96 \times 10^{-4} \text{ ft.}^2/\text{sec.}$

| x/c | x
ft. | $\frac{p}{16\sqrt{c}t^2}$ | $\frac{q}{16\sqrt{c}t^2}$ | D
ft. | V
ft./sec | $1/R_x$ | $\sqrt{1/R_x}$ | τ_0/q | $4 \frac{\tau_0}{q} \frac{q}{p} D$ |
|-------|------------|---------------------------|---------------------------|------------|----------------|------------------------|----------------|------------|------------------------------------|
| 0 | 0 | 1137 | 139.5 | 1.596 | 470 | ∞ | ∞ | ∞ | ∞ |
| .0061 | .0175 | 1174 | 152.5 | 1.575 | 494 | $.342 \times 10^{-4}$ | .00585 | .00426 | 3.73×10^{-3} |
| .0137 | .0366 | 1163 | 165 | 1.546 | 516 | $.1565 \times 10^{-4}$ | .00396 | .00239 | 2.81×10^{-3} |
| .0225 | .0599 | 1145 | 177.8 | 1.522 | 538 | $.092 \times 10^{-4}$ | .00304 | .00222 | 2.40×10^{-3} |
| .0349 | .093 | 1130 | 189 | 1.50 | 559 | $.0571 \times 10^{-4}$ | .00239 | .00174 | 2.08×10^{-3} |
| .0618 | .165 | 1116 | 204 | 1.48 | 581 | $.0303 \times 10^{-4}$ | .00174 | .00127 | 1.66×10^{-3} |

TURBULENCE BOUNDARY LAYER ZONE

| x/c | $\frac{p}{16\sqrt{c}t^2}$ | $\frac{q}{16\sqrt{c}t^2}$ | c/D | $0 \frac{q}{p} \frac{q}{p}$ | $\tau_0/2q$ | $4 \frac{\tau_0}{q} \frac{q}{p} D$ |
|-------|---------------------------|---------------------------|-------|-----------------------------|------------------------|------------------------------------|
| .0618 | 1116 | 1176 | 1.895 | 2.64 | 3.14×10^{-3} | 3.30×10^{-3} |
| .1175 | 1130 | 1130 | 1.78 | 2.305 | 2.19×10^{-3} | 5.22×10^{-3} |
| .1350 | 1145 | 1145 | 1.75 | 2.175 | 1.92×10^{-3} | 4.18×10^{-3} |
| .2520 | 1160 | 1160 | 1.725 | 1.96 | 1.77×10^{-3} | 3.47×10^{-3} |
| .319 | 1174 | 1174 | 1.675 | 1.76 | 1.69×10^{-3} | 2.95×10^{-3} |
| .400 | 1188 | 1188 | 1.665 | 1.58 | 1.60×10^{-3} | 2.53×10^{-3} |
| .542 | 1207 | 1207 | 1.61 | 1.393 | 1.51×10^{-3} | 1.975×10^{-3} |
| .700 | 1225 | 1225 | 1.555 | 1.076 | 1.415×10^{-3} | 1.52×10^{-3} |
| .877 | 1241 | 1241 | 1.498 | .867 | 1.34×10^{-3} | 1.162×10^{-3} |
| 1.000 | 1251 | 1251 | 1.455 | .736 | 1.29×10^{-3} | .850 $\times 10^{-3}$ |

1. The first part of the report is a general introduction to the subject of the study. It discusses the importance of the problem and the objectives of the research. The second part is a literature review, which summarizes the work of other researchers in the field. The third part is a description of the methods used in the study. The fourth part is a presentation of the results of the study. The fifth part is a discussion of the results and their implications. The sixth part is a conclusion and a list of references.

2. The first part of the report is a general introduction to the subject of the study. It discusses the importance of the problem and the objectives of the research. The second part is a literature review, which summarizes the work of other researchers in the field. The third part is a description of the methods used in the study. The fourth part is a presentation of the results of the study. The fifth part is a discussion of the results and their implications. The sixth part is a conclusion and a list of references.

3. The first part of the report is a general introduction to the subject of the study. It discusses the importance of the problem and the objectives of the research. The second part is a literature review, which summarizes the work of other researchers in the field. The third part is a description of the methods used in the study. The fourth part is a presentation of the results of the study. The fifth part is a discussion of the results and their implications. The sixth part is a conclusion and a list of references.

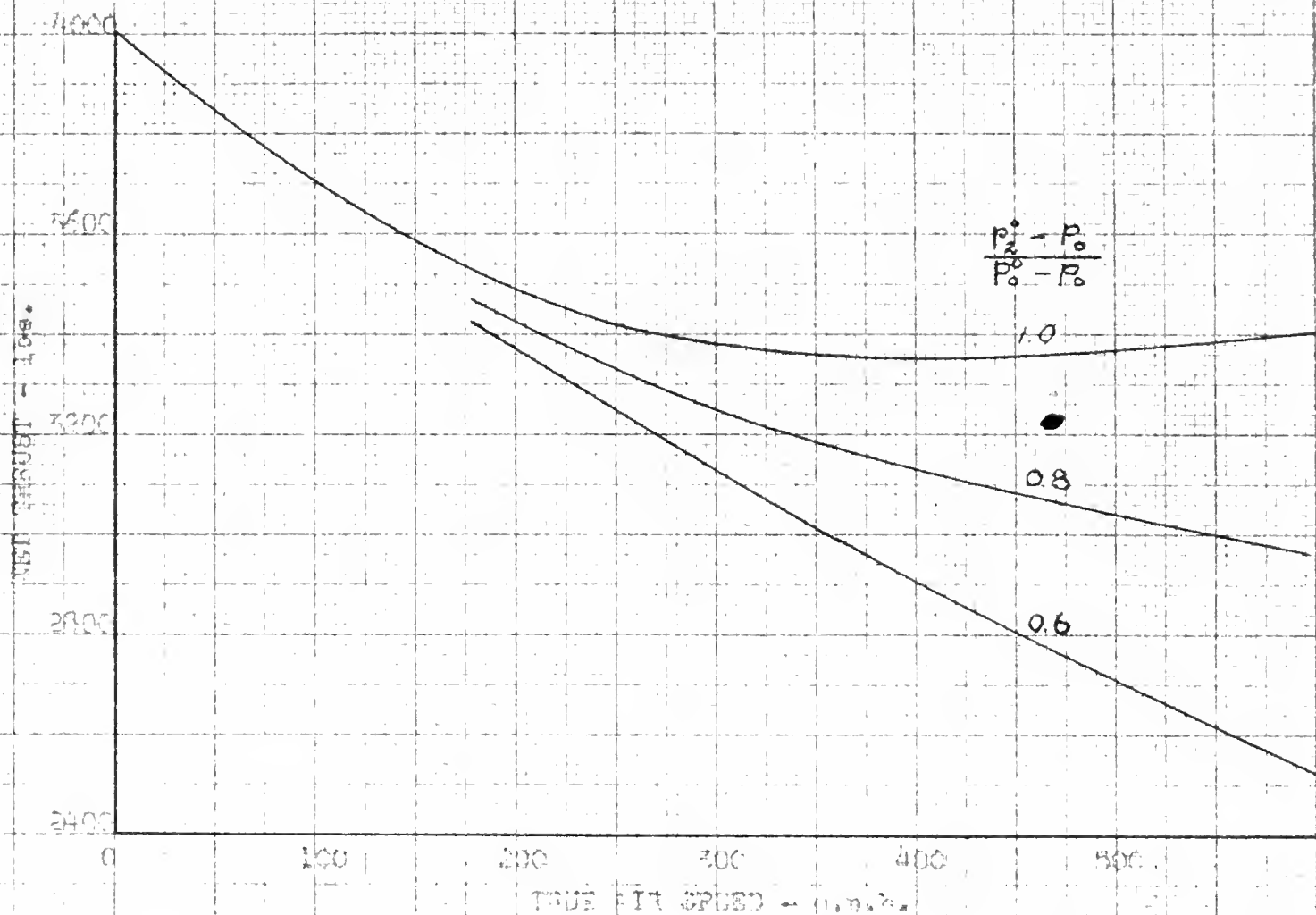


FIG. 1 - EFFECT OF RAM RECOVERY RATIO ON THE MAXIMUM AVAILABLE NET THRUST OF A TURBOJET ENGINE AT SEA LEVEL.

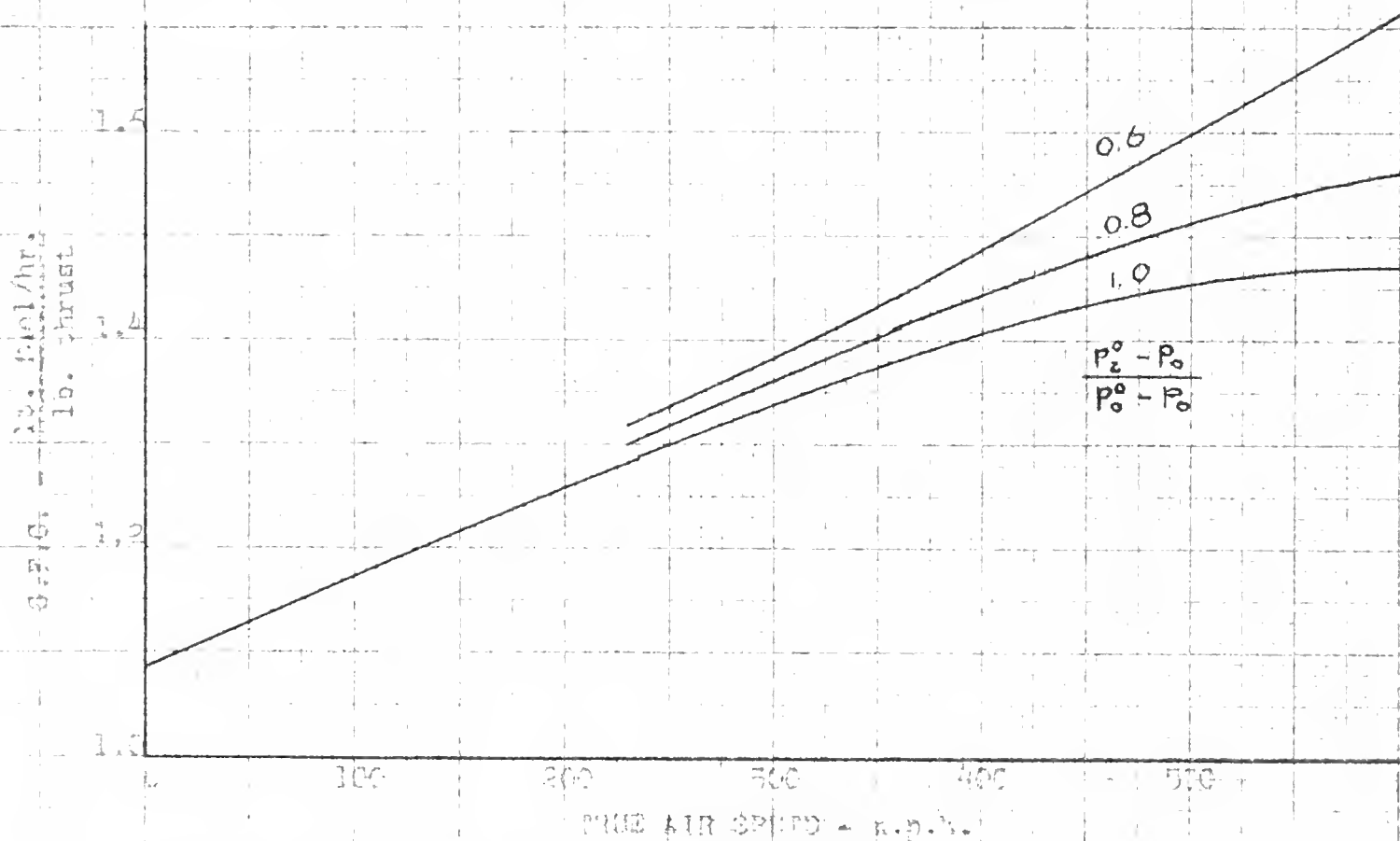
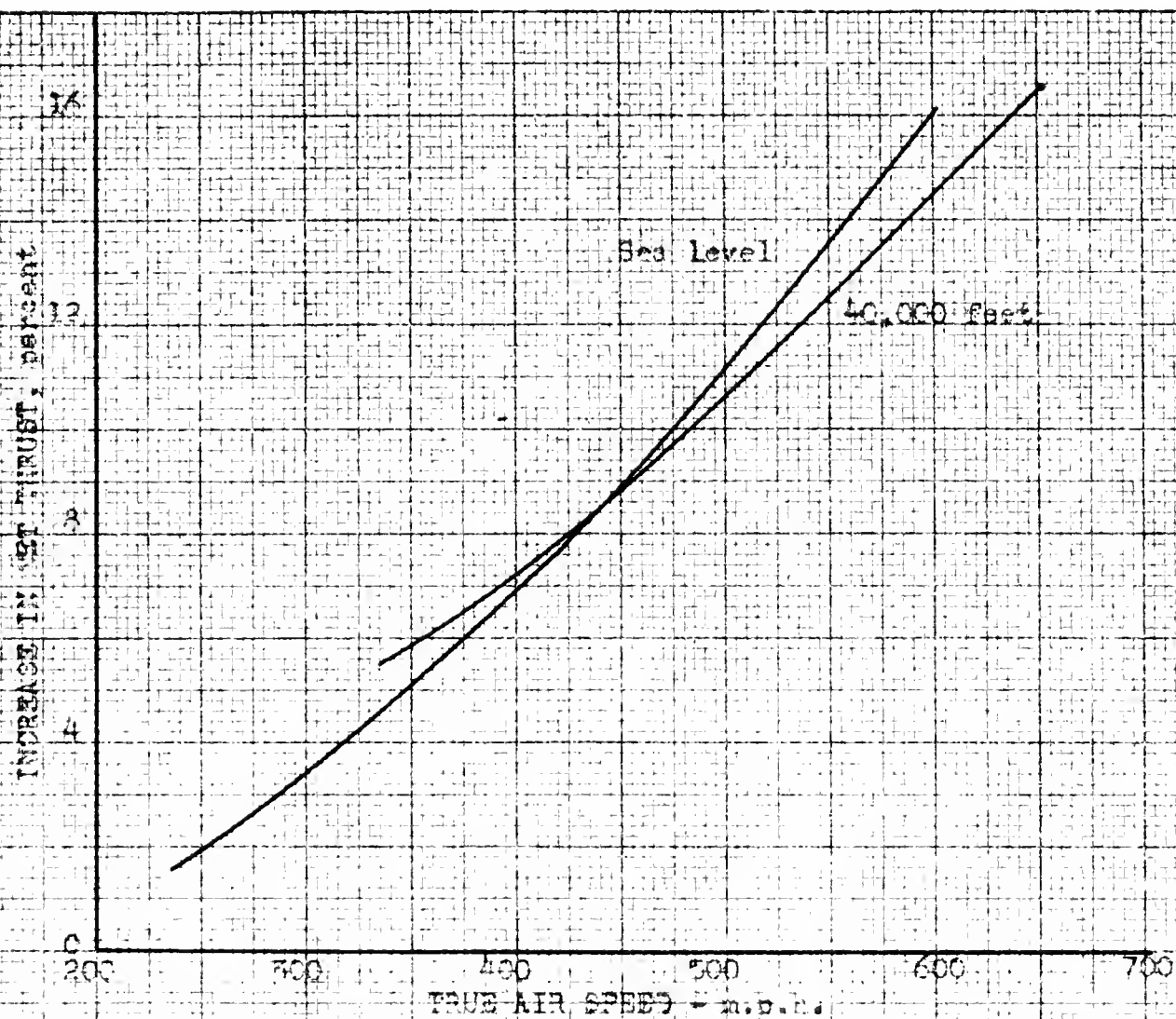
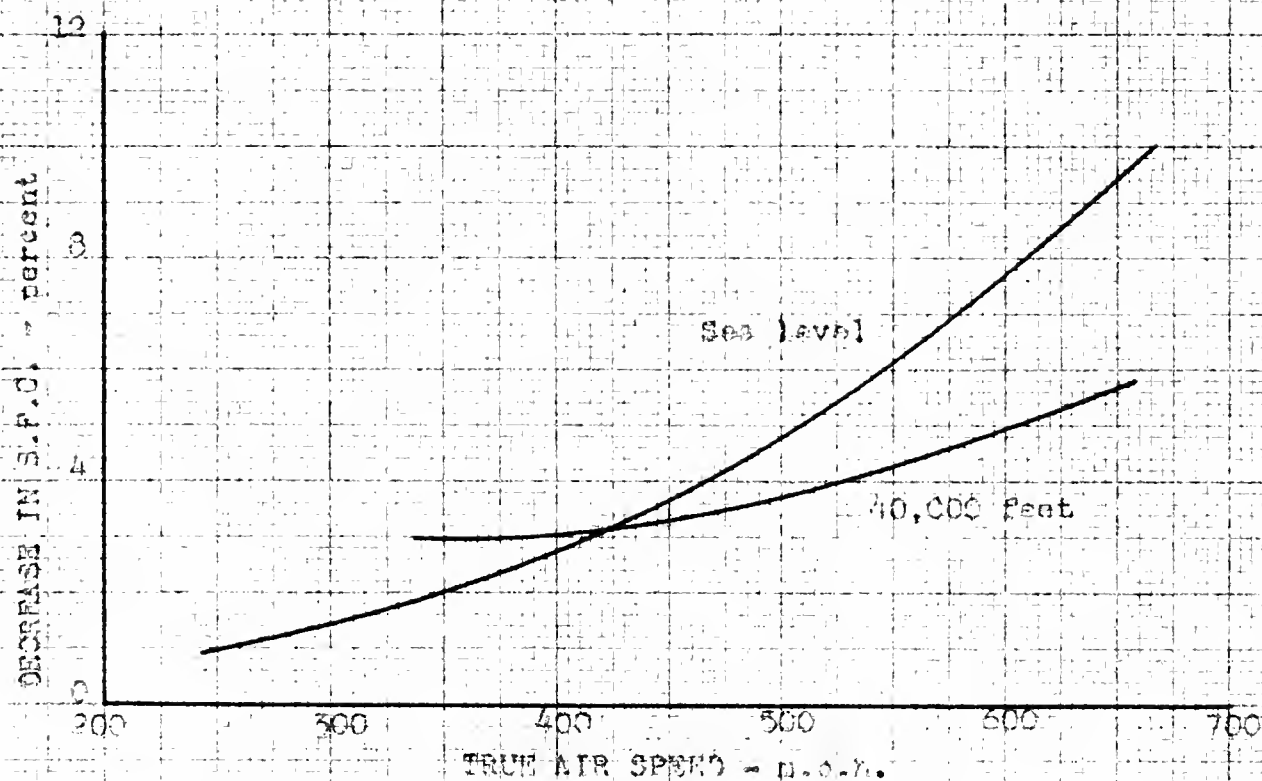


FIG. 2 - EFFECT OF RAM RECOVERY RATIO ON SPECIFIC FUEL CONSUMPTION AT MAXIMUM AVAILABLE NET THRUST OF A TURBOJET ENGINE AT SEA LEVEL.



(a) INCREASE IN NET THRUST.



(b) DECREASE IN SPECIFIC FUEL CONSUMPTION.

FIG. 5 - CHANGE IN NET THRUST AND SPECIFIC FUEL CONSUMPTION FOR AN INCREASE IN RAY RECOVERY RATIO FROM 0.70 TO 0.80.
(NACA TN 1695)

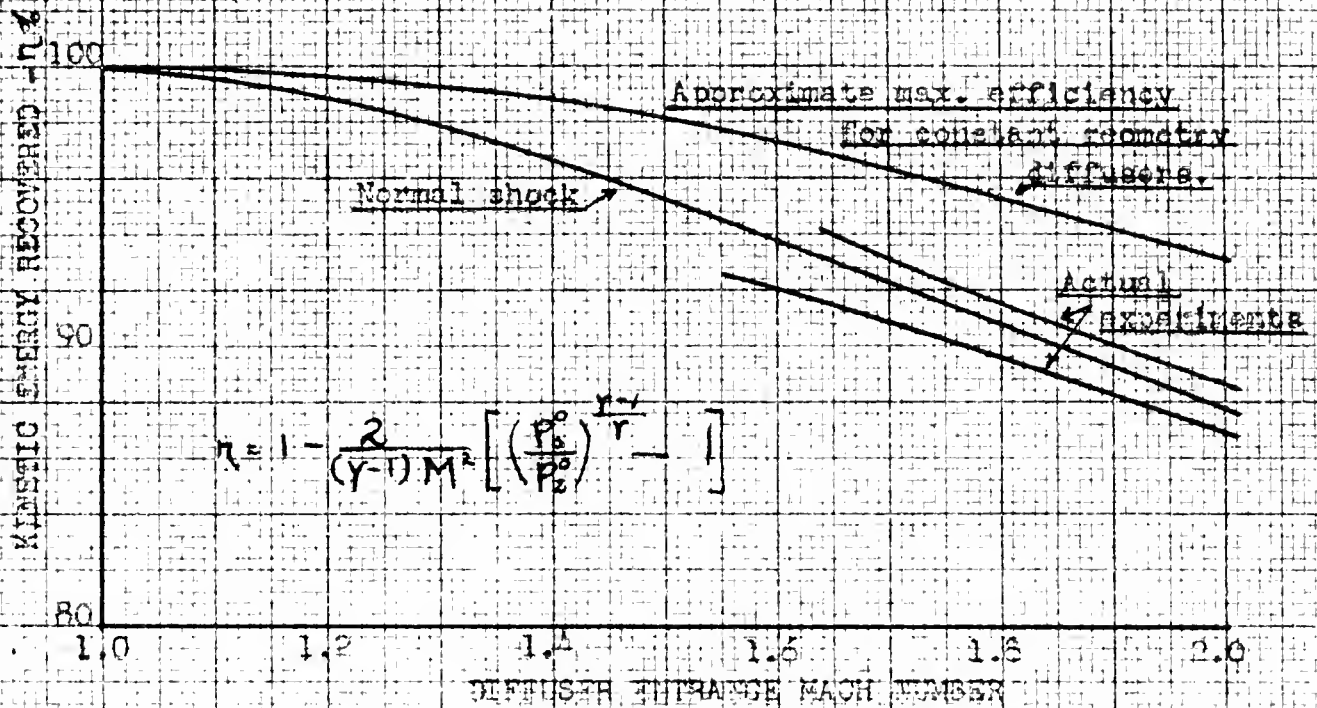


FIG. 4 - COMPARISON OF TEST RESULTS WITH THEORETICAL EXPECTATIONS FOR DIFFUSERS WITH INTERNAL SHOCK.

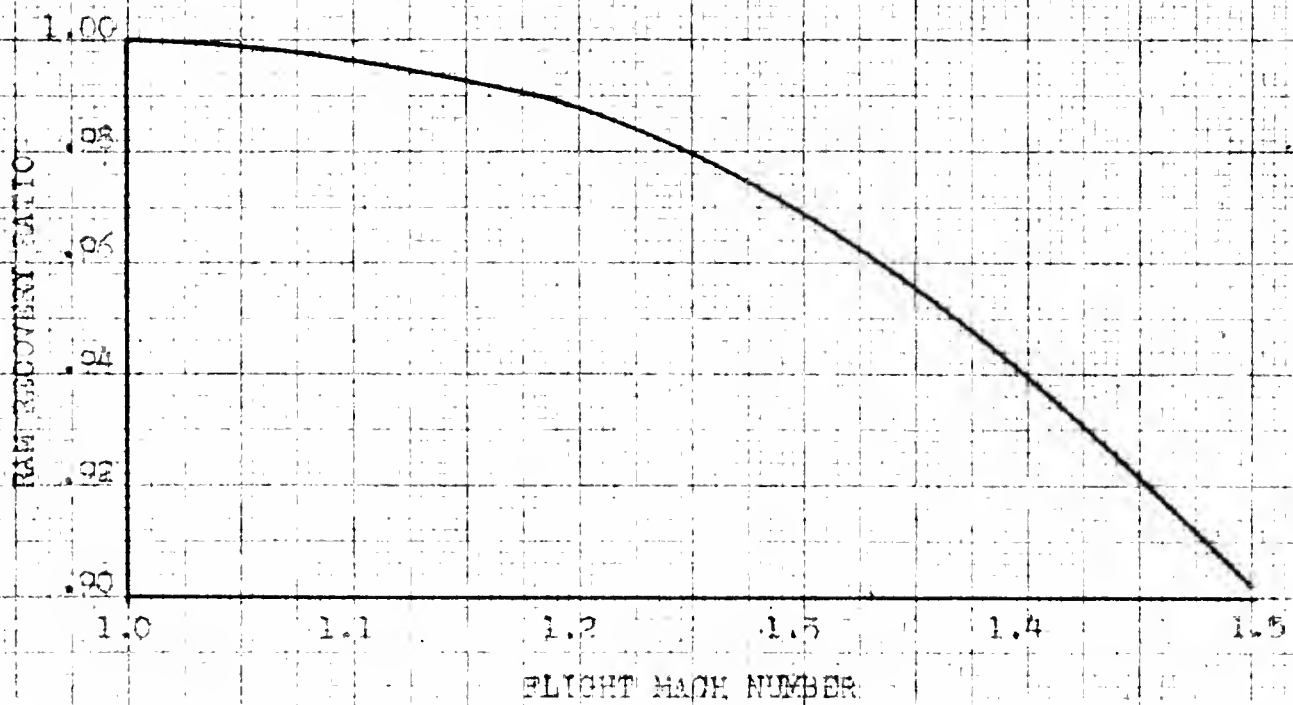


FIG. 5 - RAM RECOVERY RATIO ACROSS A NORMAL SHOCK.

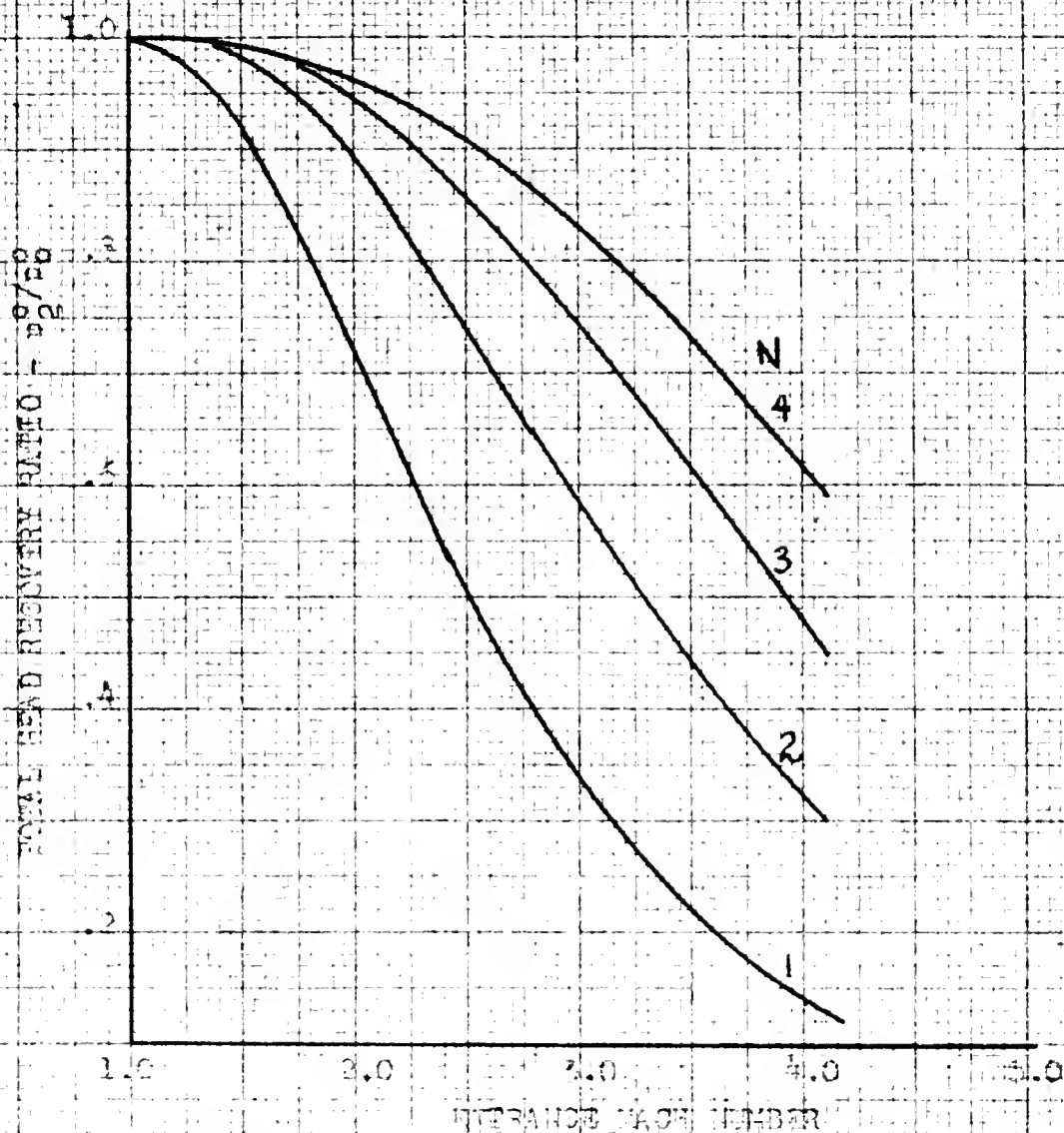


FIG. 6 - THEORETICAL PRESSURE RECOVERY RATIO AFTER "N" COMPRESSION SHOCKS. (NACA TM 1140)

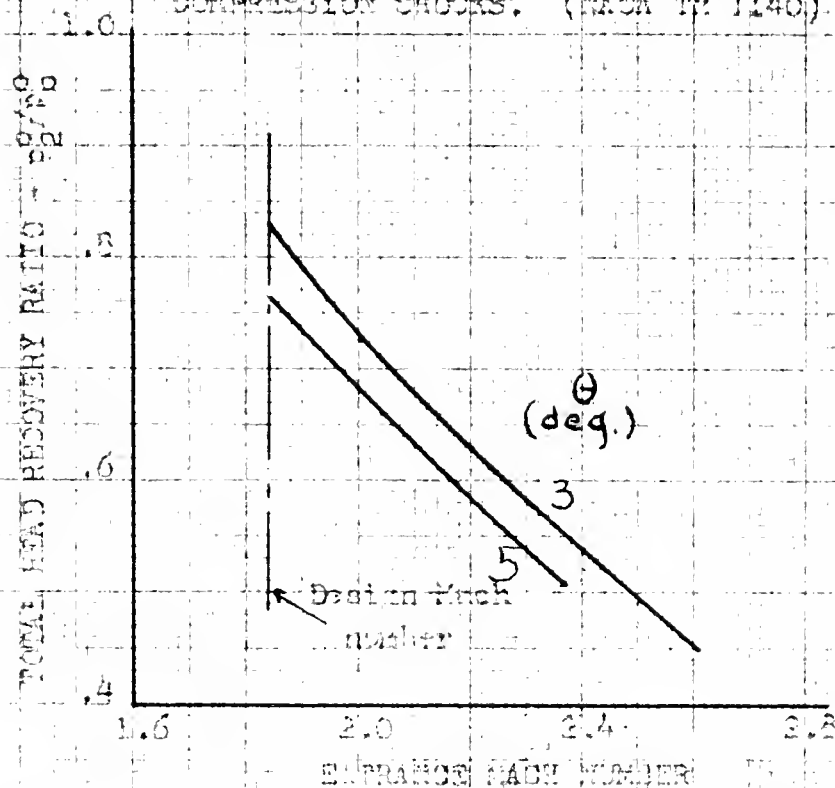


FIG. 7 - EFFECT OF EXIT CONE ANGLE ON THE PERFORMANCE OF TWO SUPERSONIC DIFFUSERS WITH EQUAL CONTRACTION RATIOS AND ENTRANCE CONE ANGLES.

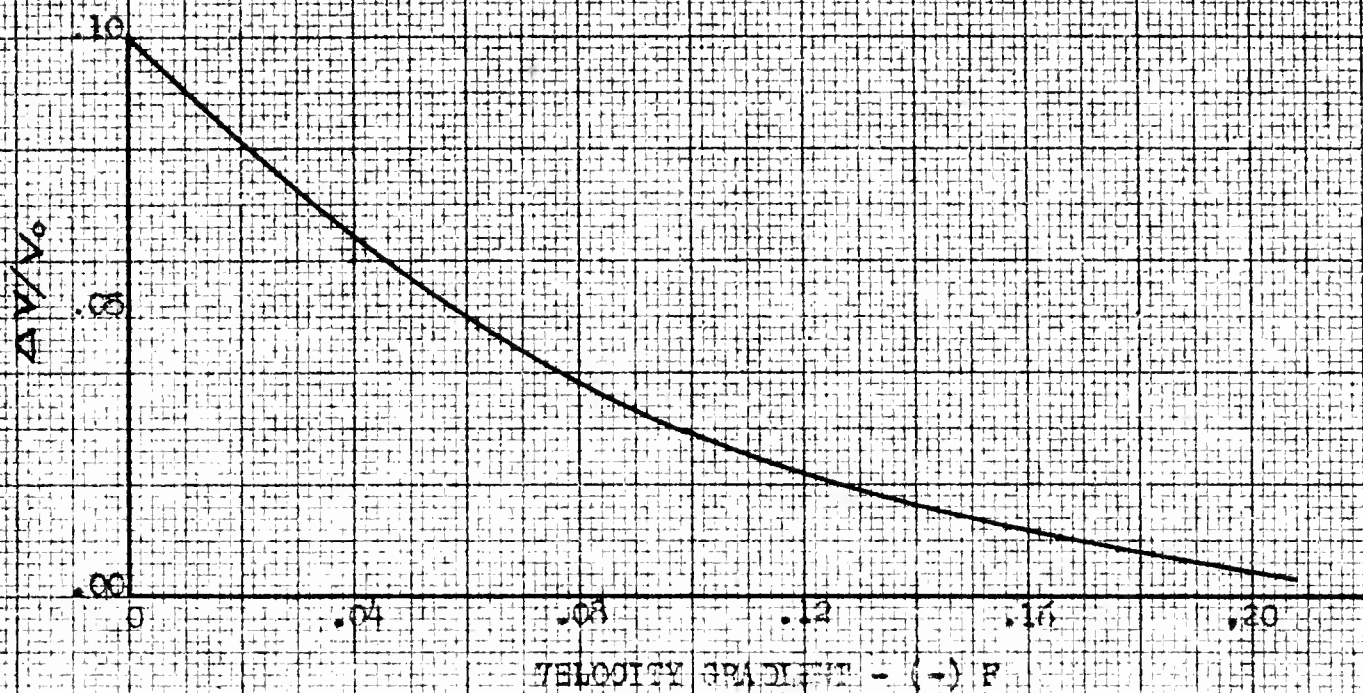


FIG. 8 - VELOCITY DECREMENT OBTAINABLE BEFORE LAMINAR SEPARATION OCCURS. (NACA TN 671)

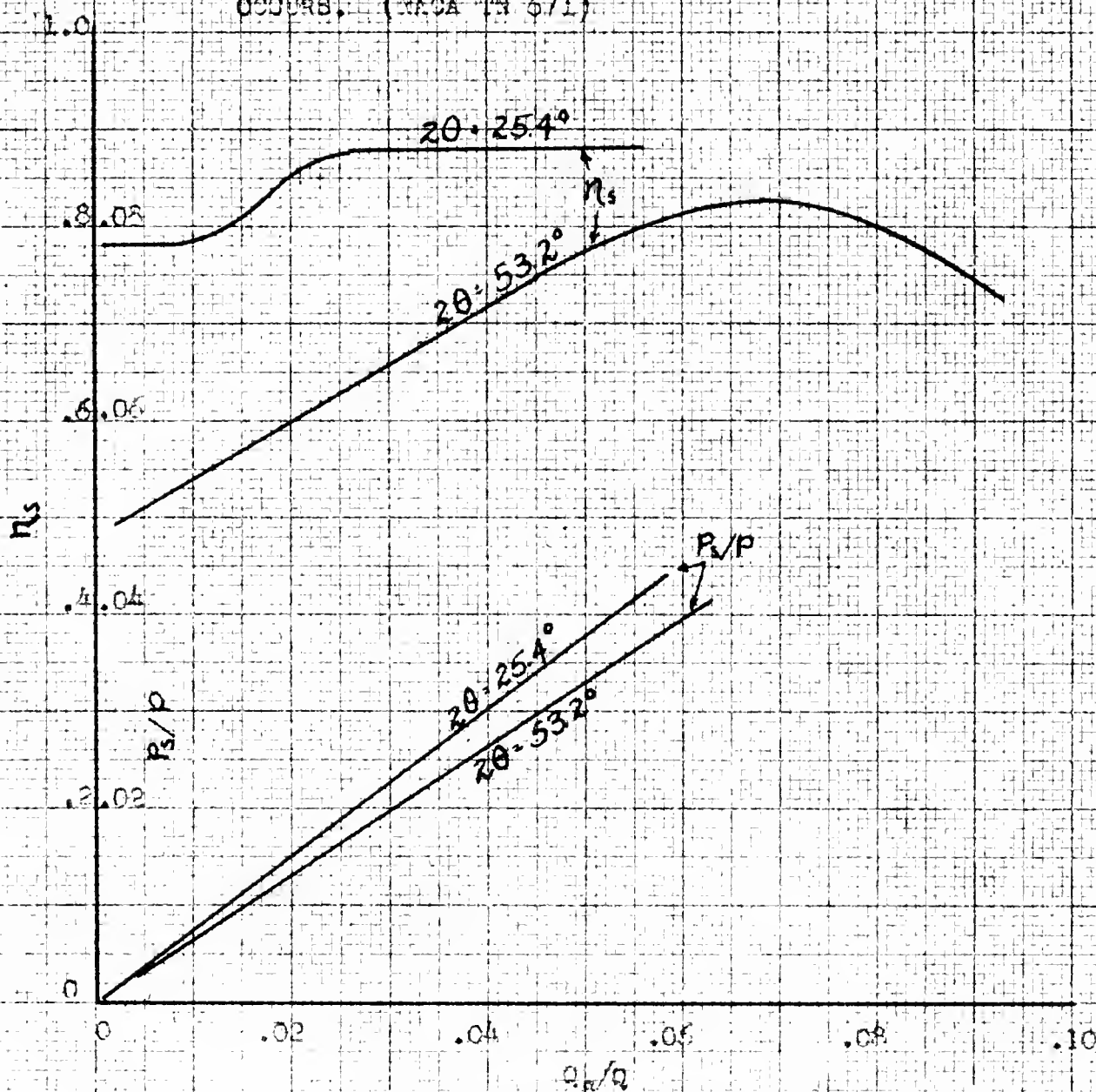
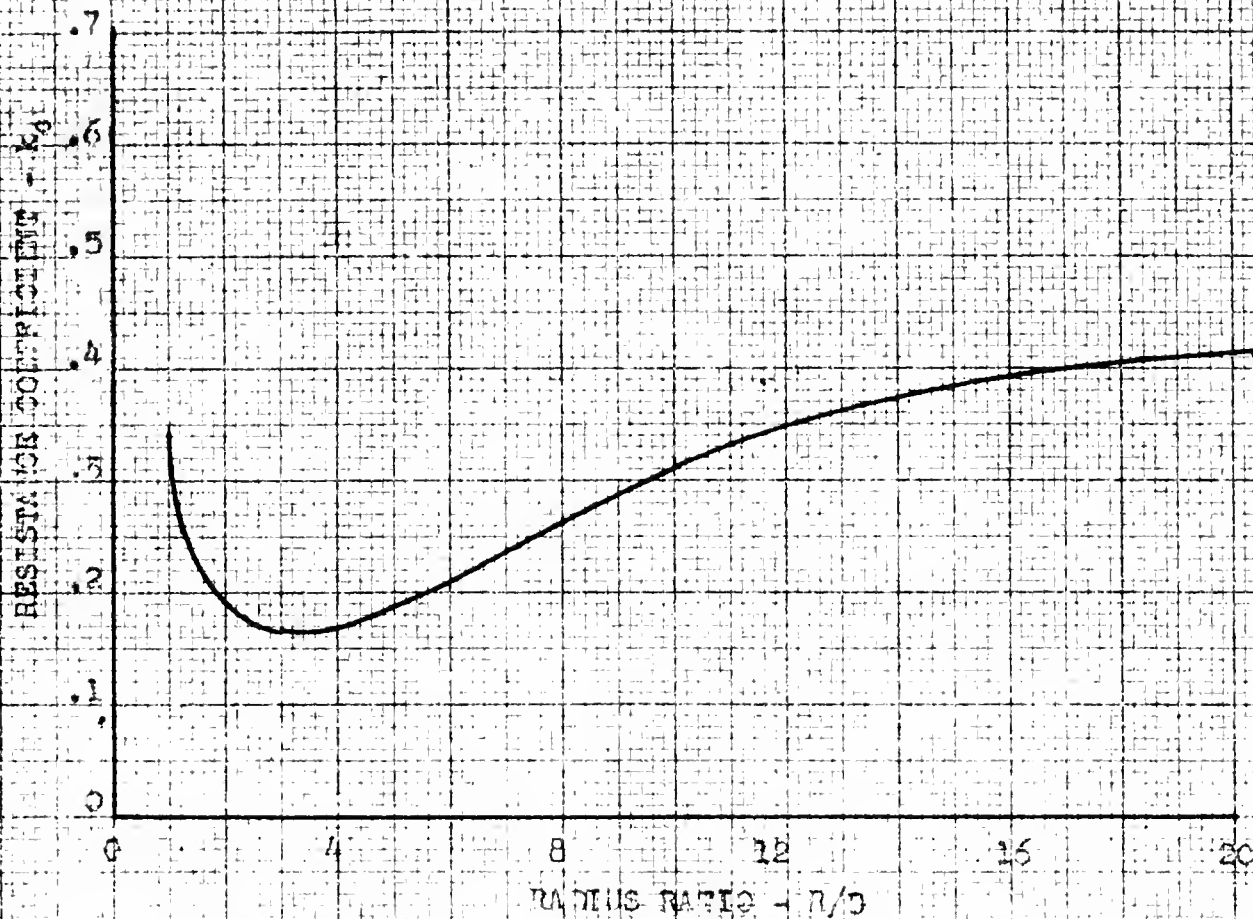
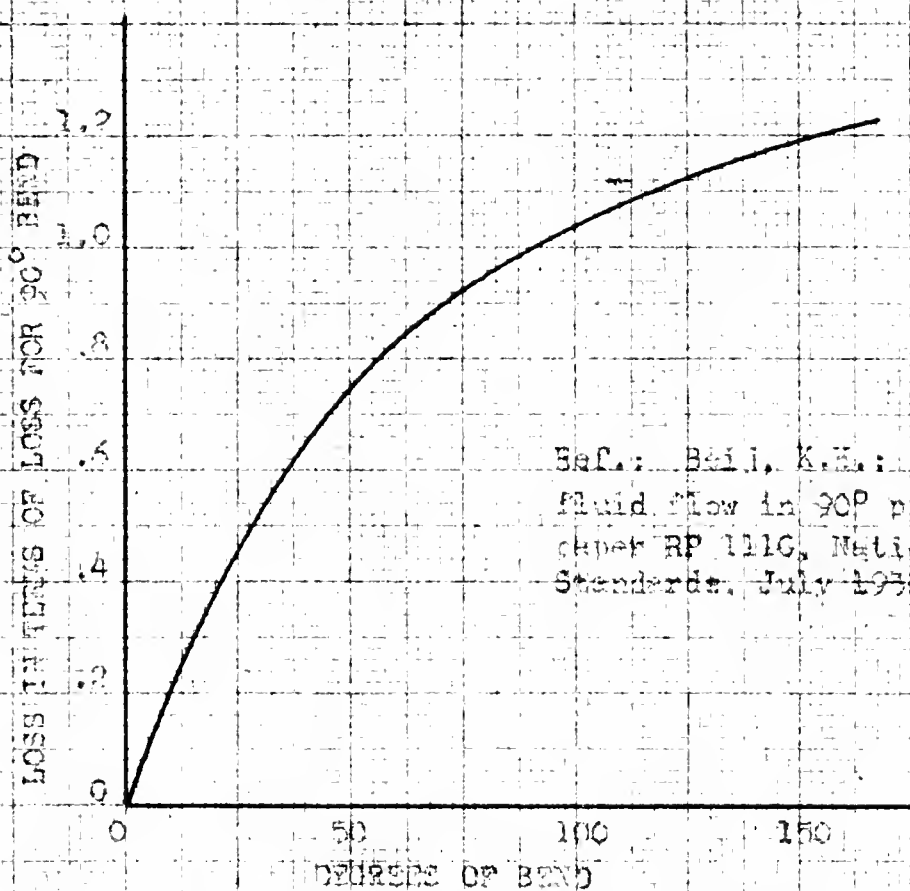


FIG. 9 - IMPROVEMENT OF DEFUSER EFFICIENCY WITH SUCTION.



(a) RESISTANCE COEFFICIENT IN A 90 DEG. BEND.



Ref.: Baile, K.H.: Pressure losses for fluid flow in 90° pipe bends, Research paper RP 1110, National Bureau of Standards, July 1958.

(b) CORRECTION FOR DEGREE OF BEND.

FIG. 10 - EFFECT OF RADIUS RATIO AND DEFLECTION ANGLE ON TURNING LOSSES IN DUCTS.

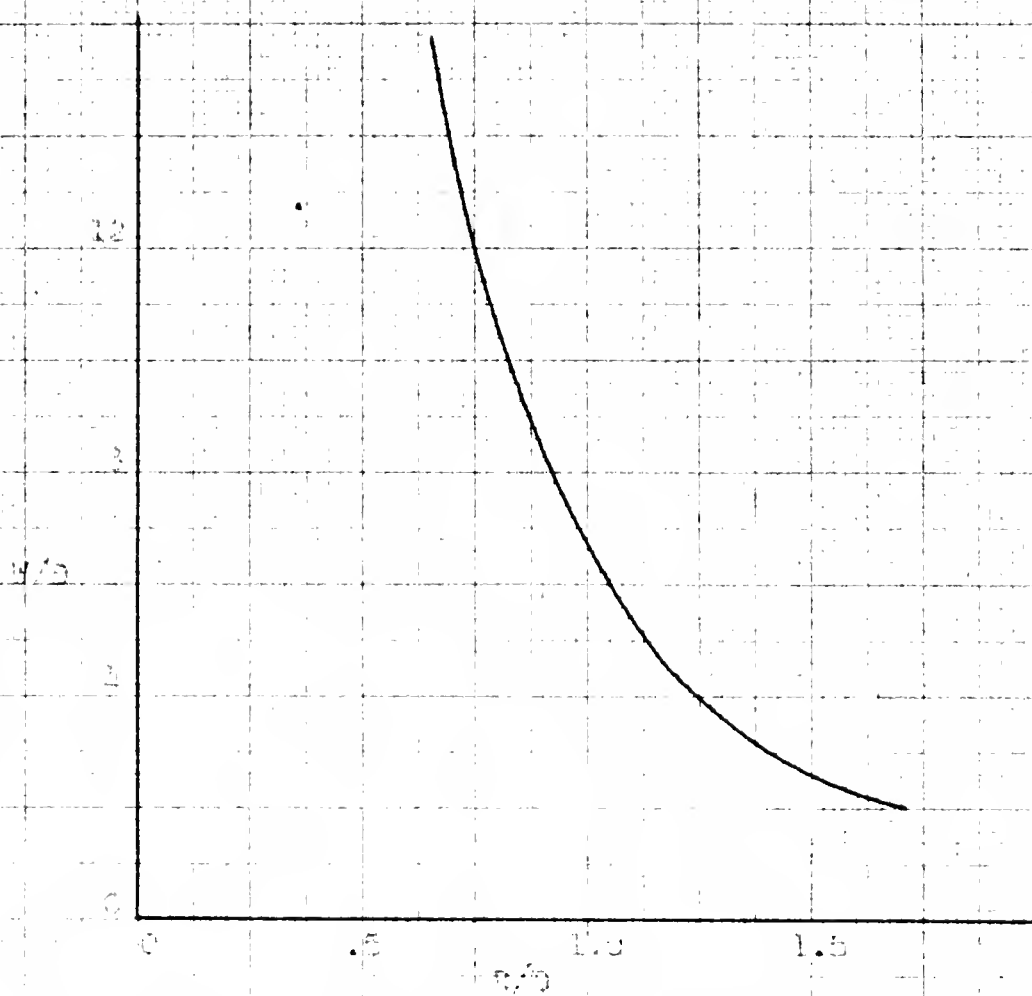


FIG. 11 - ASPECT RATIO VERSUS RADIUS RATIO TO MAINTAIN A COEFFICIENT OF CORRELATION OF 0.25

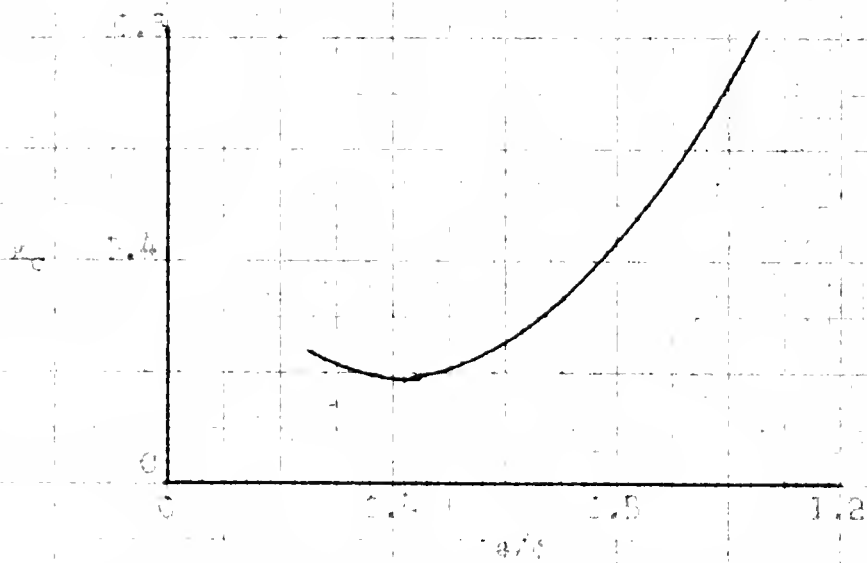
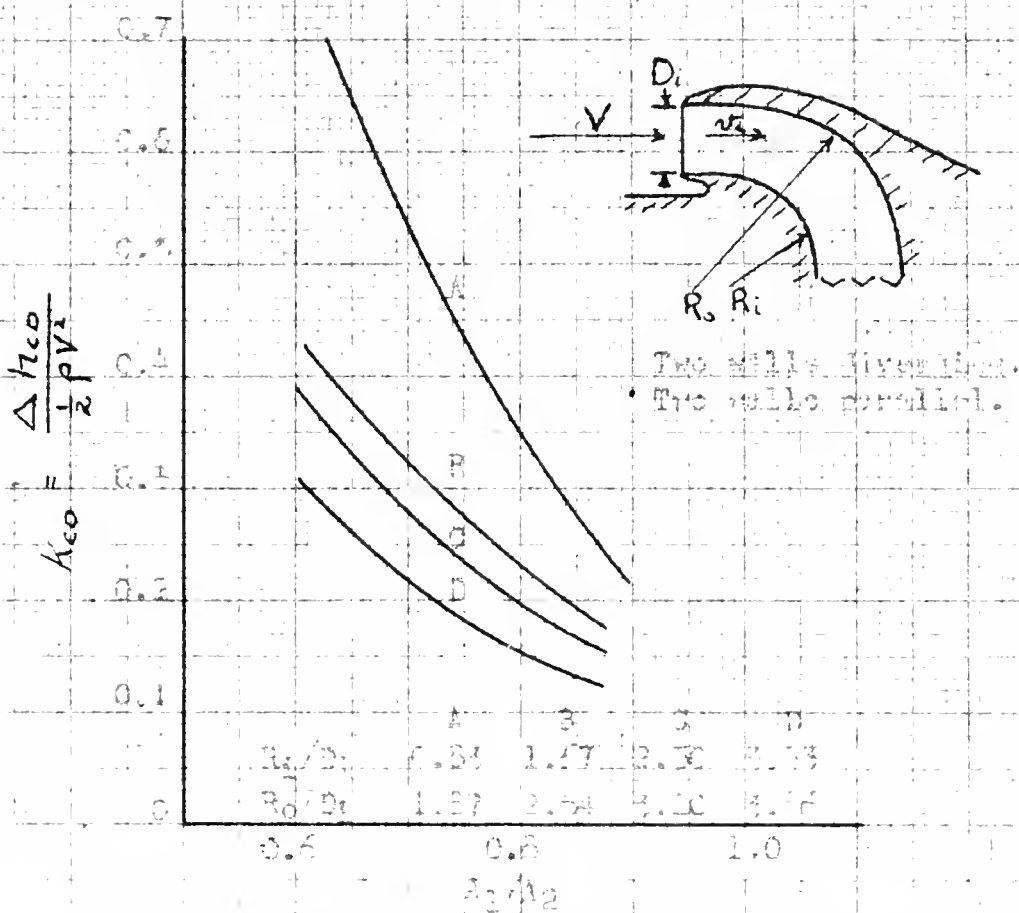
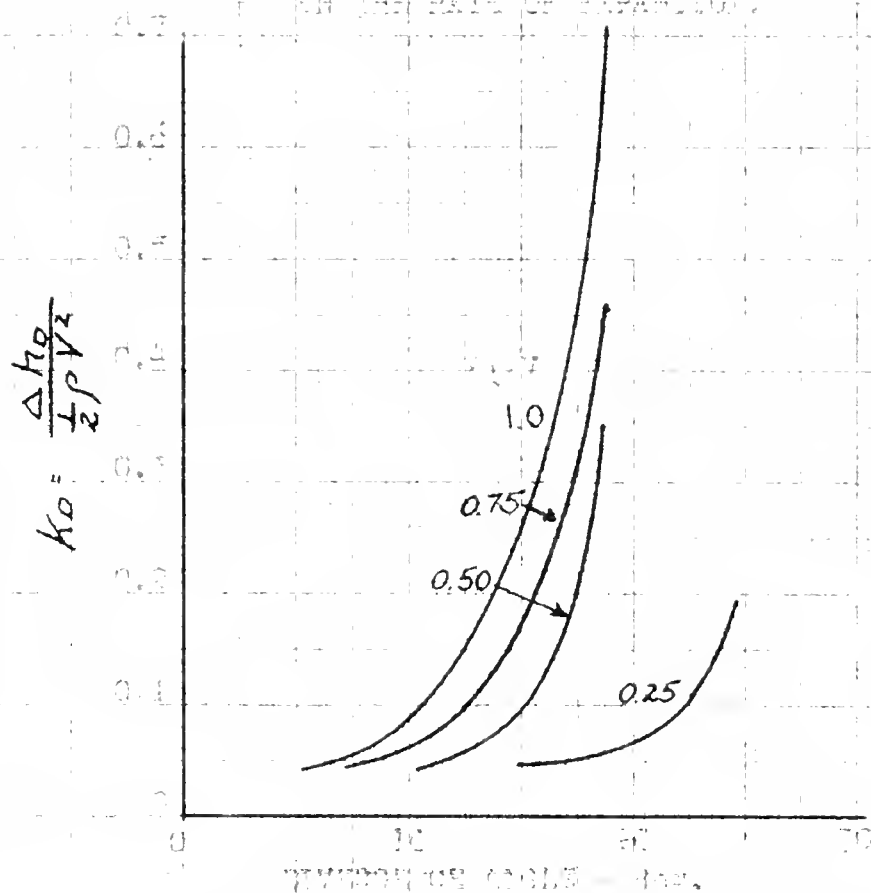


FIG. 12 - EFFECT OF GAS/CHORD RATIO ON RADIUS RATIO COEFFICIENT.



(c) DEPENDENCE OF THE LOSS IN A CURVED ENTRY ON THE RATE OF EXPANSION.



(d) VARIATION OF LOSS IN A STRAIGHT EXPANDING ENTRY WITH INTERNAL AND EXTERNAL EXPANSION.

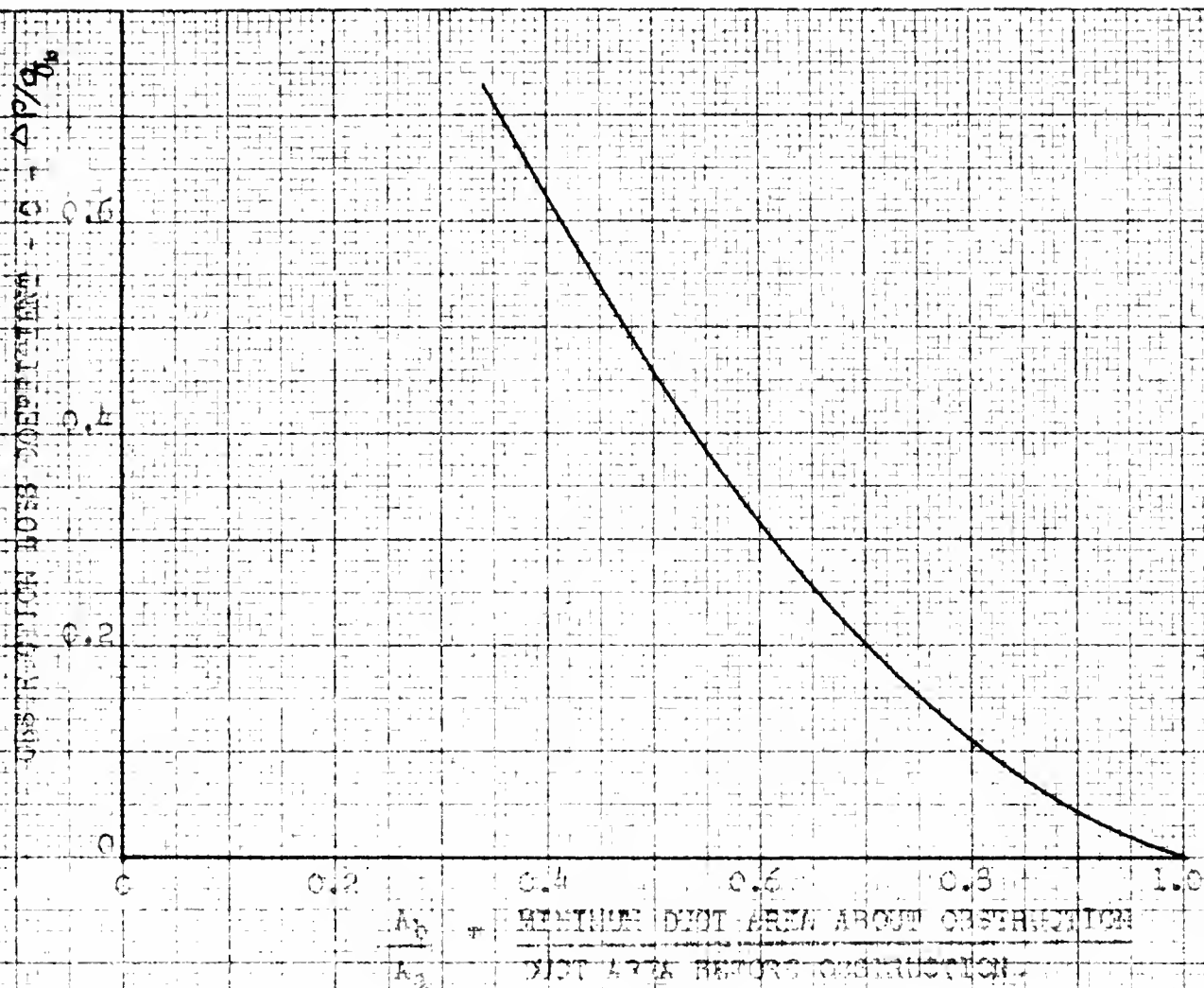


FIG. 14 - OBSTRUCTION LOSS COEFFICIENT IN A DUCT.

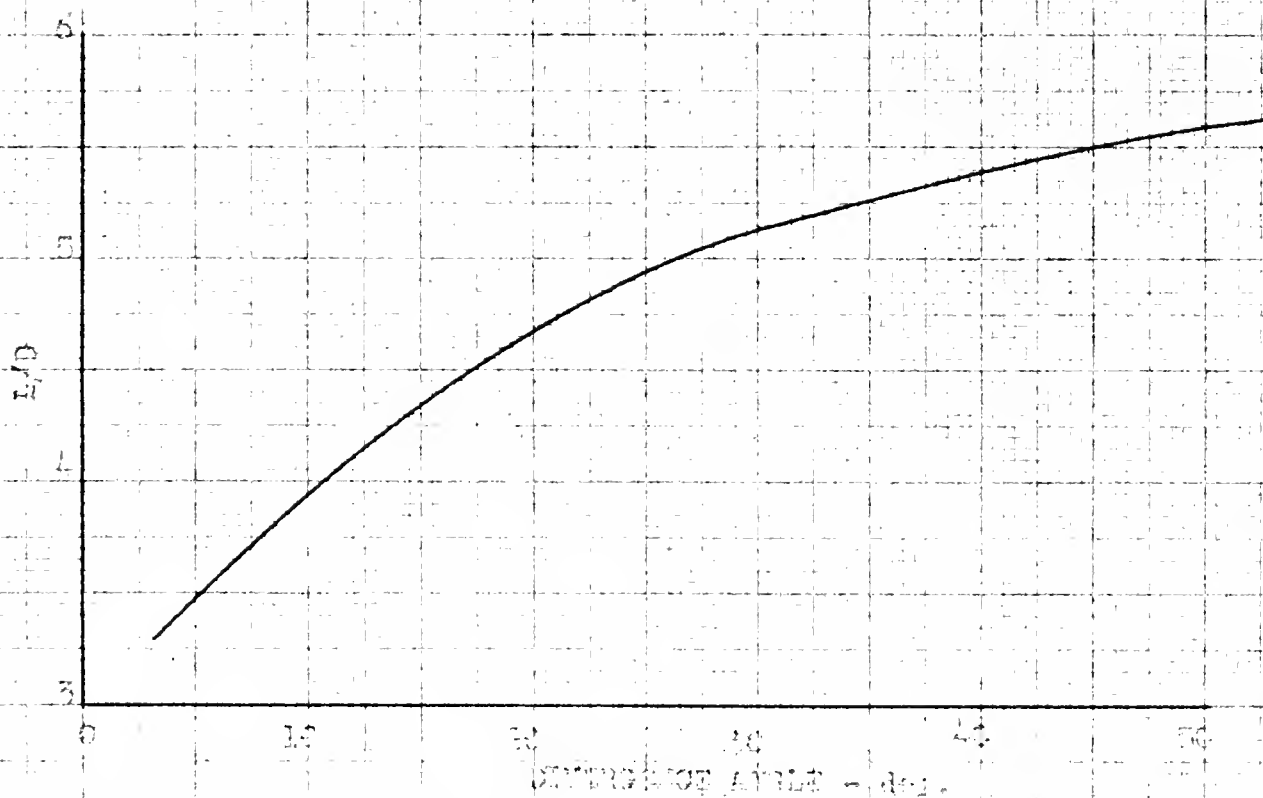


FIG. 15 - LENGTH OF DIFFUSANT AREA DUCT FOLLOWING A DIFFUSER NECESSARY FOR COMPLETE PRODUCT RECOVERY.

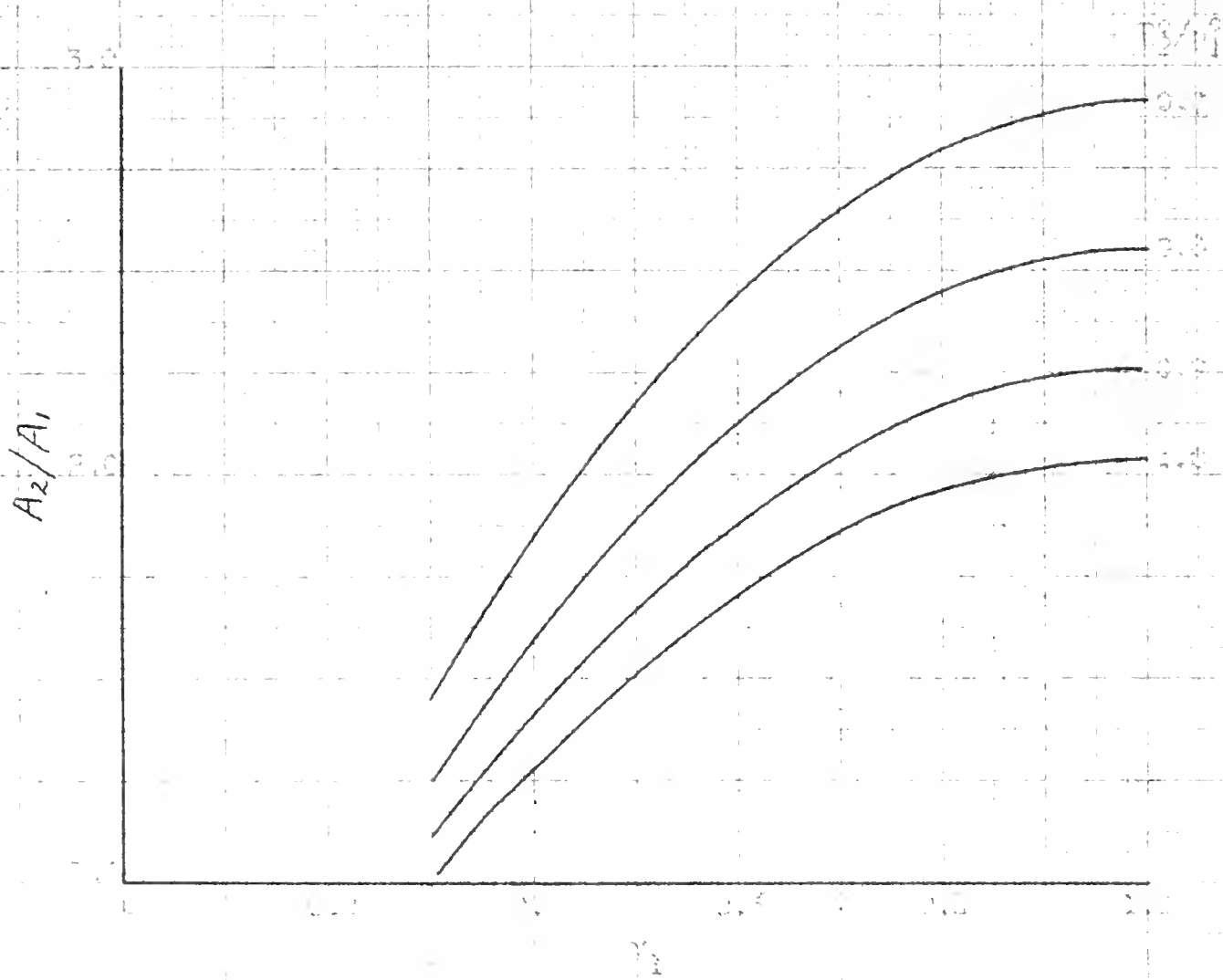


FIG. 10 - VARIATION OF THE RATIO WITH DISTANCE INSIDE THE BAG
FOR DIFFERENT VALUES OF T_3/T_1 (0.2, 0.3, 0.4, 0.5)

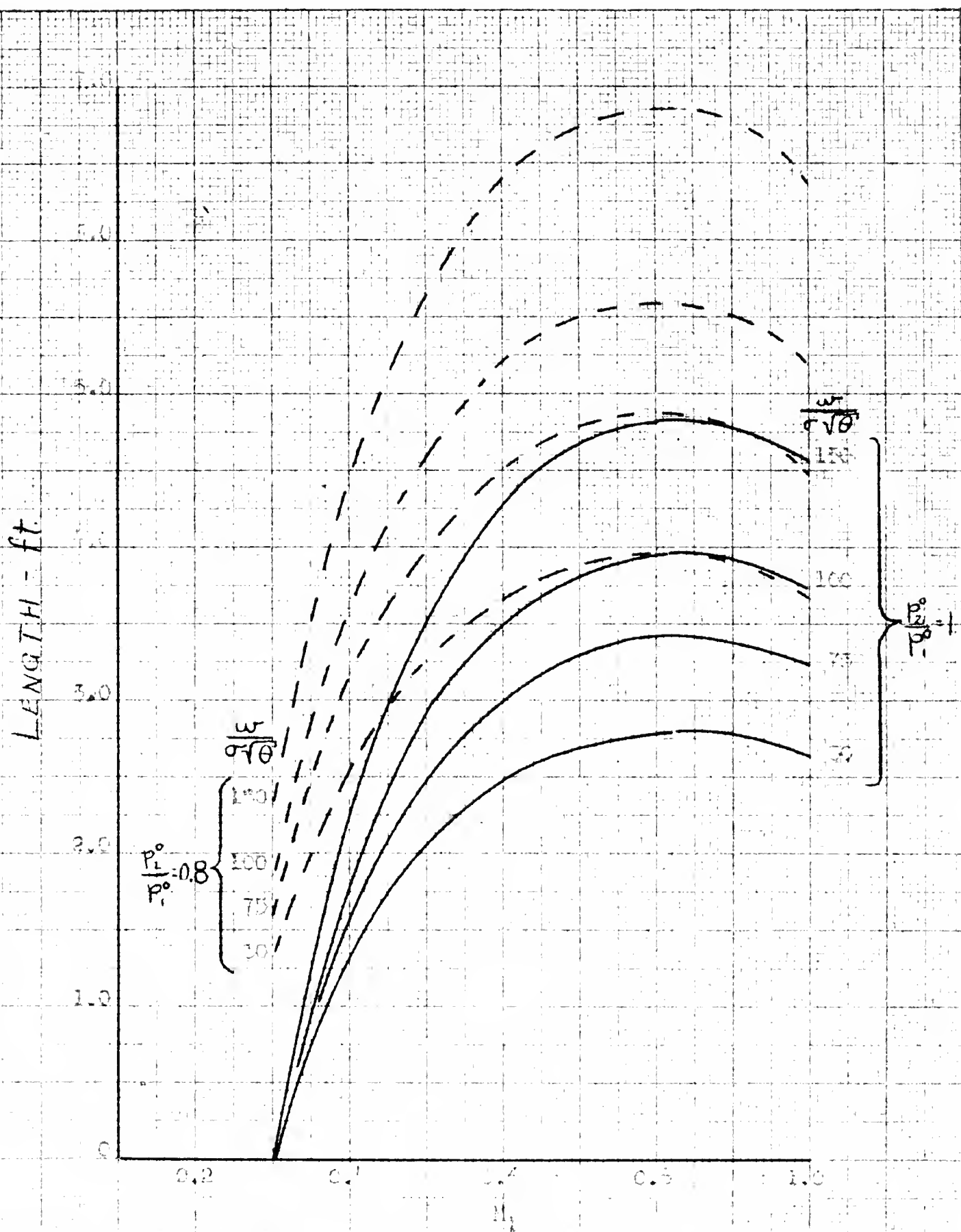


FIG. 17 LENGTH OF ORBITAL TRAJECTORIES REQUIRED FOR VARIOUS RETARDATION MACH NUMBERS. UNIT MACH NO. 0.5. INFLUENCE WIND - 30°.

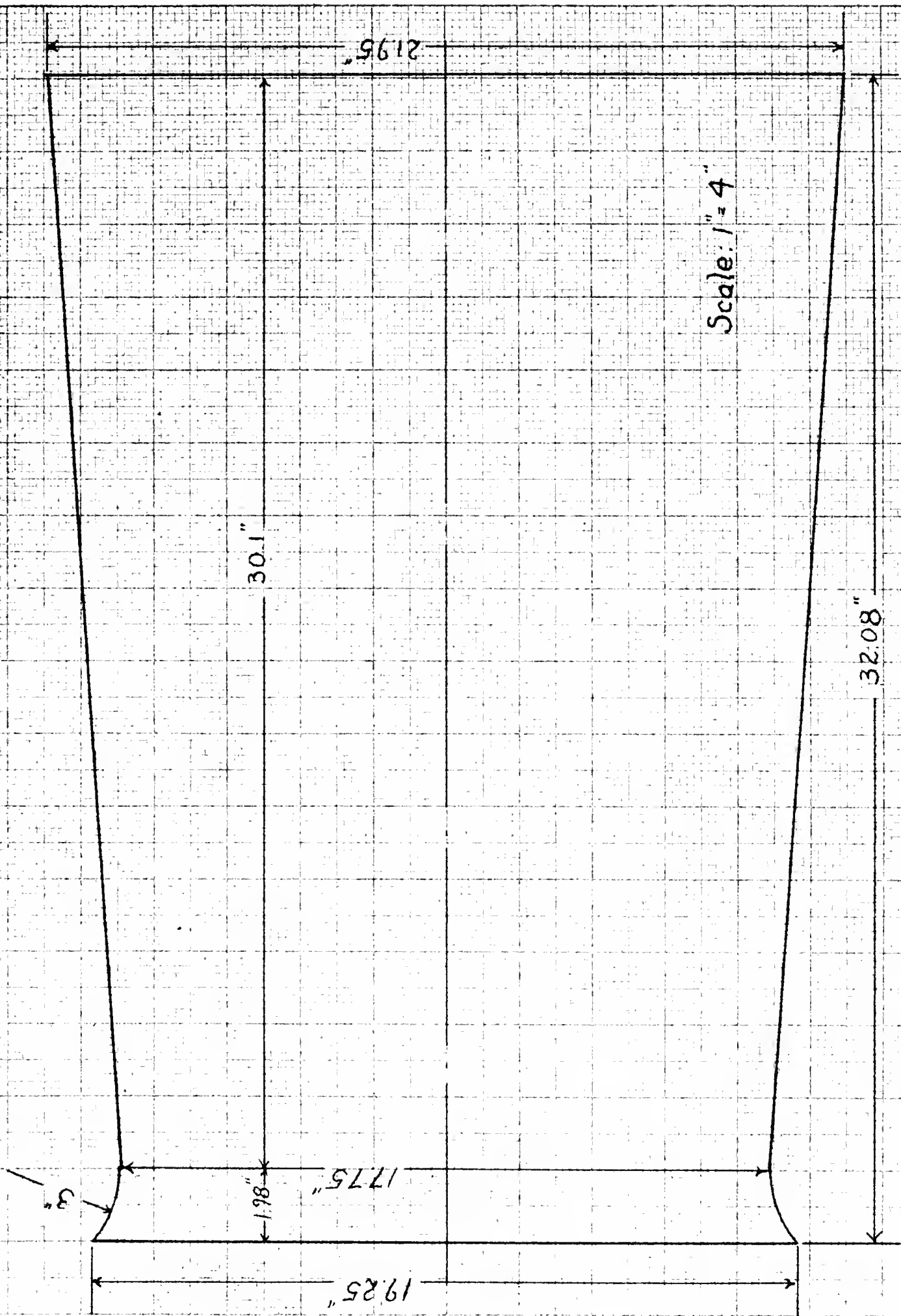
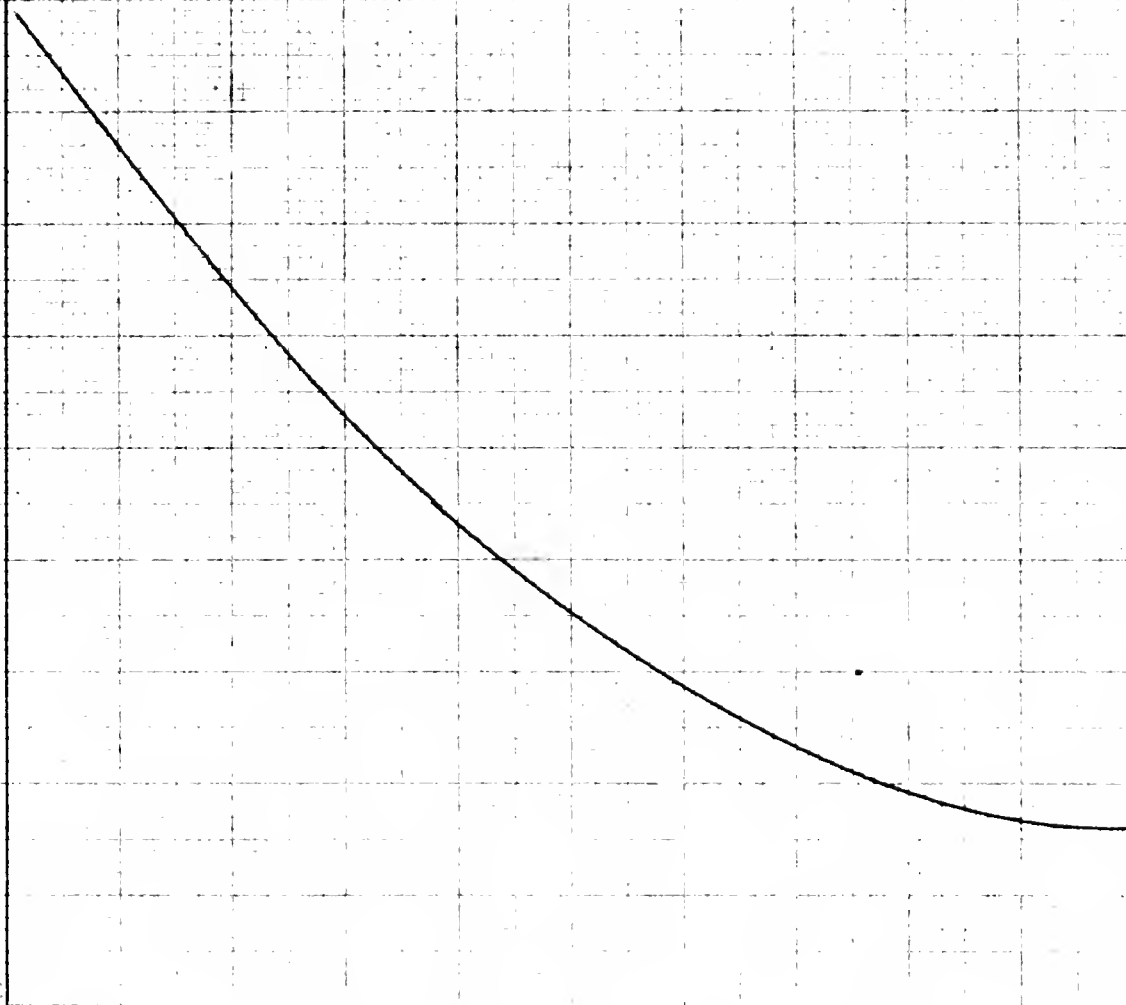
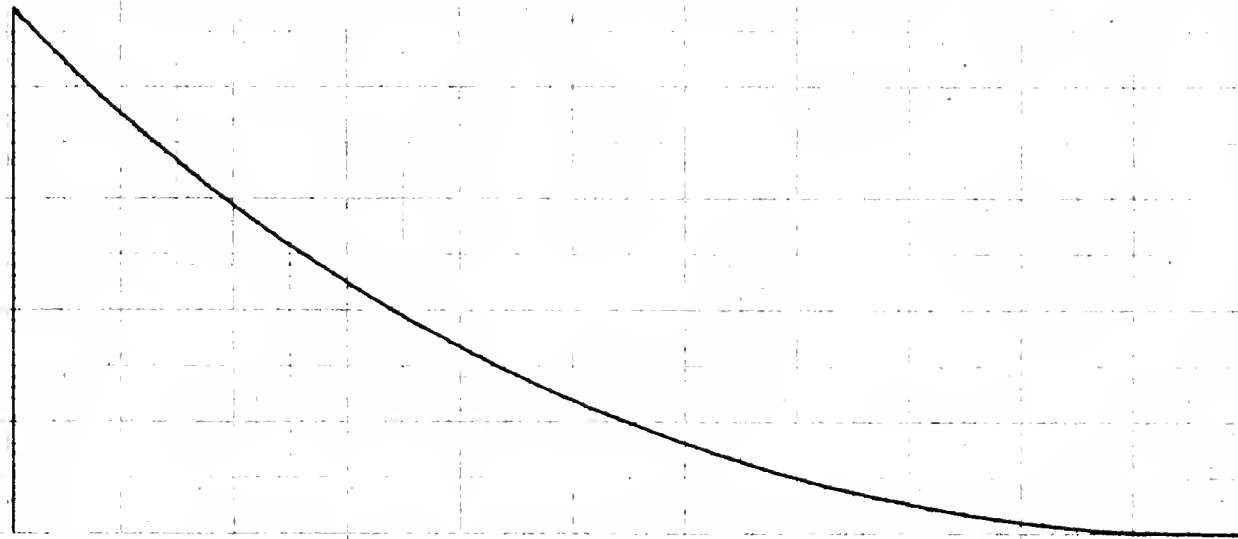


FIG. 18 - DIFFUSER FOR ILLUSTRATIVE PROBLEM.

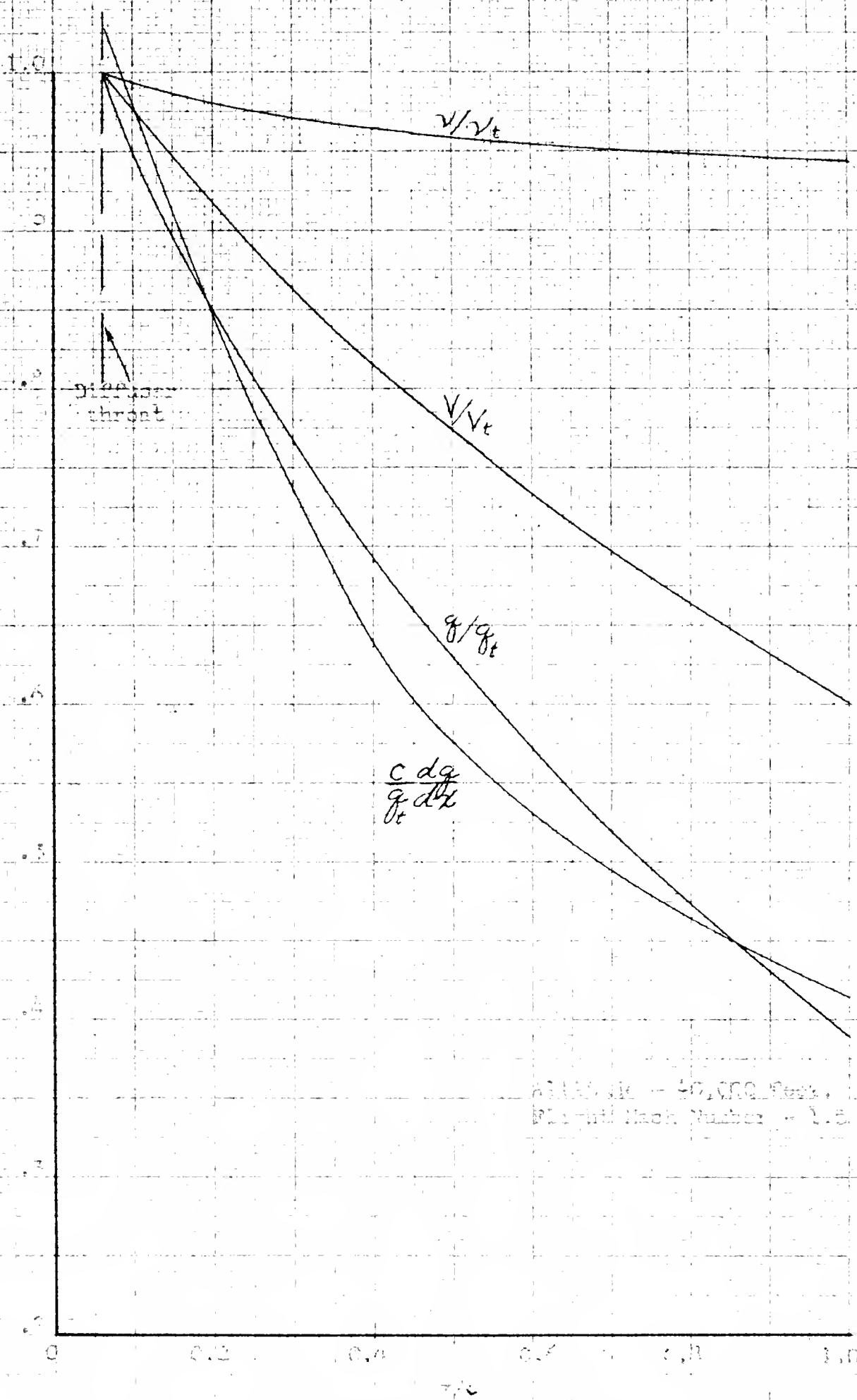
PRESSURE - lb/sq. ft.



(A) STATIC PRESSURE DISTRIBUTION AT DIAMETER 1.000.
 LENGTH = 1.000 - FEET - FROM ORIGIN - 1.0



(B) STATIC PRESSURE DISTRIBUTION AT DIAMETER 1.000.
 LENGTH = 1.000 - FEET - FROM ORIGIN - 1.0



Area at $x = 40$ ft. g_t
 Flow Mach Number = 1.0

FIG. 9 - INTERNAL CONDITIONS IN THE DIFFUSER

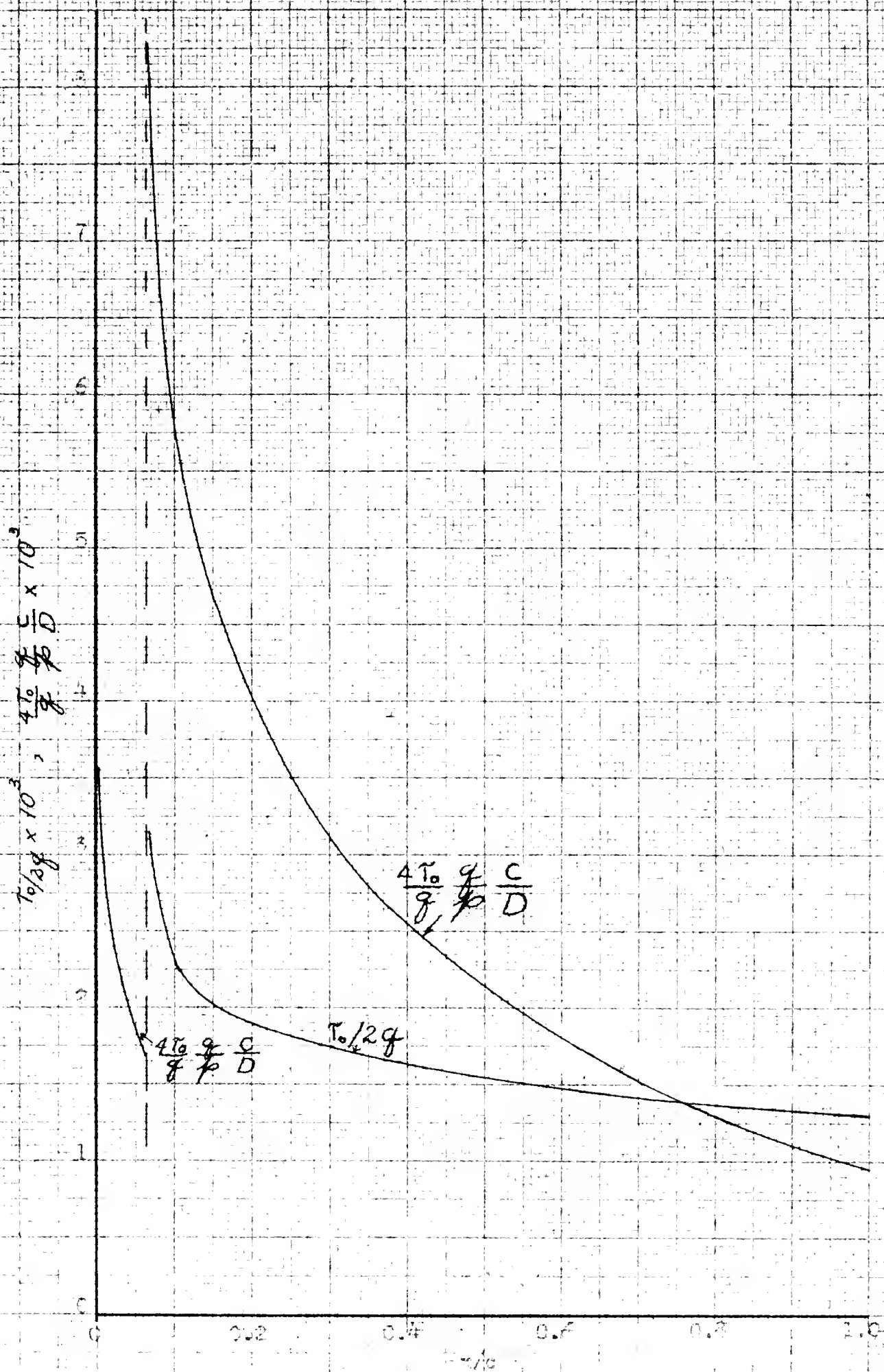


FIG. 2A - FRICTION EFFECTS IN THE RESERVOIR.

PRESSURE LOSS IN CONSTANT AREA DUCT
 $\Delta p - \text{lb./sq. ft.}$

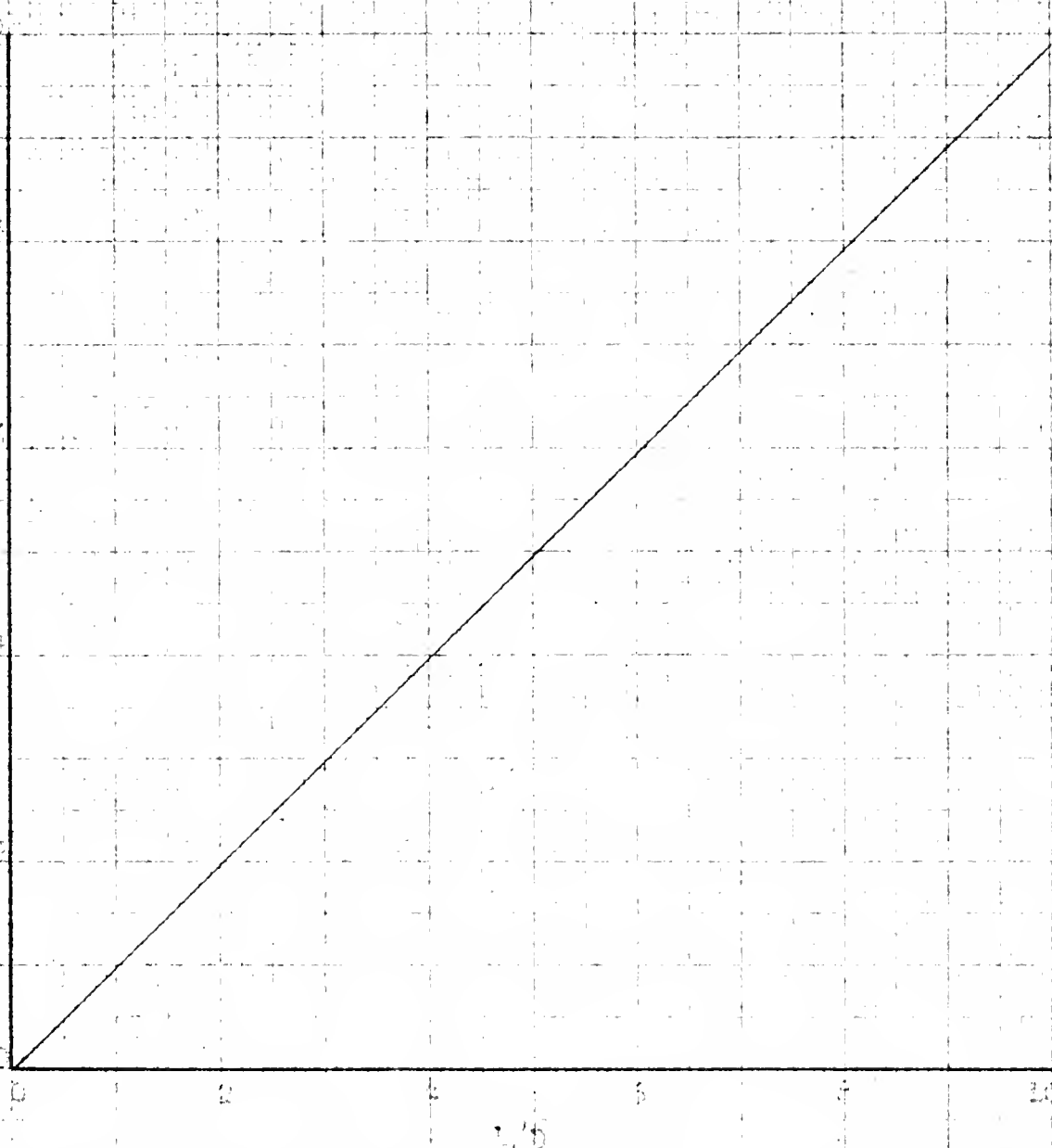


FIG. 12 - VALIDATION OF RECEIVED LOSS IN THE CONSTANT AREA DUCT
 FROM DIFFUSER EXIT TO COMPRESSOR INTAKE WITH
 1.00000 LB./FT.

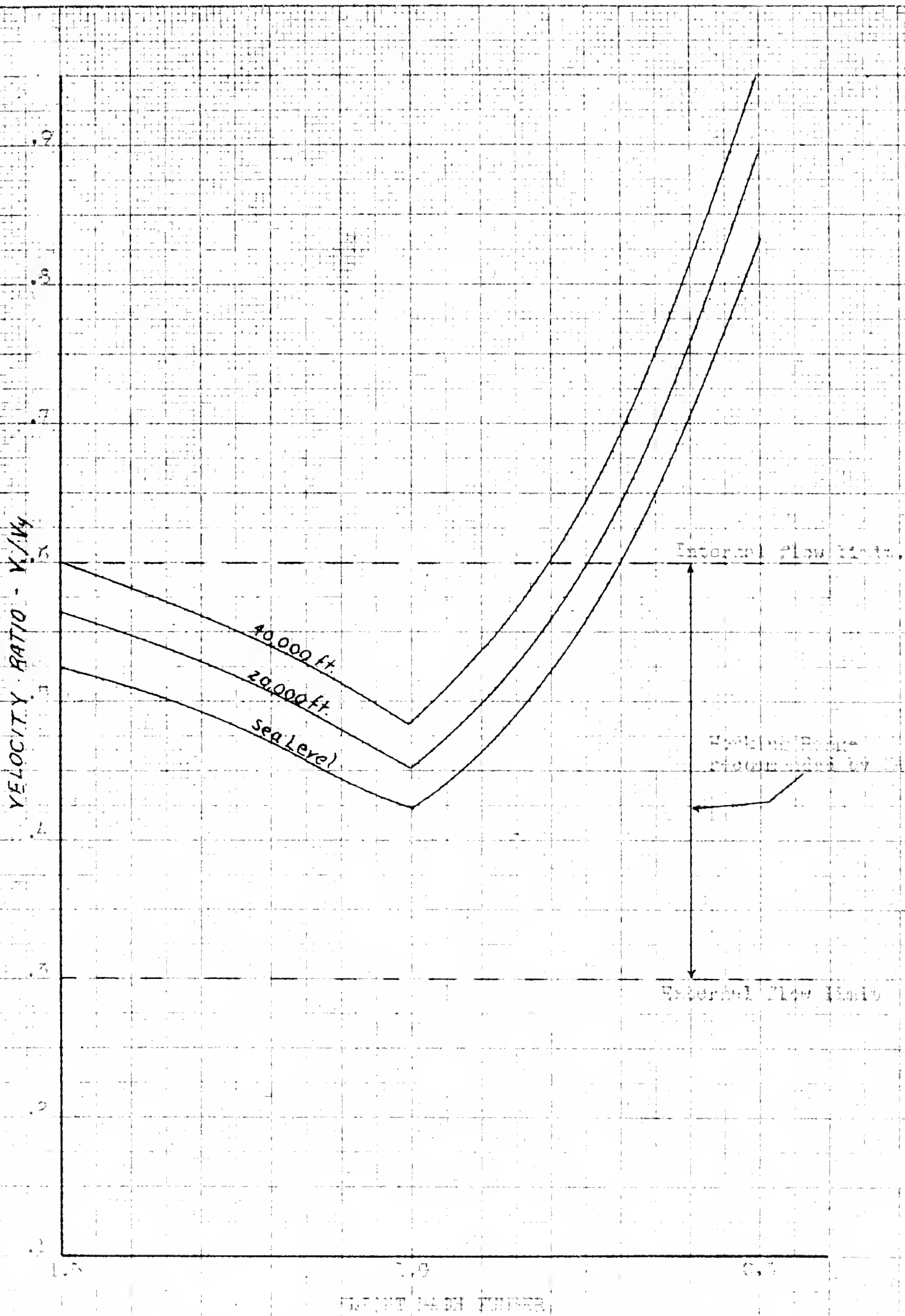


FIG. 22 - VARIATION OF VELOCITY RATIO WITH FRONT FACE STRIKE.

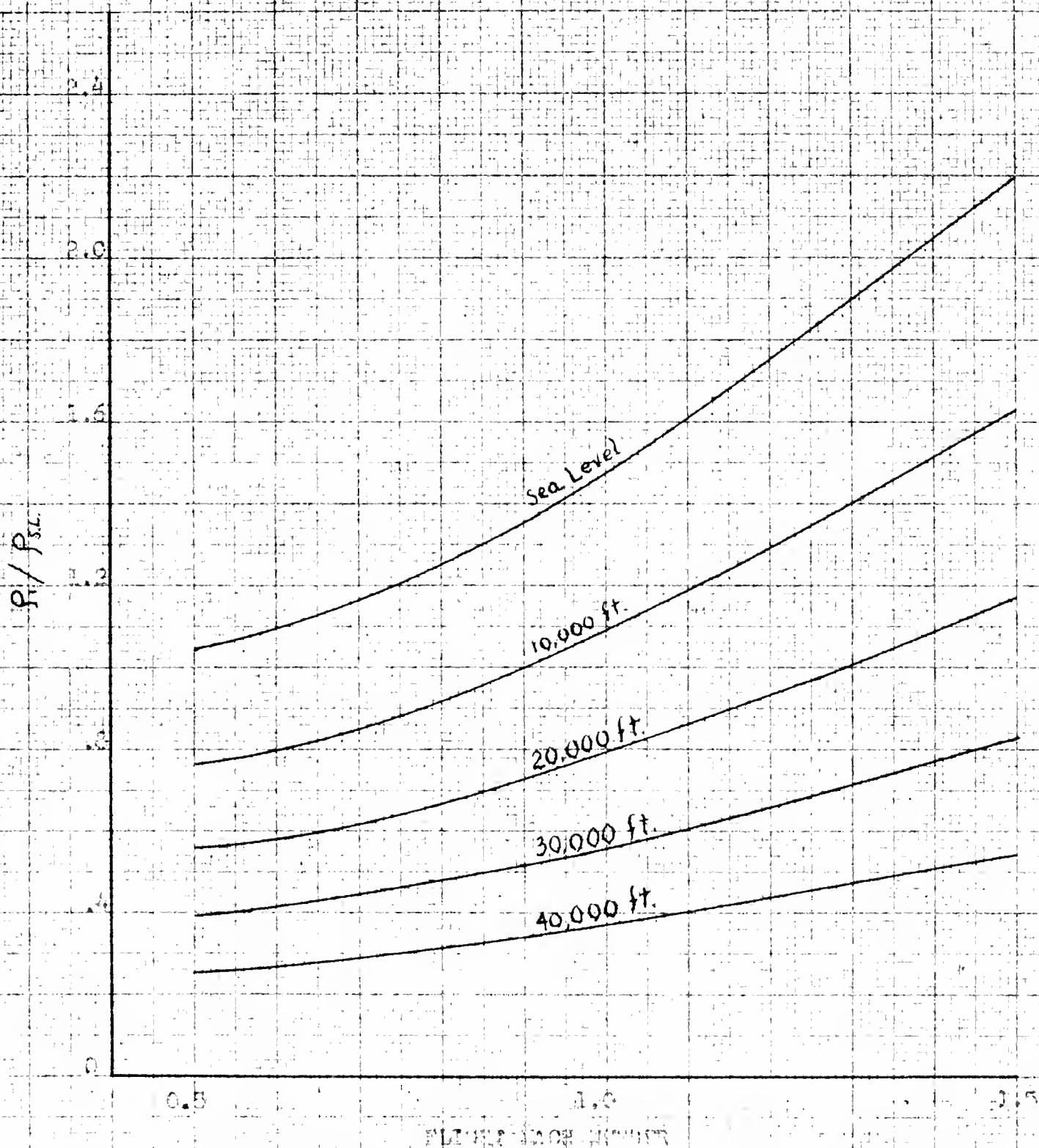


FIG. 24 - VARIATION OF AIR DENSITY WITH SPEED AND ALTITUDE.

DATE DUE

[illegible]

Thesis 11465
C78 Coyle

Air inlets for turbo-
jet engines through the
transonic speed range.

Thesis 11465
C78 Coyle

Air inlets for turbo-
jet engines through the
transonic speed range.

the
Air inlets for turbojet engines through



3 2768 002 09035 9
DUDLEY KNOX LIBRARY